CAPE PENINSULA UNIVERSITY OF TECHNOLOGY

Ethylene-1-octene elastomers: Molecular structure characterization by advanced analytical methods

Mawande Sigwinta

Thesis submitted in fulfilment of the requirements for the degree Master of Applied Sciences: Chemistry in the Faculty of Applied Sciences

Supervisors

Dr. Francois Wewers (CPUT, Department of Chemistry)

Prof. Harald Pasch (Stellenbosch University, Department of Chemistry & Polymer Science)

December 2019

Declaration

I, Mawande Sigwinta, declare that the content of this dissertation represents my own unaided work, and that the dissertation has not previously been submitted for academic examination towards any qualification. Furthermore, it represents my own opinions and not necessarily those of the Cape Peninsula University of Technology.

_____ _____

Signed Dated

Abstract

Polyolefin elastomers are non-crystallising materials which are challenging to characterize with conventional crystallization-based techniques such as crystallization analysis fractionation (CRYSTAF) and temperature rising elution fractionation (TREF). However, interaction chromatography (IC) offers an alternative pathway for the chemical composition distribution definition of these materials. This work details the development of comprehensive characterization methods of linear low-density polyethylene (LLDPE) elastomers. In the first part of this work, four preparative fractionation methods namely, solution crystallization fraction (p-SCF), preparative temperature rising elution fractionation (p-TREF), modified p-TREF, and preparative molar mass fractionation (p-MMF) were compared for the analysis of an LLDPE elastomer with 12.8 mol% 1-octene content. While p-TREF showed the coelution effect at low elution temperatures, sufficient amount of fractions with narrow molar mass dispersity were obtained with the p-MMF method. Despite the limitations with the TREF method, it was demonstrated that both fractionation techniques provide detailed information on the complex nature of the LLDPE elastomer molecular structure after subsequent analysis with several other offline techniques such as solvent gradient interaction chromatography (SGIC). The modified p-TREF method also produced fractions with interestingly narrow dispersities and showed significant molar mass influence on its fractionation mechanism. The molar mass influence on the collected fractions was also observed with the p-SCF method, and both methods are a subject for future study. It was shown that when using a binary solvent mixture in which one of the solvents limits the solubility of the polyolefin chains, the separation is molar mass dependent even if column temperature is the active variable. In the second part of this work, four LLDPE copolymers with increasing amounts of 1-octene but similar molar masses were utilized to investigate the influence of chemical composition on the p-MMF technique. For all four LLDPE copolymers, eight fractions with decreasing molar masses were collected at different non-solvent/solvent ratios as the amount of non-solvent in the non-solvent/solvent mixture was increased. It was shown that chemical composition of these samples was independent of the fraction number, but was influenced by the average chemical composition of their respective bulk sample. Consequently, it was concluded that the molecular structure complexity of the four samples decreased with increasing 1-octene content. Finally, three commercial LLDPE elastomers with high 1-octene contents were comprehensively

studied. Preparative molar mass fractionation was employed to obtain fractions which were further analysed using size exclusion chromatography (SEC) and differential scanning calorimetry (DSC). It was found that at bulk level, the samples appear to exhibit microstructural homogeneity, however, their respective p-MMF fractions exhibit multimodal chemical composition distributions. Furthermore, the p-MMF fractions showed an increase in their chemical composition heterogeneity as the molar mass decreased. Ultimately, it was concluded that the p-MMF method is the most suitable technique that provides in-depth insight on the molecular structure complexity of LLDPE elastomers.

Acknowledgements

I would like to extend my gratitude and render my warmest thanks to my supervisor, Professor Harald Pasch, who facilitated a platform for me to conduct my project at Stellenbosch University (Department of Chemistry and Polymer Science) and made this work possible. His friendly guidance and expert advice have been invaluable throughout all stages of the work. I would also wish to express my indebtedness to Dr. Francois Wewers for the extended discussions and valuable suggestions, which have contributed greatly to the improvement of the thesis. The thesis has also benefited from comments and suggestions made by my mentor, Dr. Anthony Ndiripo, who has read through the manuscript and contributed greatly to the experimental section of the work. Furthermore, I would like to acknowledge Dr. Paul Eselem Bungu for his contribution to the discussion of the results and encouragement. I cannot forget Dr Reuben Pfukwa for his continuous motivation and words of encouragement. Special thanks are due to my siblings, Phakama Sigwinta and Nosiphiwo Sigwinta for their continuous moral support, encouragement and understanding. The person with the greatest indirect contribution to this work is my mother, Nojongile Sigwinta who has made countless sacrifices and encouraged me to further my studies. This thesis has been conducted during my stay at the Department of Chemistry and Polymer Science. I would like to thank the Stellenbosch University for providing excellent working conditions, and National Research Foundation (NRF) for the financial support.

Dedication

To my mother, Nojongile Sigwinta

Table of Contents

List of Figures

List of Tables

List of abbreviations

CC	Chemical composition
CCD	Chemical composition distribution
^{13}C-NMR	Carbon-thirteen nuclear magnetic resonance spectroscopy
CRYSTAF	Crystallization analysis fractionation
SCB	Short chain branching
SCBD	Short chain branching distribution
DSC	Differential scanning calorimetry
ESL	Ethylene sequence length
ESLD	Ethylene sequence length distribution
EPS	Expanded polystyrene
FTIR	Fourier-transform infrared spectroscopy
HDPE	High density polyethylene
HT-2D-LC	High temperature two-dimensional liquid chromatography
LDPE	Low density polyethylene
LLDPE	Linear low density polyethylene
MFI	Melt flow index
MW	Molecular weight
MM	Molar Mass
MMD	Molar mass distribution
MMF	Molar mass fractionation

HT-HPLC	High-temperature high performance liquid chromatography
HT-SEC	High-temperature size exclusion chromatography
HT-SGIC	High-temperature solvent gradient interaction chromatography
PE	Polyethylene
PET	Polyethylene terephthalate
PP	Polypropylene
PS	Polystyrene
PVC	Polyvinyl chloride
SGF	Solvent gradient fractionation
SGIC	Solvent gradient interaction chromatography
TGIC	Thermal gradient interaction chromatography
TREF	Temperature rising elution fractionation

Chapter 1

Introduction

This chapter introduces the problems to be addressed in the present work. The challenges faced in the characterisation of ethylene-co-1-octene elastomers are mentioned and classified into a list of objectives, which are addressed experimentally in further chapters.

1.1 Background

Synthetic polyolefins have become part of our daily life and have a wide variety of applications from food packaging to transport and building infrastructure.[1,2] The major types of synthetic polyolefins are polypropylene (PP) and polyethylene (PE). PP is by volume the largest polyolefin material.[3] However, PE materials are much more versatile and can also be produced from the copolymerisation of ethylene and a variety of other comonomers.

PE is a thermoplastic that is produced via catalytic or radical polymerization. Various grades of PE can be synthesised depending on the end-use requirements. These grades of polyethylene can be classified according to their density, which is in turn influenced by the degree and type of branching[4]. The three main classes of PE include low density polyethylene (LDPE), linear low density polyethylene (LLDPE) and high density polyethylene (HDPE). Detailed information regarding these different classes of PE will be provided in Chapter 2.

LLDPE is produced through the copolymerization of ethylene with a variety of 1-olefins e.g. 1-butene, 1-hexene and 1-octene.[5] The 1-olefins introduce short branches to the polyethylene backbone. As a result, these materials can be tailored to have different densities by simply altering the comonomer content/chemical composition (CC).[1,5] This is achieved by varying the ethylene-to-comonomer ratios during synthesis.[2]

Due to the better properties of LLDPE over LDPE, its market share has continued to grow over the recent past.[3] Depending on the comonomer content, a wide range of products can be made from LLDPE. On the other hand, LDPE is much more challenging to tailor for such

applications due to its complex branching architecture and the harsh conditions required for its production.

Polyolefins are semi-crystalline materials.[6] Over the years, crystallization-based techniques have been developed that form the backbone of polyolefin characterization. These include differential scanning calorimetry (DSC), crystallization analysis fractionation (CRYSTAF), temperature rising elution fractionation (TREF) and more recently crystallization elution fractionation (CEF).[6] With the exception of DSC, the other mentioned techniques exploit the dissolution and recrystallization properties of polyolefins in solution. Since the distribution of polyolefin chains is statistical, the distribution of the comonomer in the different polymer chains i.e. chemical composition can affect crystallizability in solution.

Therefore, distributions relating temperature to the dissolved polyolefin chains in solution can be obtained. These distributions can be used to describe the chemical composition distributions of polyolefins. However, high comonomer content LLDPEs, also known as elastomers, fail to crystallise from solution owing to their very low crystallinity or amorphous nature. Therefore, the crystallization-based techniques become redundant when elastomers are to be analysed. A few recent works have been done to address these challenges.[7,8]

LLDPE resins can be made using different catalyst types (discussed briefly in Chapter 2) which further complicates the microstructure of the materials. In addition, batch-to-batch variations may occur during synthesis. As a way of continuously improving synthetic methods and catalyst systems, suitable analytical techniques for elastomers must be developed and used. High-temperature interaction chromatography (HT-IC) and high-temperature size exclusion chromatography (HT-SEC) are two important chromatographic techniques for the characterization of polyolefins. HT-SEC provides information on the molar masses of the polyolefin samples.

However, this technique does not provide information on the distribution of the comonomer units on the polyolefin backbone. Despite having capabilities of being coupled to information-rich detectors such as the infrared detector, the separation is based on size rather than functionality. HT-IC separates polyolefin chains based on their selective interaction with a porous graphitic carbon (PGC) stationary phase or silica in the case of functionalised polyolefins. The interactions on PGC are governed by weak dispersion forces which can be overcome by applying a temperature or a solvent gradient.[6] The main advantage of HT-IC is

that it is not governed by crystallizability. Therefore, a wide range of non-crystallizing elastomers with different comonomer contents can be analysed. Preparative fractionation has been largely employed to aid in the unravelling of the complete microstructure of polyolefins. Fractionating polyolefins prior to analysis serves two important purposes. The first is that chemically homogenous polymer chains are concentrated into narrowly distributed fractions allowing for gravimetric quantification. Secondly, smaller fractions of chemically different polymer chains that may go undetected during bulk analysis can be concentrated and analysed further. As previously indicated, the majority of fractionation techniques are crystallization-based.

Therefore, the arsenal of otherwise useful techniques becomes redundant in the preparative fractionation of non-crystallizing elastomers. In this work, we explore a molar mass-based preparative fractionation technique as an alternative to crystallization-based ones. This technique has been previously reported by Bungu et al.[9] for the preparative fraction of LDPE. When a suitable fractionation technique is coupled to HT-IC, more information on the elastomers can be obtained. In addition, HT-IC can be coupled to HT-SEC in high-temperature two-dimensional liquid chromatography (HT-2D-LC) to give information relating chemical composition distribution to molar mass distribution.[11]

1.2. Problem statement

LLDPEs are complex polyolefin materials which exhibit a molecular structure heterogeneity, including distributions in molar mass and chemical composition. Both the molar mass distribution and the chemical composition distribution affect the processability and overall mechanical properties of the final polymer product. Therefore, adequate structural elucidation of LLDPEs is a vital step in ensuring that the designed polymer material meets the desired final mechanical and physical properties. However, classical crystallization-based analytical techniques such as TREF, DSC and CRYSTAF have shortcomings as they are limited only to the analysis of crystallisable molecular chains. As a result, these techniques do not provide adequate information with regard to the microstructure of non-crystalline polyolefins.

LLDPEs with 1-olefin contents of greater than 7 mol% have very low crystallinities, consequently it is very challenging to fully characterize them. Furthermore, this class of

LLDPEs has not received much research attention owing to challenges associated to characterization of amorphous materials using the above mentioned classical analytical methods. Therefore, analytical techniques that are able to fractionate LLDPE elastomers irrespective of their degree of crystallinity are excellent potential alternatives to the crystallization-based techniques. Preparative molar mass fractionation (p-MMF) techniques separate molecular chains based on their solubility in a suitable solvent system, regardless of their crystallinity. Therefore, the task of the present study is to develop a suitable analytical method for comprehensive characterization of amorphous LLDPE elastomers.

1.3. Research questions

A comprehensive characterization of polymers, polyolefins in particular, requires fractionation of the bulk samples to obtain fractions with narrow CCD or MMD. However, the p-TREF fractionation method is limited to crystallisable materials. Therefore, it would be interesting to investigate the adequacy of p-MMF as an alternative technique to p-TREF for fractionation of LLDPEs with very low crystallinities. Furthermore, it would be interesting to study fractions obtained using the p-SGF method using a combination of analytical techniques such as DSC, CRYSTAF, SEC, SGIC, HT-2D-LC.

1.4. Objectives

There is an increasing interest for investigating the molecular structure of LLDPE elastomers due to their industrial importance. However, as previously mentioned, there are challenges associated with the characterization of this class of LLDPE. These challenges require adequate analytical approaches that can provide comprehensive information regarding the molecular heterogeneity of LLDPE elastomers. Therefore, the main objectives of this work are summarized as follows: -

- To analyse bulk samples using advanced analytical techniques.
- To fractionate the bulk samples to obtain fractions i.e. simplify the CC or MM dimensions for further analysis.
- To analyse fractions with advanced analytical techniques to obtain more information regarding the microstructure.

- To compare findings of different samples with different comonomer contents for future molecular structure-property correlations.

1.5. Hypothesis and assumptions

The success of TREF as a fractionation method mostly depends on how efficient the dissolved polymer molecules crystallize onto the inert silica support as the temperature is decreased. The solubility of polymer molecules at a constant temperature is largely influenced by their molar mass and solvent power. Therefore, since LLDPE elastomers are largely amorphous, the following assumptions and hypothesis can be made:

1.5.1. Hypothesis

- Appropriate fractions for further analysis will be obtained by p-MMF methods, rather than p-TREF.
- The proposed set of analytical tools is suitable for an adequate comprehensive analysis of the molecular heterogeneity of the elastomers under study.

1.5.2. Assumption(s)

- p-MMF can fractionate and, thus, simplify the molar mass distribution of LLDPE elastomers irrespective of the crystallinity of the polymer chains.

1.6. Layout of dissertation

Chapter 1

This chapter broadly highlights the challenges associated with crystallization-based analytical techniques for the characterization of ethylene-1-octene LLDPE copolymers that have very low crystallinity. These crystallization-based techniques include p-TREF, CRYSTAF and DSC, and potential alternative fractionation methods which are column-based are discussed. In addition, concepts of previously published work on the characterization of elastomers is highlighted. This includes the application of HT-HPLC using solvent gradient mode for the characterization of LLDPE elastomers. This chapter further highlights the objectives and hypothesis of this work.

Chapter 2

The literature review on polyethylene synthesis, role of catalysis in polyolefin synthesis and the characterization methods of LLDPEs are provided herein. Various fractionation methods including p-TREF, p-SCF, p-MMF and spectroscopic methods of molar mass and chemical composition analysis are introduced.

Chapter 3

This chapter highlights the materials including chemicals, samples and experimental procedures that were employed.

Chapter 4

Herein, the adequacy of four preparative fractionation techniques, namely p-SCF, p-TREF, p-TREF using special conditions, and p-MMF, is evaluated for the characterization of LLDPE elastomers.

Chapter 5

This chapter presents and discusses results obtained from the analyses of p-MMF fractions from four EO-LLDPE samples with varying comonomer contents.

Chapter 6

This chapter discusses results obtained from the analyses of p-MMF fractions of three commercial LLDPE elastomers with comonomer contents above 10 mol%.

Chapter 7

This chapter summarises the results obtained from the employed characterization techniques, draws a conclusion, and gives recommendations for future work based on the findings.

1.7. References

1. Sauter, D. W.; Taoufik, M.; Boisson, C. Polymers 2017, 9, 185.
2. Sturzel, M.; Mihan, S.; Mulhaupt, R. Chem. Rev. 2016, 116, 1398–1433.

3. Galiè, F., Global Market Trends and Investments in Polyethylene and Polypropylene; Reed Business Information: www.ics.com, 2016.

4. Alt, H. G.; Köppl, A. Chem. Rev. 2000, 100, 1205–1221.

5. Spalding, M. A.; Chatterjee, A. Handbook of Industrial Polyethylene and Technology: Definitive Guide to Manufacturing, Properties, Processing, Applications and Markets Set; John Wiley & Sons: New York, 2017.

6. Pasch, H.; Malik, M. I. Advanced separation techniques for polyolefins; Springer: New York, 2014.

7. Ndiripo, A.; Albrecht, A.; Monrabal, B.; Wang, J.; Pasch, H. Macromol. Rapid Commun. 2018, 39, 1700703.

8. Arndt, J.-H.; Brüll, R.; Macko, T.; Garg, P.; Tacx, J. Polymer 2018, 156, 214–221.

9. Eselem Bungu, P.; Pasch, H. Polym. Chem. 2017, 31, 4565–4575.

Chapter 2

Literature review

This chapter reviews the literature for relevant information on polyethylene and ethylene-based copolymers, its historical background and current developments in its synthesis and characterization. Relevant techniques used in the present work are also reviewed.

2.1. Introduction

Over the years polyolefins have developed from very simple ill-defined and difficult to synthesise materials into an array of classes governed by monomer, catalyst and reactor types. Therefore, it is important to review the development of polyolefins and more specifically polyethylene and polyethylene elastomers. This chapter reviews the development of polyolefins, catalysts and the techniques used for characterizing polyethylene elastomers.

2.2. History of polyethylene

The concept of polymers was first introduced by Herman Staudinger about three decades after the first traces of PE were reported by Hans von Pechman as a decomposition product of diazomethane into "polymethylene".[1,2] However, the first commercial production process of PE was patented in 1937 by Imperial Chemical Industry (ICI) about four years after small amounts of LDPE were discovered through an accidental free radical polymerization reaction in the presence of oxygen as an initiator.[1-3] Thereafter, PE gained more attention from both academic researchers and industry. Figure 2.1 highlights some significant discoveries in catalysis that led to improvements in the synthesis of polyolefins.

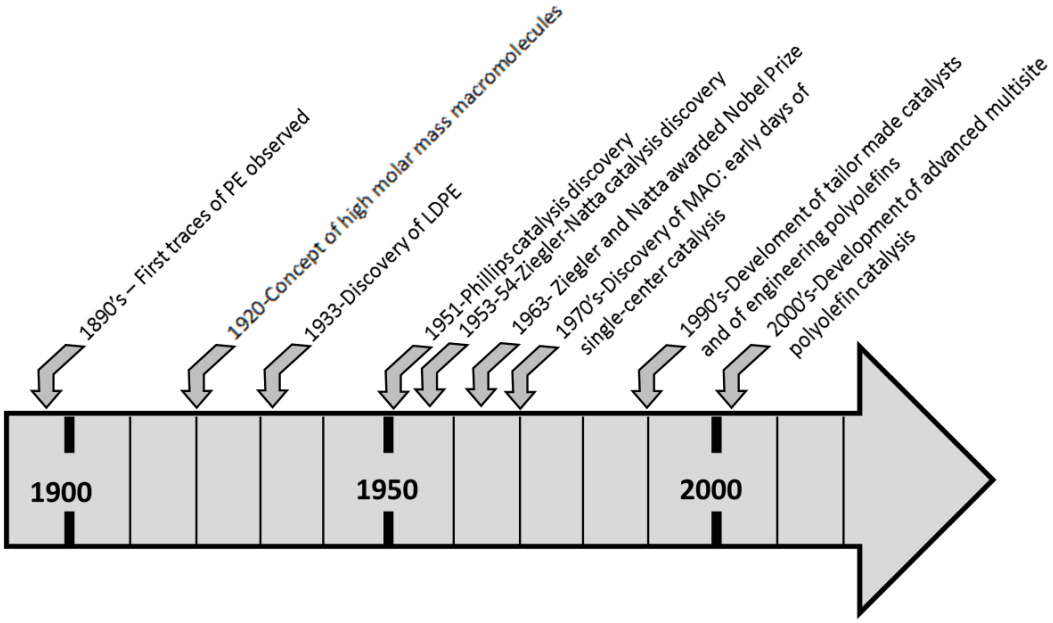

Figure 2.1. Most significant discoveries in catalysis that improved synthesis of polyolefins and their commercial applications.[1]

The main motivation was to find more sustainable PE synthetic pathways that would yield PE resins with better physical properties and processability. Consequently, major breakthroughs which significantly advanced the industrial commercialization of PE were recorded between the 1950-1990 with the introduction of catalytic polymerization of PE in various transition metal based catalytic systems. Most prominently, Ziegler recorded a triple increase in the productivity of the copolymerization reaction using zirconium acetylacetonate and triethylaluminium.[1,4]

It was later discovered that replacing zirconium acetylacetonate with titanium tetrachloride significantly improved the copolymerization process efficiency with higher ethylene conversions at lower temperature and pressure. [3,5] This new catalytic system was employed by Natta to produce stereoregular isotactic polypropylene (i-PP) thereby introducing for the first time the concept of stereoregularity in polyolefins.[1,6] Thereafter, the first industrial production of i-PP using a Ziegler-Natta system was realized in 1957[1,3,7], and gained widespread application throughout the years until to date.

Kaminsky and Sinn[8] accidentally discovered that a reaction between trimethylaluminium (TEA) and water produced a new compound called methylaluminoxane (MAO) which

significantly improved the catalytic activity of a titanocene catalyst. This discovery gave rise to the discovery of metallocene catalysts which offer high control of molar mass and chemical composition. Consequently, metallocene catalysts found wide industrial applications including Exxon-Mobil's Exxpol™ Technology for polyolefin production and the Dow INSITE™ Technology that is based on constrained geometry catalyst (CGC) to name a few.[3,7,9]

Particularly, the INSITE™ technology was used for the production of a range of speciality polyolefins such as plastomers (AFFINITY), elastomers (ENGAGE) and high performance ethylene-propylene-diene monomers (EPDM).[7] To date, Phillips-type, Ziegler-Natta (ZN) and metallocene-type catalysts are prominently used in the catalytic polymerization processes of PE.[1] Phillips-type catalysts account for 40-50% of global HDPE production.[1,3,10] It is worth noting that the evaluation of each of the catalytic systems in producing the desired end products is entirely dependent on the capabilities of the employed analytical techniques to comprehensively elucidate the microstructure of the produced polymers.

2.3. Polyolefin types

Polyolefins are now by far the largest produced synthetic polymers (by volume). Each type of polyolefin material is designed to fit a specific application, from packaging to structural applications. Part of the process of making a suitable polyolefin starts in the choice of the monomers, catalyst and the type of polymerisation process.[11,12] The most common PE types are LDPE, LLDPE and HDPE. LDPE is produced via a free radical polymerisation process.[3,13] Harsh conditions are required for this process and the cost of making and maintaining plants for such purposes is high. In addition, it is more difficult to tailor LDPE for specific functions due to its complex microstructure which involves long and short chain branching.[3]

On the other hand, HDPE and LLDPE are typically produced using ZN or metallocene type catalysts.[2,10] Philips type catalysts are also still widely used although they give resins with broad molar mass and chemical composition distributions.[10,14] HDPE consists of highly linear PE chains and consequently has high density due to the close packing of the crystallised chains. This makes HDPE suitable for applications which require strength and toughness. When a comonomer is copolymerised with ethylene, the PE backbone is modified to either incorporate short chain branches (SCBs) or functional groups.[15] The later will not be reviewed since it is

not part of the dissertation. In cases where PE is modified by introducing SCBs, the materials so formed are referred to as LLDPEs. It is, therefore, worth to review this class or type of polyolefin since it is the material used in the present work.

2.4. Linear low-density polyethylene

LLDPEs are linear copolymers that have short chain branching (SCB) which is incorporated during the copolymerization reaction.[16-19] Short chain branching refers to branches consisting of at most six carbon atoms. For LLDPEs, the branching usually results from the copolymerization of ethylene with other 1-olefins such as propylene, 1-butene, 1-pentene, 1-hexene and 1-octene, although 1-cycloalkenes are sometimes also utilized as comonomers.[20-22] A simple reaction equation for the polymerization of ethylene in the presence of a catalyst is shown in Equation 1.

$$H_2C{=}CH_2 \xrightarrow{\text{catalyst}} {\sim}(CH_2CH_2)_n{\sim} \qquad (1)$$

The reaction conditions and the type of catalyst (Figure 2.2 shows the influence of multiple active site catalyst on CCD and MMD) dictate the mechanism through which 1-olefins are introduced into the polyethylene backbone. Consequently, LLDPEs possess a molecular heterogeneity that is attributed to the molar mass distribution and the intermolecular and intramolecular short chain branching distribution.[23] The intermolecular heterogeneity is caused by the fact that each macromolecular chain has its unique composition different from any other macromolecule. Furthermore, the comonomers can be randomly distributed on the PE backbone or can have longer homopolymer segments, thus contributing to the intramolecular heterogeneity of LLDPE.

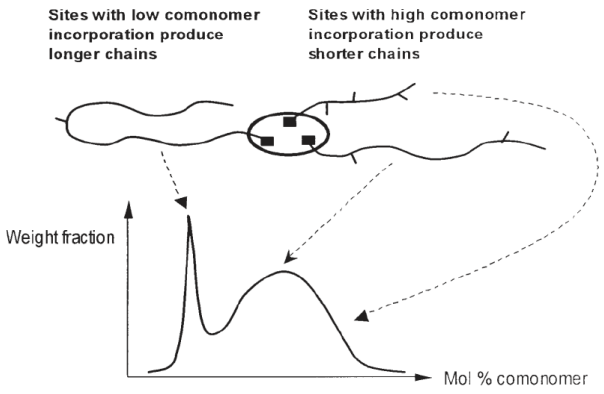

Figure 2.2. CCD and MMD resulting from multiple active sites of ZN-catalyst.[24]

Furthermore, the mechanical properties of the final polyolefin product are a function of molar mass and chemical composition of the polyolefin molecules making up the bulk resin. Thus, the melt flow index and the toughness of LLDPE material can be modified by changing the MMD and the SCB content and/or SCB type, respectively. Therefore, the physical and chemical properties of these LLDPE are often tailored to match the performance or intended use.

Thus, in order to achieve the desired end product, it is essential to fully understand the molecular heterogeneities of the elastomer material being processed. The challenge associated with characterization of bulk resin is that only average molecular structural information is revealed. However, in addition to average structural information, the distributions in both molar mass and chemical composition must be elucidated. For a comprehensive characterization of polyolefins, fractionation is inevitable as this narrows down the complexity of the polymer resin in question.[14]

Furthermore, the complexity of polyolefins requires a multiple analytical method approach in order to gain detailed information on the multidimensional heterogeneity (CCD and MMD). The most widely used characterization techniques for LLDPE microstructure elucidation include spectroscopic methods and separation methods.[14,25] Generally, in separation-based techniques the goal is to gain in-depth structural details of the bulk material, and this is best achieved by dividing the bulk molecular structure into its component parts (fractions) for further analysis.[14,25-27] For this reason, p-TREF is an ideal and well known technique for chemical composition analysis of polyolefins.[14,25,28-30]

TREF isolates groups of crystallisable polyolefin chains at each elution temperature based primarily on their degree of crystallizability. The chemical composition information is then deduced from the known relationship that crystallinity/ethylene sequence length decreases with increasing comonomer content of the LLDPE copolymer.[31-33] It has been demonstrated that the LLDPEs can be fractionated based on chemical compositions in TREF.[34,35] The success of the TREF technique in chemical composition analysis of semicrystalline LLDPE is well documented.[18,28,36]

However, attempts to study the chemical composition of elastomers using p-TREF have failed due to lack or absence of crystallisable polyolefin chains. Phiri et al.[37] demonstrated using ethylene-propylene rubber (EPR) that p-TREF is limited to the fractionation of polymer resins that have a significant amount of crystallisable polyolefin chains. Therefore, when the TREF method is employed for the fractionation of elastomers, a lot of useful compositional information is lost since, generally, more than 80 wt.% of the bulk elastomer chain segments co-elute in the first low elution temperature fraction.

Additionally, CRYSTAF, a chemical composition analysing technique which is based on measuring the concentration of the polymer dissolved in a good solvent as the temperature decreases stepwise, has also been explored.[37] Similar results to TREF were obtained with this technique. However, the effect of a strong solvent in addition to high temperature makes analysis of elastomers virtually impossible as almost all of the polymer molecules are soluble below 30 °C. Another technique which provides useful information about the chemical composition of polyolefins is differential scanning calorimetry (DSC).

DSC measures the thermal events of the polymer in a particular predetermined range of temperature and relates them to the chemical composition/molar mass of the polymer molecules. Again, the average crystallization and melting behaviour of standard LLDPE have been successfully investigated using DSC.[11,23,35,38] However, DSC analysis of LLDPE elastomers does not reveal the characteristic thermal events, consequently only limited information can be drawn from the obtained DSC results for this class of materials.[39]

Therefore, there is a need for alternative means of comprehensively probing into the microstructure of polyolefin copolymers, especially LLDPE elastomers. Fractionation techniques, which discriminate polymer molecules based on their molar mass differences rather than crystallizability possess an excellent potential. Ideally, a suitable technique should

successfully fractionate LLDPE elastomers into simpler molar mass fractions that can then be analysed using advanced analytical techniques, including HT-HPLC, HT-2D-HPLC, HT-SEC, ^{13}C-NMR. Typically, column-based techniques such as HPLC in solvent and temperature gradient mode are excellent alternatives to the crystallization-based fractionation methods.

In contrast to the crystallization-based methods, column-based methods of analysis are sensitive mostly to molar mass differences amongst polymer molecules.[40-42] Therefore, in the case of very high comonomer content LLDPE elastomers, the amorphous nature of these materials does not limit the efficiency of the fractionation, as opposed to p-TREF.

2.4.1. Types of LLDPE

Different grades of LLDPE with specifically designed properties for end-use have been widely produced. LLDPE with SCB incorporation between 20-60 CH_3/100C and densities in the range 0.91-0.94 g/cm^3 have received significant popularity.[2,35,43] This class of LLDPE exhibits large amounts of crystallisable polymer segments and their molecular heterogeneity has been characterized using various methods including p-TREF. Furthermore, these LLDPEs have high melting temperatures between 99 and 108 ˚C, and exhibit broad CCD and MMD. These LLDPEs are typically applicable in production of high impact and stress resistant products.[44,45]

On the other hand, moderate incorporation of SCB in the PE backbone leading to SCB degrees of 30 to 70 CH_3/100C further reduces the density and melting temperature of these materials to about 0.90-0.92 g/cm^3 and 83-102 ˚C, respectively.[46-48] This class of LLDPEs is mainly synthesized using metallocene-catalysts, and exhibit moderate flexibility, crystallinity and melt flow index.[49] These LLDPEs are often referred to as metallocene LLDPE (m-LLDPE).[39,49] In contrast, when SCB branching incorporation exceeds 70 CH_3/100C, the resulting LLDPE has low densities ranging between 0.86-0.90 g/cm^3, and are called ultra-low or very low density polyethylene (U/VLDPE).[49,50]

These materials have high flexibility, stress and impact strength, and thus have very high deformation recovery ability. However, owing to lack of crystallinity as well as high melt flow indexes of this type of LLDPE, not much research attention has been given to this class of LLDPEs, until recently. Therefore, this project focuses mainly on developing adequate analytical methods for the characterization elastomers with very low crystallinities.

2.4.2. Crystallinity of polyethylene

Molecular chain orientation and crystallinity are interrelated.[51] Generally, LLDPE copolymers consist of amorphous and crystalline regions in various degrees/amounts. Amorphous regions result from incomplete chain movement (in the case of a polymer melt) caused by very short cooling rates, and secondly from the structural irregularities that are caused mostly by presence of side chain branching which hinder effective close packing of the macromolecules.[51,52] Figure 2.3 shows a simplified illustration of the arrangement of molecular chain segments in different regions of a semi-crystalline polymer.

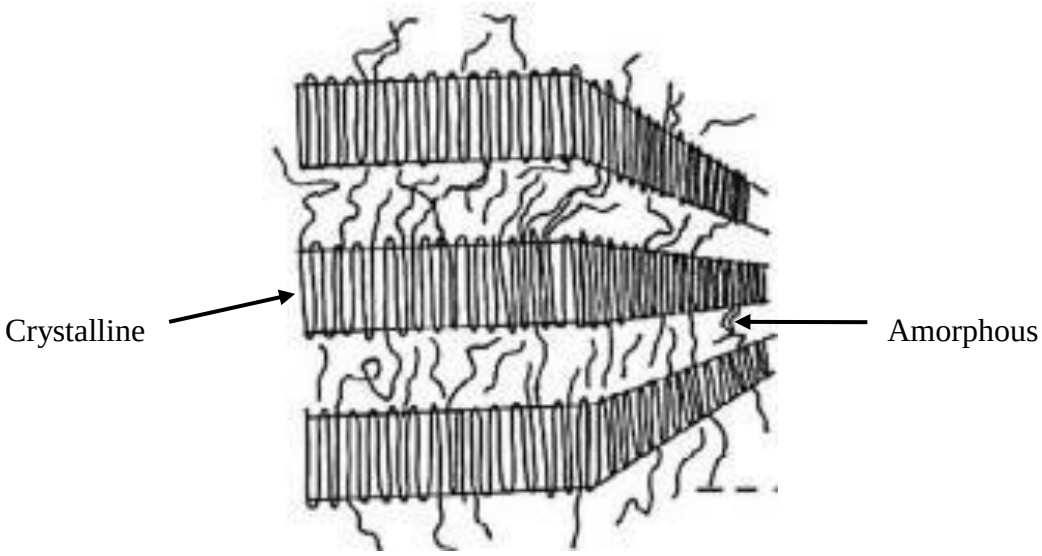

Figure 2.3. Illustration of the packing order of polymer chains in the unit cell structure of semi-crystalline polyethylene.[51]

Crystalline regions are formed by molecules with regular structures at temperatures below the crystallization point provided that sufficient time is allowed for long molecules to assume oriented solid-state arrangements.[52] Likewise, linear molecules such as PE assume a linear zigzag conformation. This allows molecules to easily pack in an orderly fashion, thus forming stronger polymer chain segment interactions.

As a result, this kind of molecular arrangement produces a tight unit cell crystal.[53] However, in poorly ordered molecules the interactive forces are relatively weak, thus less energy is required to effect chain mobility.[51] In total contrast to ordinary small organic molecules which have three phases namely:- solid, liquid and vapour state, polyethylene exhibits more than

twenty transitions that are interrelated to their physical properties.[51] Of course these transitions are relatable to the microstructure of the polymer.

As such, the melting and crystallization behaviour of LLDPE copolymer chains is largely influenced by SCB and SCBD. Thus, herein, the melting and crystallization transitions shall be utilized as means for chemical composition characterization. Furthermore, at sufficiently high temperatures the closely packed crystalline segmental chains gain mobility, which consequently disrupt their crystallinity. At low comonomer contents LLDPEs are semi-crystalline materials and, therefore, contain both molecular chain segments that are arranged in orderly close-packed crystals, and molecular chain segments that are less ordered and amorphous.[52]

The amount of the crystalline and/or amorphous regions is dependent on the amount of comonomer incorporated, since comonomer insertion disrupts the crystallisable sequence length, thereby, decreasing the crystallinity of the polymer.[49,54] Generally, for LLDPE elastomers, the amount of comonomer incorporated into the ethylene backbone is above 10 mol%., thus this class of LLDPEs contain primarily amorphous regions. The behaviour of polymers is better explained thermodynamically, hence in most cases, temperature and the type of solvent are amongst the most important variables that should be carefully controlled.

The chemical composition of LLDPEs is mostly determined using crystallization-based techniques, especially copolymers of semicrystalline LLDPEs, as has been mentioned previously, since the relationship between crystallinity and microstructure is well established.[22,55,56] With this information in mind, both the crystalline and amorphous regions of the polymer can be accessible for analysis.

2.4.3. Elastomers

Polyethylene mechanical properties including elasticity, flow-ability and stress resistance are mainly influence by the MMD and the SCB content and SCBD, as has been mentioned. Thus, PE copolymers vary from plastic to elastomers depending on the SCB content.[57] Typically, LLDPE with significantly high CC incorporation are known as POE.[1,39] This is a relatively new class of polyolefins which possess characteristically more homogeneous molecular structure compared to the regular ZN-based copolymer materials. The elastomeric nature displayed by these materials is a consequent of their narrow CCD and MMD, that is achievable

with metallocene-catalysts, and more recently, through living EO copolymerization. Polyolefin elastomers find large usage as impact modifiers, adhesives and films.[58]

Polyethylene elastomers have been blended with PP as an impact modifier resulting in improved processability.[59] The controllability of the molecular structure of these copolymer is key to their unique interesting properties, as such, various copolymerization conditions have been investigated and different metallocene-based catalytic systems been published over the recent past.[7,60-63] Ethylene-1-octene elastomer with alternative blocks of amorphous and semicrystalline segments has been recently reported.

2.5. Catalyst types

Catalysis is the driving force behind the advancement and innovative development of new polyolefin-based materials.[64,65] Catalytic polymerization has enabled the production of an array of materials ranging from linear HDPE for pipes to LLDPEs for packaging and EPDM copolymers for rubbers.[12] Thus, control of molecular structure properties in polyolefin synthesis, especially in synthesis of ethylene/α-olefin copolymers is of commercial importance to industry. The CCD and MMD of copolymers such as LLDPE are most significantly influenced by the uniformity or lack thereof, of the catalyst active sites.[6,8,10]

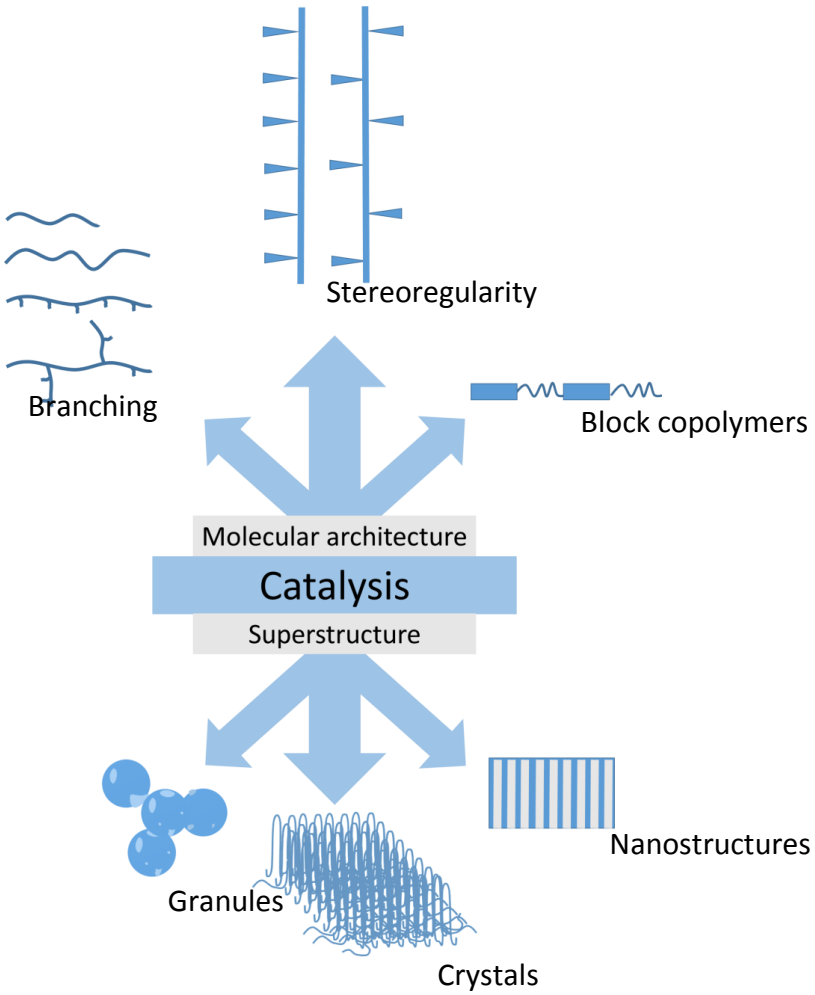

Figure 2.4. Polyolefin catalysis: from microstructure to granules and multiphase polyolefins.

Some of the high-performance polyolefins which were realized through catalysis are beyond the scope of this work (see Fig. 2.4). Several types of catalysts with a variety of properties, including variation in selectivity and performance are used for polyethylene production, in particular. A large array of PE grades with special properties for their intended application are produced mainly by changing a catalyst type or its properties.[10,12] This emphasizes the role that catalysts play in influencing the microstructure properties of polymers. The most widely used catalysts for commercial production of LLDPE include Ziegler-Natta, metallocene and Phillips-type catalysts.

Phillips-type catalysts

Phillips-type catalysts are based on Chromium (IV) that is supported on silica and alumina. The proposed structure, but not necessarily true structure of a Phillips catalyst is shown in Figure 2.5. The active sites are generated by mixing chromium oxide and silicon oxide (CrO_3/SiO_2).[3,49] Herein, the catalytically active sites are generated before the polymerization reaction takes place, thus the Phillips catalyst does not require co-catalysts. Phillips catalysts are not as popular as the ZN-catalysts and m-catalysts but also find a recognizable role in the gas phase and slurry process for PE production.[66] Phillips catalyst-produced PE exhibits characteristic broad MMDs with dispersities ranging between 12-14.[66]

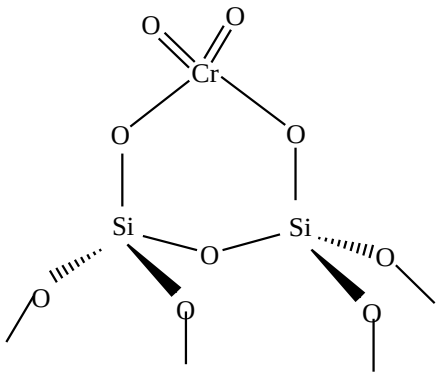

Figure 2.5. Proposed chemical structure of a typical Phillips catalyst.

Ziegler-Natta type catalysts

A Ziegler-Natta catalyst is a heterogeneous inorganic compound which consists, usually, of a $TiCl_4$ metal salt and a main-group co-catalyst.[5] The co-catalyst used for $MgCl_2$ supported catalysts is triethyl aluminium (TEAL), but triisobutyl aluminium (TIBA) is the most preferred co-catalyst type. This high performance catalyst exhibits multiple active sites which are generated by the interaction of the transition metal atoms with the co-catalyst.[4,67,68]

As a result, ZN-catalysts find worldwide usage in the production of polyolefins with broad MMD, a property which is advantageous in polymer processing. The non-uniformity in composition and molar mass of the produced ZN-LLDPE provides excellent flow index and end products with desired impact strength and stress resistance.[1] Another interesting property

of ZN-catalysts is their ability to avoid poisoning from possible oxidative reactions initiated by impurities such as oxygen, sulphur and other electron donors.[1]

Metallocene catalysts

A metallocene (m) catalyst is an organometallic coordination compound with a transition metal centre "sandwiched" by two ligands, such as, but not limited to cyclopentadiene rings thus forming a metal-ligand bond. A typical general chemical formula for a m-catalyst is Cp_2ZrCl_2. The ligand can be substituted by cyclopentadienyl rings that are single bonded to the transition metal centre. Thus, the valence ligand-metal bond is evenly shared by all five carbon atoms of the ligand, as shown Figure 2.6.

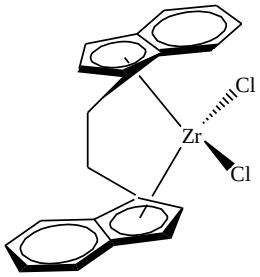

Dichloro[rac-ethylenebis(indenyl)]zirconium(IV)

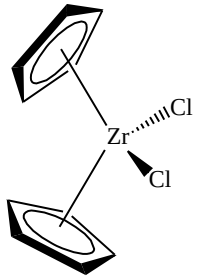

bis(cyclopentadienyl)zirconium(IV)

Figure 2.6. A typical molecular geometry of a metallocene catalyst depicting the ligand position**.**

The selectivity and performance of the m-catalyst is largely influenced by the chemical structure of the ligand, the geometry and its shape. As such, the monomer coordination geometry and insertion mechanism which dictates the orientation of the growing polymer chain during polymerization is influenced by the symmetry of the ligands relative to the catalyst active site.[3,69] The high selectivity of m-catalyst enables excellent control of the polyolefin synthesis towards materials with extraordinarily precise molar mass distributions, end-groups, SCB and LCB, and stereochemistry.[3,65]

LLDPE elastomers with very high melt flow index and narrow molar mass distribution are thus far only achievable with a m-catalyst.[3] However, advances in catalysis still continue to grow and new types of catalysts which are based on modification of the current m-catalyst and ZN-catalysts are beginning to emerge.[10,60,70] This is particularly interesting from a characterization

point of view since through these new catalysts, less complex or more complex polyolefins will be synthesized that require the development of new or more sophisticated analytical characterization techniques.

Some modified catalysts include the recently reported multisite catalysts which enable, for instance, direct comonomer insertion towards high mass molecular chains, instead of the normally favoured low molar masses.[3,12] Recently, ethylene/1-octene block copolymers with alternating flexible amorphous poly(ethylene-co-1-octene) with a low glass transition temperature (T_g) and PE segments with significantly higher melting temperature (T_m) than semicrystalline poly(ethylene-co-1-octene) have been reportedly produced by copolymerization of ethylene and 1-octene using chain shuttling on dual-site catalysts.[12]

More robust catalytic systems that couple different single-site catalysts in a "single" multisite catalyst are potential future catalytic systems towards the realization of a commercial production of "all composite polyolefins".[3,12] Other interesting polyolefin catalysts include tandem catalysis which produce a range of PE materials from stiff engineering plastics to flexible LLDPE packaging films, and thermoplastic elastomers using exclusively ethylene as feedstock. A detailed literature review on multisite catalytic systems for polyolefin production is given by Mülhaupt et al.[12]

2.6. Characterization of polyolefins

It is important to define the microstructure of polyolefins since the molecular characteristics influence the physical and mechanical properties at bulk sample level. Various analytical techniques have been developed over the last seventy years to help understand the microstructure of polyolefins. The characterization of the molecular heterogeneity of polyolefins cannot be fully studied by a single analytical technique. Several analytical techniques which were used in this work are discussed in the sections that follow.

2.6.1. Fourier-transform infrared spectroscopy (FTIR)

Infrared (IR) spectroscopy is a widely known identification technique for functionalized organic compounds. In the field of polyolefins, IR spectroscopy is mostly used to measure the branching content and crystallinity of polyethylene, in particular.[71] Most commonly, IR

spectrometers for analysis consist of five components namely: 1. light source, 2. IR inactive transparent sample holder, 3. monochromator, 4. detector and, 5. recording system (see Figure 2.7).[49] Large molecules such as LLDPE have localized bonds that absorb light at frequencies which are characteristic of the localized bonds present in the molecule.[71] This forms the basis for the analysis of branching in LLDPE. Modern IR spectrometers employ Fourier transformation (FT) which simplifies the interferogram obtained by, most typically, the Michelson interferometer.

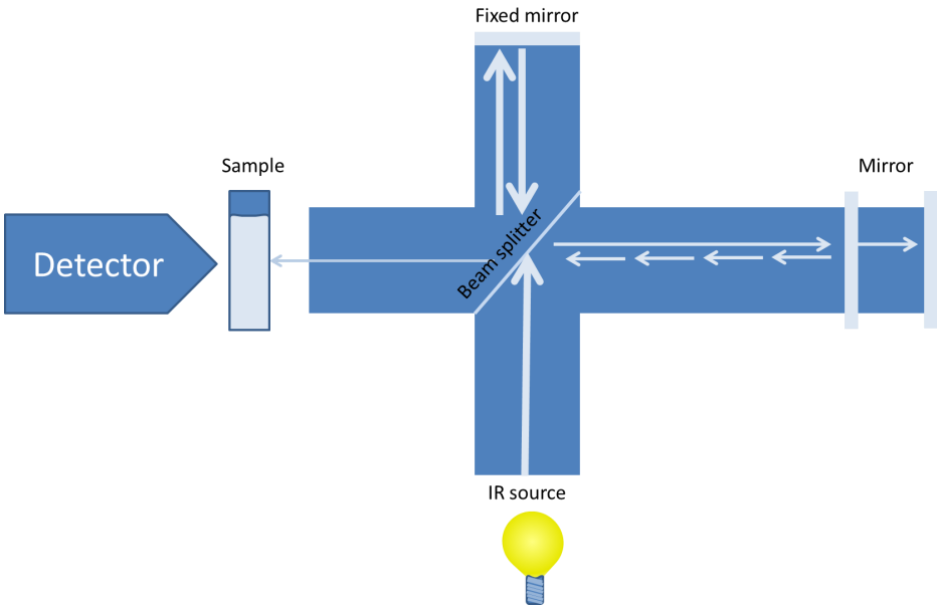

Figure 2.7. Illustration of typical components of FTIR-Michelson interferometer.

In FTIR spectroscopy, the complex frequencies resulting from the localized bonds are converted into a readable frequency domain by the computer using FT.[71,72] Infrared dispersive instruments have also been employed to a limited extent for polymer analysis.[73] Unlike FTIR, dispersive instruments physically split the radiation into its various wavelengths using a monochromator. This technique is rather time consuming, hence FTIR is the preferred choice of the analytical method. The typical IR frequency absorption range for polymers is between 4000-400 cm^{-1}.[71]

Typically, in FTIR analysis the IR radiation is passed through the analyte and the fraction of the absorbed light is measured either as transmittance or absorbance.[27] For instance, C-H stretching bonds have characteristic frequencies in the range between 2880-2900 cm^{-1}.[74-76]

Furthermore, FTIR has the advantage over other compositional analysis methods that sample preparation might not be required.[76] It offers rapid analysis and does not destroy the sample. Moreover, it allows enhancement of the signal-to-noise ratio through programmed signal averaging.[71,76]

LLDPE consists of CH_2 and CH_3 bond types throughout the molecular chain. Since atoms of the LLDPE backbone are less mobile compared to those of the side chains, the vibrational modes of interest for branching analysis of LLDPE are those of side chain branches.[71] Thus, the average comonomer content in LLDPE can be quantified since FTIR is able to detect polymer regions that have varying arrangements of repeat units[73,77].

Cheruthazhekatt et al.[78] conducted a qualitative study on the chemical composition differences of ethylene-propylene copolymer fractions obtained by p-TREF and preparative solution crystallization fractionation (p-SCF) using FTIR spectroscopy. They demonstrated that p-SCF gives more homogenous fractions with less co-crystallization effects. Phiri et al[37]. investigated the chemical composition of p-TREF fractions of ethylene-propylene rubbers using FTIR coupled to HT-HPLC. They concluded that the TREF fractions were indeed fractionated according to their respective ethylene contents. Jorgensen et al.[79] studied the SCB of LLDPE using SEC-FTIR in which FTIR was specifically used for the measurement of methyl contents on molar mass fractions. They concluded that SEC-FTIR provides comprehensive chemical composition information compared to the cross-fractionation technique. In this work FTIR is used to investigate average short chain branching of fractions obtained by p-TREF, p-SCF and p-MMF in comparison to the bulk samples.

2.6.2. Carbon-thirteen nuclear magnetic resonance spectroscopy (^{13}C NMR)

Polymer molecules consist of carbon and hydrogen atoms which have radiofrequency active nuclei. When the nucleus of a carbon or hydrogen atom is exposed to a magnetic field it can, depending on its spin quantum number (I), either split into multiple energy levels or not have any energy level. Thus, atoms that have both even atomic mass and atomic number like ^{12}C possess I=0 and are NMR-inactive, while ^{13}C is NMR active.[80]

In a typical solution NMR analysis, a dissolved sample is placed in a magnetic field and is exposed to a radiofrequency resulting in excitation of its nuclei. The excited nuclei relax at rates that are dictated by the local magnetic environment in the sample.[49] The resulting

frequency from the spin relaxation is recorded by the spectrometer as the time-domain, also known as free induction decay (FID).

This FID is converted to a frequency domain by Fourier transformation (FT). The sensitivity of, particularly, ^{13}C NMR to microstructural differences in a polymer sample makes it suitable for chemical composition analysis of complex polymers.[49] Consequently, for an LLDPE that has 1-octene branching, the second CH_2 from the 1-octene (branch) end is characterized by the resonances at about 33 and 32 ppm, respectively.[20] Therefore, the average SCB content and SBCD for 1-octene incorporated LLDE can be determined by integrating the peak intensity of the signals.[20] Thus, it has been widely used for compositional analysis of LLDPE copolymers.[47,76,81]

However, a limitation of this technique is the longer relaxation time which consequently decreases the life-span of the spins in both the upper and lower energy level thus, resulting in broadening of the resonance lines.[49] Spin-lattice relaxation time (T_1), is the necessary time taken for the difference between the actual spin population and its equilibrium value to be reduced by a factor of an electron charge *e*.[49] In addition, broadening may also result from the anisotropic effect of molecular chain segments with different orientation with respect to the magnetic field, interaction with the neighbouring nuclear spin dipoles and/or broadening due to interactions caused by constant flexing and tumbling of the molecules.[81,82]

However, the broadening effects can be eliminated or at least reduced by techniques such as magic-angle spinning (MAS).[80,83] Herein, a frequency is applied at a particular angle (usually 54.7°) between the spin-spin interactions and the external magnetic field so that good resolution between the resonances is achieved.[49] This technique not only removes the broadening due to spin-spin interaction but, also the broadening due to anisotropic effects.[49] While dipolar decoupling (DD) is a known method employed for eliminating the spin-spin coupling in ^{13}C NMR analysis, cross-polarization (CP) receives much attention. Often, MAS is used together with a CP technique for compositional analysis of polyolefins [84].

Since several pulse sequence scans are required in order to increase resolution, the CP technique advantage is its shorter lattice relaxation time which result in very short analysis time while maintaining the simplicity of the proportionality of the signal of the number of spins at various chemical environments.[49,84]

Hence, MAS is often combined with the CP technique which has shorter T_1 values, and therefore, reduces analysis time. A typical NMR instrument consist of the basic components shown in Figure 2.8.

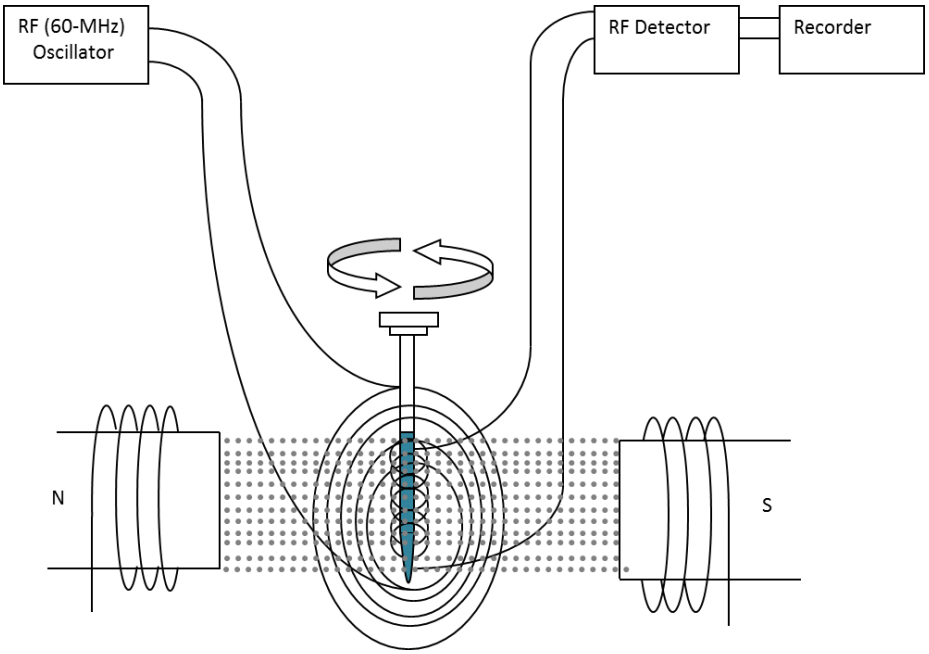

Figure 2.8. Schematic diagram illustrating the general components of an NMR instrument.

Owing to its sensitivity and robustness, ^{13}CNMR is used for the determination of the branching content and the size of branches (to a limited extent) of polymers. Galland et al.[81], studied the chemical composition of LLDPEs produced by homopolymerization of ethylene with [η^3-methallyl-nickel-dad]PF_6 catalyst using ^{13}C-NMR and found that paired methyl-methyl branches form due to high concentration of methyl isolated groups in the polyethylene chain. Furthermore, ^{13}C-NMR has been coupled with HT-SEC and HT-HPLC techniques to comprehensively characterize the microstructure of complex polyolefins.[42,85,86]

2.6.3. Differential scanning calorimetry

For copolymers, crystallizability is dependent on the comonomer content, and forms the basis for the study of chemical composition of polyolefins by crystallization-based techniques such as DSC and CRYSTAF (CRYSTAF is discussed in Section 2.6.4). DSC is widely used for characterization of physical properties of polymer materials including melting, crystallization, and mesomorphic transition temperatures.[87] In this technique, the heat capacity and heat of

transition of polymer samples is thermodynamically correlated to the physical properties (total thermal motion, energy, extent of disorder, and degree of stability) of the material.

Furthermore, its broad dynamic range is important in evaluating the thermal behaviour of semicrystalline materials, since the phase transitions of these materials are dependent mainly on time.[87] In addition to its ability to study kinetics of transitions in a broad dynamic range, DSC is a reliable technique that provides heat capacities at high temperatures. DSC instruments generally have two sample positions, one crucible for the analyte and the second empty crucible is used as a reference. Sometimes an inert material is filled in the second crucible to serve as a reference. In Figure 2.9, a schematic illustration of the two sample positions in a DSC instrument are presented.

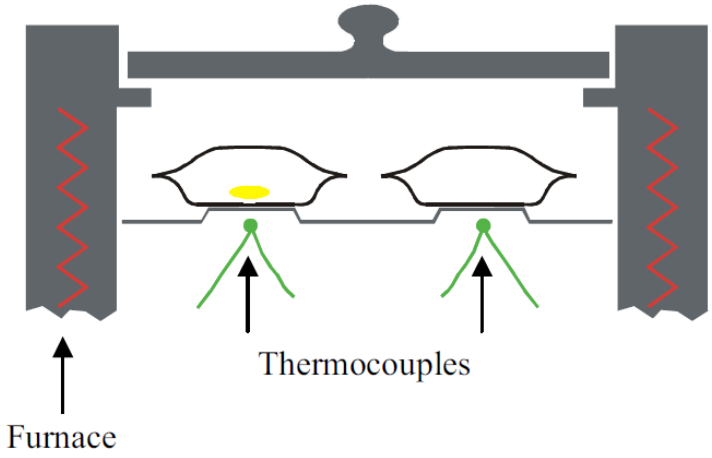

Figure 2.9. Polymer sample placed in a heated pan in a furnace.[88]

The total enthalpy change of the polymer sample at a constant pressure is given by the integral under the DSC peak which is automatically calculated by the system software. Therefore, for DSC measurements, the difference in heat capacity of the sample and the reference is given by:

$$\Delta C_p = C_p(\text{sample}) - C_p(\text{reference}) \qquad (2)$$

For semicrystalline polymers which show multiple melting peaks, the average melting temperature is obtained by drawing the line from the maximum of the peak to the baseline.[87] DSC analysis for polyolefins show two most important phase transitions, including the

exothermic (crystallization) and endothermic (melting) events. These events are influenced by the chemical composition, in particular SCB content in LLDPE copolymers.[11,87]

During the crystallization phase heat is given out while on the melting phase the heat is absorbed, thus, these transitions are said to be exothermic and endothermic, respectively. Schick[87,88] studied the temperature dependence of crystalline, semicrystalline and the liquid amorphous fractions, including the lamellae thickness distributions of polyethylene samples using DSC and found good correlation between results obtained from X-ray analysis.

Furthermore, the chemical composition distribution of LLDPE was successfully studied using a special thermal treatment called successive self-nucleation and annealing (SSA) and concluded that the obtained results were in agreement with data obtained from ^{13}C-NMR analysis of fractions.[11] More recently, several researchers have successfully used DSC for chemical composition analysis of LLDPEs.[28,39,79] In this work, the crystallization and melting behaviour of elastomers will be investigated using DSC to establish the chemical composition of the samples including fractions thereof.

2.6.4. Crystallization analysis fractionation

The CRYSTAF technique was developed in the early 90s by Monrabal.[89] The CRYSTAF technique fractionates polymer molecules in a dilute solution (0.1 – 1.0 mg/mL) as the solution temperature is decreased. For copolymers, crystallizability is dependent on the comonomer content and this dependence forms the basis for the fractionation. Figure 2.10 shows a typical CRYSTAF instrument setup.

The CRYSTAF technique involves dissolving an amount of polymer in a good solvent (typically 1,2,4-trichlorobenzene) in a stirred (200 rpm stirring rate) stainless steel vessel housed in an oven at high temperature. Upon slowly cooling (0.1 – 0.2 °C/min) the polymer solution by sequentially decreasing the oven temperature, polymer molecules form crystals which precipitate out of solution (during crystallization the stirring rate is reduced to about 100 rpm). Consequently, the concentration of the solution decreases. Ideally, the highly crystalline (lowest comonomer content) molecules precipitate first and the low crystalline (highest comonomer content) molecules precipitate last.

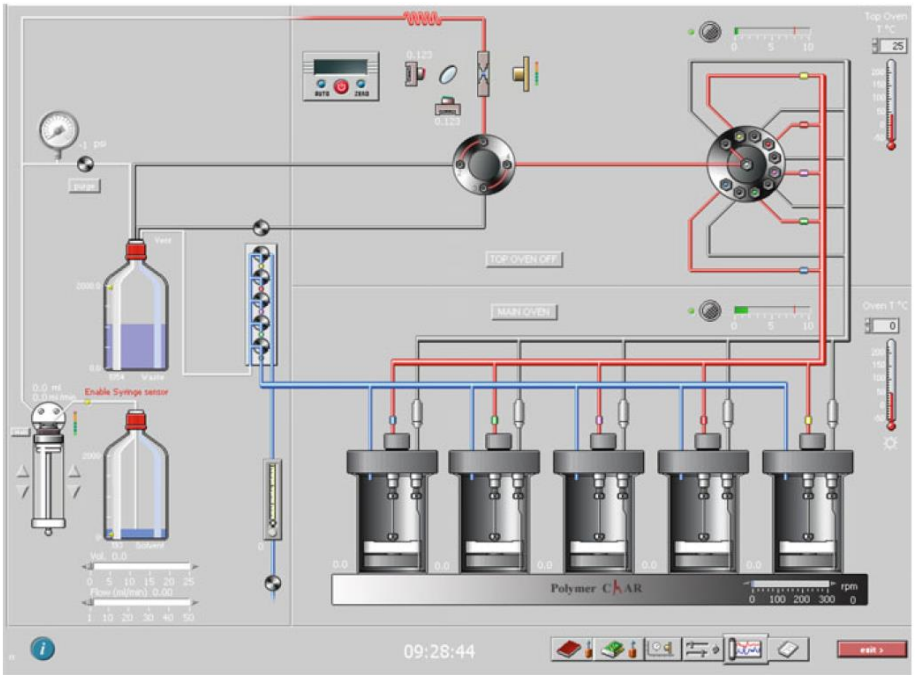

Figure 2.10. Schematic diagram of a CRYSTAF instrument.[90]

The CRYSTAF instrument is equipped with an IR concentration detector operating at high temperature (150 °C) which measures the concentration of the solution as a function of temperature. The experimental conditions of CRYSTAF analysis are obtained by using a calibration curve developed using polyolefins with narrow CCD. Even though CRYSTAF operates based on a similar principle as TREF, it has the advantage that it is faster and involves only two steps (the dissolution and the crystallization step). On the other hand, amongst the known drawbacks of CRYSTAF, co-crystallization is the most prominent.[14,90] However, the success of CRYSTAF in the analysis of complex polyolefins including homogeneous EO copolymers, blends of PE/PP and other ethylene-α-olefin copolymers is well documented in literature.[25,91 92]

2.6.5. Chromatographic techniques

2.6.5.1. High-temperature size exclusion chromatography

SEC, also known as gel permeation chromatography (GPC), is a widely used technique for the molar mass analysis of macromolecules, particularly polyolefins (see a schematic diagram of a typical HT-SEC system in Figure 2.11). A typical SEC column consists of silica or polymer

particles (i.e. cross-linked polystyrene) of uniform pore size, through which the polymer molecules are separated based on their hydrodynamic volumes in solution, rather than their chemical interactions with the stationary phase. Therefore, depending on the type of polymer in question, among other important factors, the choice of stationary phase, particle size and pore size is central to the success of this technique.

The smaller macromolecules are trapped in the particle pores while larger macromolecules flow with the mobile phase, thus largest molar mass molecules elute first and the smallest molar mass fractions elute last. Unlike the classical chromatography techniques, HT-SEC operates at high temperatures above the melting point of polyolefins (110 to 160 °C) so as to prevent molecules from precipitating out of solution.

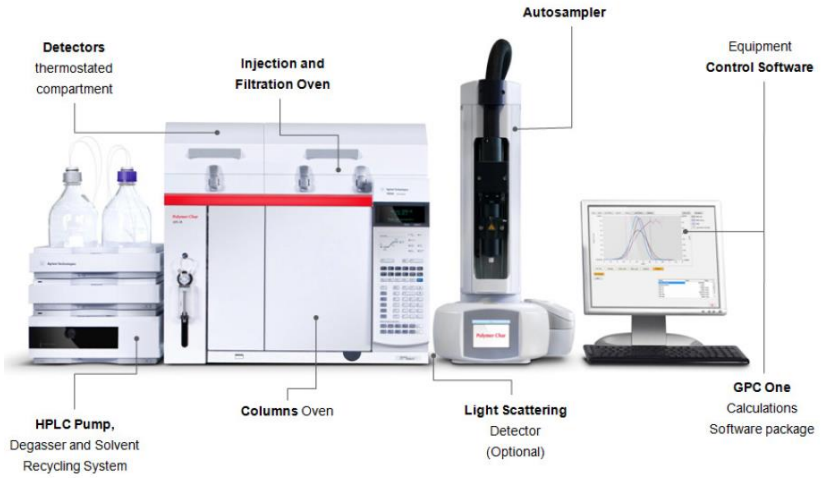

Figure 2.11. An illustrative diagram of a SEC/GPC system equipped with infrared and an optional light scattering detector.[93]

Various detectors have been used with SEC instruments including refractive index, viscometer (Visco), light scattering (LS) and IR. However, depending on the complexity of the sample to be analysed, more than one detector can be coupled to the SEC instrument in order to obtain adequate information pertaining to the molar mass of the material.[27,94] As such, three online detectors (Visco, RI and multiangle laser light scattering (MALLS)) have been used simultaneously in a single SEC system, known as triple detector SEC (3D-SEC), to achieve absolute molar mass information of complex polyolefins.

Polyolefins dissolve only at high temperatures and the sample has to remain in solution throughout the analysis (from sample injection to the detector).Therefore, high boiling point solvents such as 1,2,4-trichlorobenzene (TCB), ortho-dichlorobenzene (ODCB), decalin, methylcyclohexane and other solvents with similar properties are used.[90] Furthermore, polymer chains are susceptible to degradation at high temperatures when exposed to oxygen or under shear stress, which may consequently result in inaccurate molar mass determinations. As a result, butylated hydroxytoluene (BHT) has been widely used as a stabilizer to prevent thermo-oxidative degradation.[95] Herein, HT-SEC will be used to study the molar mass and molar mass distribution of the samples in question.

2.6.5.2. High-temperature high performance liquid chromatography

The analysis of the chemical composition distribution of polyolefins by interactive HPLC at ambient or elevated temperatures was only developed about 50 years after the industrial production of polyolefins. The first initiative to develop HPLC systems suitable for the analysis of polyolefin chemical compositions based only on chemical interaction of polymer chains with the stationary phase rather than on crystallinity were made by Pasch and Macko at the German Institute of Polymers,[96-98] which then gave rise to a new range of applications for known methods.

HT-HPLC separates crystalline and amorphous polymer molecules based on their selective interactions with the stationary phase (usually porous graphite, Hypercarb®). The development of this technique was prompted by findings which were made by Lehtinen and Paukkeri[99] through which they observed that ethylene glycol monobutyl ether (EGMBE) was a good solvent for isotactic PP, but a non-solvent for PE. Macko et al.[100] demonstrated the effect of different solvent polarities on the elution behaviour of PE using silica gel with a covalently bonded layer of oligo(dimethylsiloxane) as stationary phase at elevated temperatures (100 – 150 °C).

The operation of HT-SGIC includes injection of a sample into a porous graphitic carbon (Hypercarb®) stationary phase followed by running a mobile phase solvent gradient with increasing solvent strength. The elution order is dependent on the affinity of the molecules for the stationary phase which is in turn governed by their chemical composition. The elution order is generally from high comonomer content polymer chains (short uninterrupted ethylene

sequences) to low comonomer content (long uninterrupted ethylene sequences) for ethylene copolymers.[78,101,102] Based on the elution volume and peak area obtained from the chromatogram, qualitative and quantitative information is obtained. In this work, HT-HPLC will be employed for the separation according to chemical composition of the elastomers.

2.6.5.3. High-temperature two-dimensional liquid chromatography

HT-2D-LC is achieved by coupling HT-HPLC to HT-SEC. The combination of different chromatographic techniques to improve analysis is not a new phenomenon. However, separation of complex polymers using HT-2D-LC was only introduced for the first time in 2010.[103] Figure 2.12 shows the diagram of a typical 2D-LC separation setup. In 2D-LC the polymer chains are separated based on their selective interaction with the carbon-based stationary phase, Hypercarb®, using a solvent gradient as described above (starting with a non-solvent, such as 1-decanol and increasing the percentage of the good solvent in the mixture, e.g. TCB).

In 2D-LC, the first dimension separates polymer chains based on their chemical composition and the second dimension according to molar mass. This ability to simultaneously provide information about the chemical composition and the molar mass of the polymer chains that are being analyzed makes 2D-LC the most powerful technique for analysis of complex polyolefins.[14,104,105]

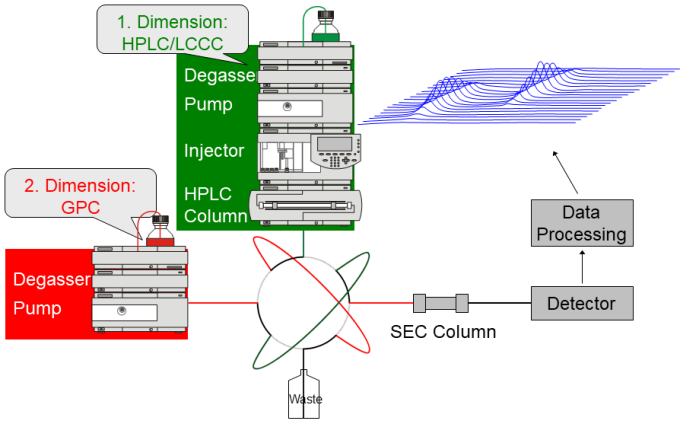

Figure 2.12. Schematic representation of a 2D-LC instrument.[14]

The outcome is the separation according to both chemical composition and molar mass to yield contour plots as shown in Figure 2.13. HT-2D-LC is especially excellent for separation of complex polyolefins and elastomeric polymers that have multiple distributions that are interdependent. TGIC is developed by replacing the solvent gradient in SGIC with a thermal gradient using an isocratic mobile phase. TGIC and SGIC have been successfully employed to study the chemical composition distribution and microstructure of ethylene-1-octene copolymers, ethylene-propylene copolymers, and high impact polypropylene as well as other complex polyolefins.[106-108]

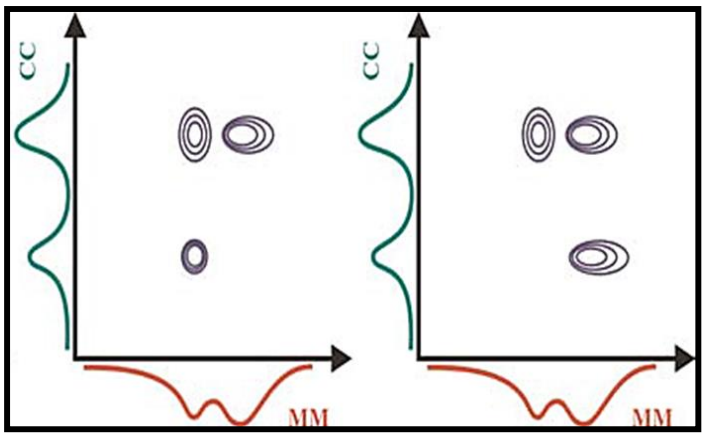

Figure 2.13. Schematic 2D contour plots illustrating 2D-LC separations.

2.7. Preparative fractionation

Generally, the separation of polymer molecules requires comprehensive knowledge of their chemical and physical properties and behaviour thereof in different media. Conventional separation methods used for separation of small molecules are often inadequate for polymer molecules, especially polyolefins. Polymer molecules which constitute only carbon and hydrogen atoms require separation mechanisms which are sensitive to molecular properties such as architecture, topology and functionality, to name a few. Therefore, from literature it is known that variables such as temperature and solvents have a certain influence on the behaviour of polymer chains.[49,58,109]

Depending on the intramolecular and intermolecular structure differences of molecular chains, some chains will behave in a particular manner in a particular solvent system or at certain temperature. The solubility of a polymer molecule in a particular solvent can be well explained thermodynamically by the Flory-Huggins theory using Gibbs-Helmholtz equation as shown in equation 3:

$$\Delta G_m = \Delta H_m - T\Delta S_m \qquad (3)$$

where ΔS_m is the change of entropy upon mixing and decreases with increasing polymer molar mass. ΔH_m is the change of enthalpy upon mixing and is directly proportional to the square root of the difference between the solubility parameter of the solvent (δ_s) and polymer (δ_p).

The fractionation methods employed in this work including p-TREF, p-SCF and p-MMF are based on the Flory-Huggins theory.

2.7.1. Preparative temperature rising elution fractionation (p-TREF)

Figure 2.14 shows a typical p-TREF instrument which is used to perform fractionation of polyolefin samples into separate polyolefin fractions according to their crystallizability. The TREF technique is one of the oldest techniques for polyolefin fractionation and is still the most important technique for the fractionation of semicrystalline copolymers.[28,29,110] The first step includes dissolving the polymer sample in a suitable good solvent, such as xylene, at high temperature (130 – 140 °C), and allowing time (minimum of 2 hours) for a complete dissolution of the sample. Thereafter, an inert support (e.g. sea sand) which has been preheated to 140 °C is transferred into the polymer solution. The reactor with its contents is then placed in an oil bath to cool down at a programmed cooling rate (1 – 2°C/hour), thus facilitating a controlled crystallization process.[90]

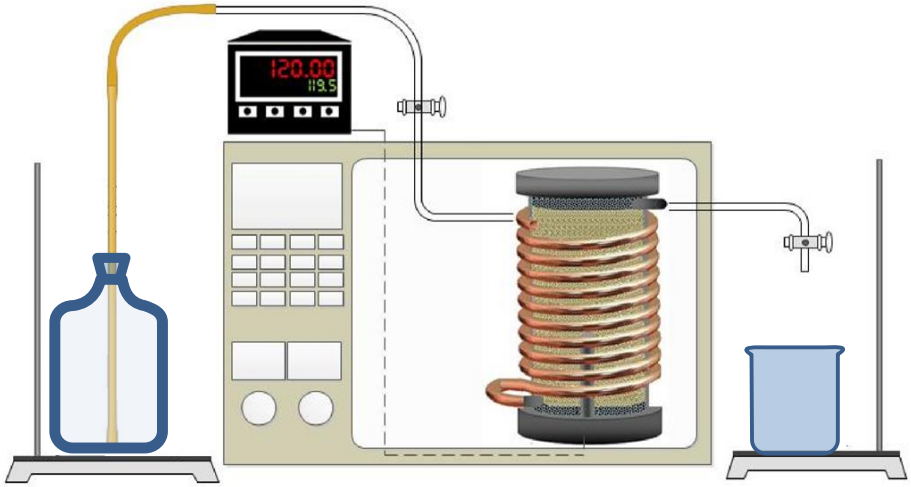

Figure 2.14. Preparative TREF setup during the elution step.[30]

As the temperature decreases, the polymer chains in solution adsorb onto the sand particles as they crystallize and form polymer layers, with the most crystalline polymer chains forming the inner layer, the least crystalline forming the outer layer and non-crystalline chains remain in solution. Then lastly, the sample is transferred into a TREF column, which has a solvent supplier, an oven with programmable temperature, and a sample collector (shown in Figure 2.14). The elution includes pumping the good solvent (xylene) into the column and increasing the temperature of the column in a predetermined temperature sequence. The fractions are then collected at each temperature and prepared for further analyses.

2.7.2. Preparative solution crystallization fractionation (p-SCF)

The preparative solution crystallization fractionation (p-SCF) method was developed by Cheruthazhekatt et al.[111] as an alternative preparative fractionation method to the solvent and time consuming TREF. Similar to p-TREF, the fractionation mechanism is based mainly on crystallizability of molecular chains. However, in p-SCF crystallization occurs in the absence of an inert support (sand).

The solution crystallization fractionation method involves dissolving the polymer in a suitable solvent at high temperatures (130-150 °C). Upon decreasing the temperature of the polymer solution stepwise, the molecules crystallize and are collected at each temperature. The most

crystalline molecules precipitate out of solution as the temperature decreases. p-SCF is a faster fractionation technique that consumes less solvent as compared to p-TREF. Moreover, it was shown that p-SCF has a better sensitivity to chemical composition and can fractionate copolymers with very low crystallizability.[112]

Moreover, Cheruthazhekatt et al.[111] demonstrated that p-SCF can fractionate molecules in a broad range of crystallinities, from amorphous to highly crystalline material. When p-SCF is combined with DSC, CRYSTAF, ^{13}CNMR and HT-SGIC a comprehensive chemical composition of complex copolymers is achievable.[111] This makes p-SCF a potential fractionation method for the microstructure characterization of the LLDPE elastomers in question.

2.7.3. Preparative molar mass fractionation (p-MMF)

Fractionation by molar mass is a well-documented technique. This technique thrives on the fact that the solubility of polymer molecules is dependent on their molar mass, thus in preparative molar mass fractionation (p-MMF) method the mode of fractionation is controlled to discriminate molecular chains of different molar masses based primarily on their solubility in a particular solvent system. Figure 2.15 shows a typical p-MMF experimental setup. Preparative-MMF involves dissolving a polymer sample in a good solvent at high temperatures. Reactor temperature between 130-150°C is achieved by heating silica oil using an oil circulating device that has a temperature control. The heated silicon oil circulates from the oil circulating device to the reactor as depicted in Figure 2.15. The temperature is kept constant by the circulating silicon oil that jackets the reactor inner layer contains the dissolved polymer.

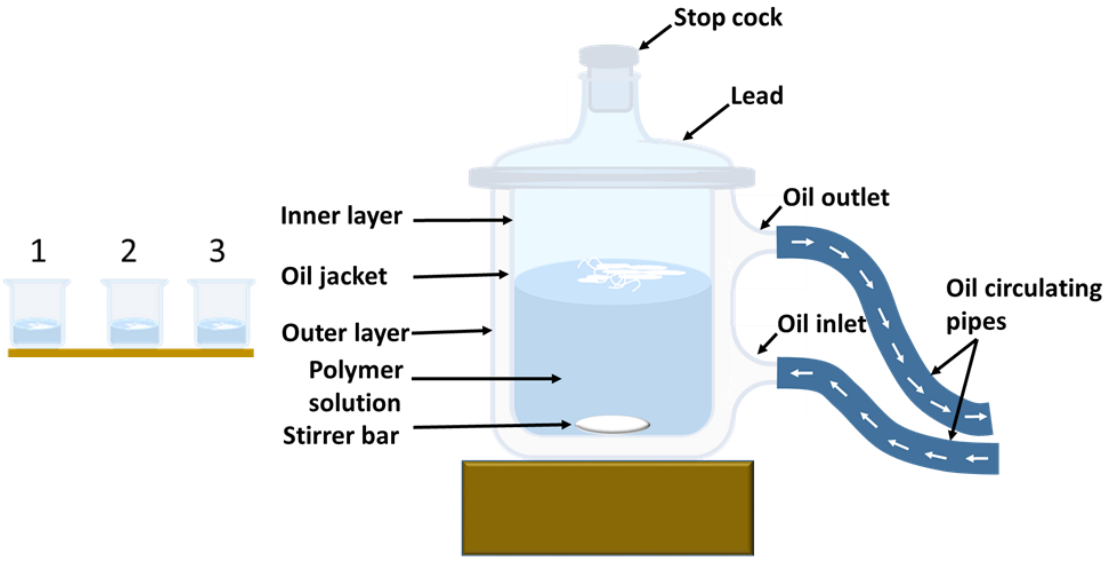

Figure 2.15. Typical setup of a p-MMF experiment.

The optimum temperature for fractionation is the minimum temperature at which the sample completely dissolves (good solvent/non-solvent).[113] After the polymer has completely dissolved, aliquots of a non-solvent are added into the polymer solution until the polymer precipitates out of solution. The precipitated polymer is isolated from the polymer solution and forms the first fraction. More non-solvent is added until the polymer precipitates out of solution again to form the second fraction. This process is repeated until all the polymer has precipitated out of solution.

The non-precipitated polymer is collected as the "soluble fraction". The high molar mass molecules (least soluble) precipitate first at minimal non-solvent amounts, while lowest molar mass material precipitate at large amounts of non-solvent. This is an excellent fractionation method for low crystalline materials since the success of the fractionation is independent of the crystallinity or chemical composition of the molecules. Furthermore, adequate amounts of homogenous fractions with narrow molar mass distributions are obtained in a single experiment and can be further analysed using various characterization techniques available to provide meaningful MMD and CCD correlation.

2.8. References

1. Sauter, D. W.; Taoufik, M.; Boisson, C. Polymers 2017, 9, 185.
2. Alt, H. G.; Köppl, A. Chem. Rev. 2000, 100, 1205–1221.
3. Spalding, M. A.; Chatterjee, A. Handbook of Industrial Polyethylene and Technology: Definitive Guide to Manufacturing, Properties, Processing, Applications and Markets Set; John Wiley & Sons: New York, 2017.
4. Kaminsky, W. Catal. Today 1994, 20, 257–271.
5. Kaminsky, W. In MMI Press Symposium Series (Michigan Molecular Institute), Quirk, R. P., Ed.; Harwood academic publishers, 1983, pp 225–244.
6. Kaminsky, W.; Laban, A. Appl. Catal., A 2001, 222, 47–61.
7. Chum, P. S.; Swogger, K. W. Prog. Polym. Sci. 2008, 33, 797–819.
8. Kaminsky, W. Catal. Today 2000, 62, 23–34.
9. Askeland, D.; Fulay, P. The Science & Engineering of Materials; Cengage Learning: United States, 2005.
10. Bazvand, R.; Bahri-Laleh, N.; Nekoomanesh, M.; Abedini, H.; Hanifpour, A. Communications In Catalysis 2018, 1, 1–10.
11. Balbontin, G.; Camurati, I.; Dall'Occo, T.; Finotti, A.; Franzese, R.; Vecellio, G. Angew. Makromol. Chem. 1994, 219, 139–160.
12. Sturzel, M.; Mihan, S.; Mulhaupt, R. Chem. Rev. 2016, 116, 1398–1433.
13. Shamiri, A.; Chakrabarti, M. H.; Jahan, S.; Hussain, M. A.; Kaminsky, W.; Aravind, P. V.; Yehye, W. A. Materials 2014, 7, 5069–5108.
14. Pasch, H.; Malik, M. I. Advanced separation techniques for polyolefins; Springer: New York, 2014.
15. Malpass, D. B. Handbook to Industrial Polyethylene; John Wiley & Sons: New Jersey, 2012, p 59–133.
16. Hsieh, E. T.; Randall, J. C. Macromolecules 1982, 15, 1402–1406.
17. Chien, J. C.; He, D. J. Polym. Sci., Part A: Polym. Chem. 1991, 29, 1603–1607.
18. Gupta, P.; Wilkes, G. L.; Sukhadia, A. M.; Krishnaswamy, R. K.; Lamborn, M. J.; Wharry, S. M.; Tso, C. C.; DesLauriers, P. J.; Mansfield, T.; Beyer, F. L. Polymer 2005, 46, 8819–8837.

19. De Pooter, M.; Smith, P.; Dohrer, K.; Bennett, K.; Meadows, M.; Smith, C.; Schouwenaars, H.; Geerards, R. J. Appl. Polym. Sci. 1991, 42, 399–408.

20. Usami, T.; Gotoh, Y.; Takayama, S. Macromolecules 1986, 19, 2722–2726.

21. Adisson, E.; Ribeiro, M.; Deffieux, A.; Fontanille, M. Polymer 1992, 33, 4337–4342.

22. Hosoda, S. Polym. J. 1988, 20, 383–397.

23. Balbontin, G.; Camurati, I.; Dall'Occo, T.; Zeigler, R. C. J. Mol. Catal. A: Chem. 1995, 98, 123–133.

24. Anantawaraskul, S.; Soares, J. B. P.; Wood-Adams, P. M.; Monrabal, B. Polymer 2003, 44, 2393–2401.

25. Albrecht, A.; Brüll, R.; Macko, T.; Sinha, P.; Pasch, H. Macromol. Chem. Phys. 2008, 209, 1909–1919.

26. De Goede, E.; Mallon, P.; Pasch, H. Macromol. Mater. Eng. 2010, 295, 366–373.

27. Pasch, H. Polym. Chem. 2013, 4, 2628–2650.

28. Ndiripo, A.; Joubert, D.; Pasch, H. J. Polym. Sci., Part A: Polym. Chem. 2016, 54, 962–975.

29. Cheruthazhekatt, S.; Pijpers, T. F. J.; Mathot, V. B. F.; Pasch, H. Macromol. Symp. 2013, 330, 22–29.

30. Monrabal, B.; Sancho-Tello, J.; Mayo, N.; Romero, L. Macromol. Symp. 2007, 257, 71–79.

31. Anantawaraskul, S.; Soares, J. B. P.; Wood-Adams, P. M. J. Polym. Sci., Part B: Polym. Phys. 2003, 41, 1762–1778.

32. Cheruthazhekatt, S.; Pijpers, T. F. J.; Harding, G. W.; Mathot, V. B. F.; Pasch, H. Macromolecules 2012, 45, 2025–2034.

33. Tso, C. C.; DesLauriers, P. J. Polymer 2004, 45, 2657–2663.

34. Ndiripo, A. Comparative study on the molecular structure of ethylene/1-octene, ethylene/1-heptene and ethylene/1-pentene copolymers using advanced analytical methods. MSc thesis, Stellenbosch University, South Africa, 2015.

35. Zhang, M.; Lynch, D. T.; Wanke, S. E. J. Appl. Polym. Sci. 2000, 75, 960–967.

36. Zhou, X.; Hay, J. N. Eur. Polym. J. 1993, 29, 291–300.

37. Phiri, M. J.; Cheruthazhekatt, S.; Dimeska, A.; Pasch, H. J. Polym. Sci., Part A: Polym. Chem. 2015, 53, 863–874.

38. Gabriel, C.; Lilge, D. Polymer 2001, 42, 297–303.

39. Liu, W.; Zhang, X.; Bu, Z.; Wang, W.-J.; Fan, H.; Li, B.-G.; Zhu, S. Polymer 2015, 72, 118–124.

40. Bungu, P. E.; Pasch, H. Polym. Chem. 2018, 9, 1116–1131.

41. Maiko, K.; Pasch, H. Macromol. Rapid Commun. 2015, 36, 2137–2142.

42. Pasch, H.; Heinz, L. C.; Macko, T.; Hiller, W. Pure Appl. Chem. 2008, 80, 1747–1762.

43. Garoff, T.; Mannonen, L.; Väänänen, M.; Eriksson, V.; Kallio, K.; Waldvogel, P. J. Appl. Polym. Sci. 2010, 115, 826–836.

44. Sukhadia, A. M.; Krishnaswamy, R. K.; Welch, M. B.; Palackal, S. J. In TAPPI - Polymers, Laminations and Coatings Conference, 2000, pp 825–832.

45. Joubert, D. Macromol. Symp. 2002, 178, 69–80.

46. Al-Malaika, S.; Peng, X.; Watson, H. Polym. Degrad. Stab. 2006, 91, 3131–3148.

47. Luruli, N.; Heinz, L. C.; Grumel, V.; Brüll, R.; Pasch, H.; Raubenheimer, H. G. Polymer 2006, 47, 56–66.

48. Hindryckx, F.; Dubois, P.; Jérome, R.; Garcia Marti, M. Polymer 1998, 39, 621–629.

49. Rodriguez, F.; Cohen, C.; Ober, C. K.; Archer, L. Principles of polymer systems; CRC Press: United States of America, 2014.

50. Razavi-Nouri, M. Polym. Test. 2006, 25, 1052–1058.

51. Ward, I. M.; Sweeney, J. An introduction to the mechanical properties of solid polymers; John Wiley & Sons, 2004.

52. Sperling, L. Introduction to physical polymer science, 1992, 4th Edition ed.; John Wiley & Sons: New Jersey, 2005, p 880.

53. Pasch, H.; Trathnigg, B. HPLC of Polymers; Springer Science & Business Media: Berlin, 1999.

54. Mirabella, F. M.; Bafna, A. J. Polym. Sci., Part B: Polym. Phys. 2002, 40, 1637–1643.

55. Cady, L. Plast. Eng. 1987, 43, 25–27.

56. Sarzotti, D. M.; Soares, J. B. P.; Simon, L. C.; Britto, L. J. D. Polymer 2004, 45, 4787–4799.

57. Bensason, S.; Minick, J.; Moet, A.; Chum, S.; Hiltner, A.; Baer, E. J. Polym. Sci., Part B: Polym. Phys. 1996, 34, 1301–1315.

58. Xu, J.; Feng, L. Eur. Polym. J. 2000, 36, 867–878.

59. Da Silva, A. L. N.; Tavares, M. I. B.; Politano, D. P.; Coutinho, F. M.; Rocha, M. C. J. Appl. Polym. Sci. 1997, 66, 2005–2014.

60. Zhang, K.; Liu, P.; Wang, W.-J.; Li, B.-G.; Liu, W.; Zhu, S. Macromolecules 2018, 51, 8790–8799.

61. Liu, W.; Wang, W.-J.; Fan, H.; Yu, L.; Li, B.-G.; Zhu, S. Eur. Polym. J. 2014, 54, 160–171.

62. Ribeiro, R.; Ruivo, R.; Nsiri, H.; Norsic, S. b.; D'Agosto, F.; Perrin, L.; Boisson, C. ACS Catal. 2016, 6, 851–860.

63. Leone, G.; Mauri, M.; Pierro, I.; Ricci, G.; Canetti, M.; Bertini, F. Polymer 2016, 100, 37–44.

64. Boor, J. Ind. Eng. Chem. Res. 1970, 9, 437–456.

65. Brintzinger, H. H.; Fischer, D.; Mülhaupt, R.; Rieger, B.; Waymouth, R. M. Angew. Chem. Int. Ed. 1995, 34, 1143–1170.

66. McDaniel, M. P. Adv. Catal. 2010, 53, 123–606.

67. Helfferich, F. G. In Comprehensive Chemical Kinetics, Helfferich, F. G., Ed.; Elsevier: The Netherlands, 2001, pp 299–354.

68. Sinn, H.; Kaminsky, W. In Advances in Organometallic Chemistry, Stone, F. G. A.; West, R., Eds.; Academic Press, 1980, pp 99–149.

69. Quijada, R.; Dupont, J.; Miranda, M. S. L.; Scipioni, R. B.; Galland, G. B. Macromol. Chem. Phys. 1995, 196, 3991–4000.

70. Zhang, J.; Li, B.-G.; Fan, H.; Zhu, S. J. Polym. Sci., Part A: Polym. Chem. 2007, 45, 3562–3569.

71. Gulmine, J. V.; Janissek, P. R.; Heise, H. M.; Akcelrud, L. Polym. Test. 2002, 21, 557–563.

72. Marengo, E.; Longo, V.; Robotti, E.; Bobba, M.; Gosetti, F.; Zerbinati, O.; Di Martino, S. J. Appl. Polym. Sci. 2008, 109, 3975–3982.

73. Bower, D. I. An introduction to polymer physics; Cambridge University Press: United States of America, 2002, p 425.

74. Graef, S. M.; Brüll, R.; Pasch, H.; Wahner, U. M. e-Polymers 2003, 3, 51–59.

75. Gulmine, J. V.; Akcelrud, L. Polym. Test. 2006, 25, 932–942.

76. Su, Z.; Zhao, Y.; Xu, Y.; Zhang, X.; Zhu, S.; Wang, D.; Han, C. C.; Xu, D. Polymer 2004, 45, 3577–3581.

77. DesLauriers, P. J.; Rohlfing, D. C.; Hsieh, E. T. Polymer 2002, 43, 159–170.

78. Cheruthazhekatt, S.; Mayo, N.; Monrabal, B.; Pasch, H. Macromol. Chem. Phys. 2013, 214, 2165–2171.

79. Jørgensen, J. K.; Larsen, A.; Helland, I. e-Polymers 2010, 10, 1596–1612.

80. Ortin, A.; Monrabal, B.; Sancho-Tello, J. Macromol. Symp. 2007, 257, 13–28.

81. Galland, G. B.; de Souza, R. F.; Mauler, R. S.; Nunes, F. F. Macromolecules 1999, 32, 1620–1625.

82. Randall, J. C. J. Polym. Sci., Part B: Polym. Phys. 1973, 11, 275–287.

83. Randall, J. C. Macromolecules 1978, 11, 592–597.

84. Klimke, K.; Parkinson, M.; Piel, C.; Kaminsky, W.; Spiess, H. W.; Wilhelm, M. Macromol. Chem. Phys. 2006, 207, 382–395.

85. Hiller, W.; Sinha, P.; Hehn, M.; Pasch, H. Prog. Polym. Sci. 2014, 39, 979–1016.

86. Hehn, M.; Maiko, K.; Pasch, H.; Hiller, W. Macromolecules 2013, 46, 7678–7686.

87. Schick, C. In Polymer Science: A Comprehensive Reference, Möller, K. M., Ed.; Elsevier: Amsterdam, 2012, pp 793–823.

88. Schick, C. Anal. Bioanal.Chem. 2009, 395, 1589–1611.

89. Monrabal, B. Journal of Applied Polymer Science 1994, 52, 491–499.

90. Pasch, H.; Malik, M. I.; Macko, T. In Polymer Composites–Polyolefin Fractionation–Polymeric Peptidomimetics–Collagens; Springer: New York, 2013, pp 77–140.

91. Cheruthazhekatt, S.; Mayo, N.; Monrabal, B.; Pasch, H. Macromol. Chem. Phys. 2013, 214, 2165–2171.

92. Brüll, R.; Grumel, V.; Pasch, H.; Raubenheimer, H. G.; Sanderson, R.; Wahner, U. M. In Macromol. Symp.; Wiley Online Library, 2002, pp 81–92.

93. Monrabal, B.; Sancho-Tello, J.; Montesinos, J.; Tarín, R.; Ortín, A.; del Hierro, P.; Bas, M. In The applications book, Europe, L., Ed.; LCGC Europe: Chester, 2012.

94. Boborodea, A.; Collignon, F.; Brookes, A. Int. J. Polym. Anal. Charact. 2015, 20, 316–322.

95. Heinz, L. C.; Macko, T.; Pasch, H.; Weiser, M. S.; Mülhaupt, R. Int. J. Polym. Anal. Charact. 2006, 11, 47–55.

96. Macko, T.; Denayer, J. F.; Pasch, H.; Baron, G. V. J. Sep. Sci. 2003, 26, 1569–1574.

97. Macko, T.; Pasch, H.; Denayer, J. F. J. Chromatogr. A 2003, 1002, 55–62.

98. Macko, T.; Pasch, H.; Denayer, J. F. J. Sep. Sci. 2005, 28, 59–64.

99. Lehtinen, A.; Paukkeri, R. Macromol. Chem. Phys. 1994, 195, 1539–1556.

100. Macko, T.; Pasch, H.; Kazakevich, Y. V.; Fadeev, A. Y. J. Chromatogr. A 2003, 988, 69–76.

101. Mekap, D.; Macko, T.; Brull, R.; Cong, R.; deGroot, A. W.; Parrott, A.; Cools, P. J. C. H.; Yau, W. Polymer 2013, 54, 5518–5524.

102. Cheruthazhekatt, S.; Pasch, H. Macromol. Symp. 2014, 337, 51–57.

103. Ginzburg, A.; Macko, T.; Dolle, V.; Brüll, R. J. Chromatogr. A 2010, 1217, 6867–6874.

104. Ginzburg, A.; Macko, T.; Dolle, V.; Brüll, R. Eur. Polym. J. 2011, 47, 319–329.

105. Cheruthazhekatt, S.; Harding, G. W.; Pasch, H. J. Chromatogr. A 2013, 1286, 69–82.

106. Al-Khazaal, A. Z.; Soares, J. B. P. Macromol. Chem. Phys. 2017, 218, 1600332.

107. Ndiripo, A.; Pasch, H. Anal. Chem. 2018, 90, 7626–7634.

108. Phiri, M. J.; Dimeska, A.; Pasch, H. Macromol. Chem. Phys. 2015, 216, 1619–1628.

109. Soares, J. B. P.; Hamielec, A. E. Polymer 1995, 36, 1639–1654.

110. da Silva Filho, A. A.; dal Pizzol, M. F.; de Galland, G. B.; Soares, J. B. P. In Brazilian congress on polymers: Brazil, 1999.

111. Cheruthazhekatt, S.; Pasch, H. Anal. Bioanal.Chem. 2014, 406, 2999–3007.

112. Cheruthazhekatt, S.; Robertson, D. D.; Brand, M.; van Reenen, A.; Pasch, H. Anal. Chem. 2013, 85, 7019–7023.

113. Fan, Y.; Xue, Y.; Nie, W.; Xiangling, J.; Bo, S. Polym. J. 2009, 41, 622–628.

Chapter 3

Methodologies

This chapter provides detailed information on the instrumentation, samples and procedures used in the present work. The employed procedures were adopted from literature, and modified.[1,2 3]

3.1. Material and reagents

The supplier of Lucene LC 160 (abbreviated as LC 160) is LG Chem (PTY) LTD. Samples 1-4 were supplied by Borealis, and the commercial samples including ENGAGE 8100 and ENGAGE 8842 were obtained from Dow Chemical, and Tafmer H-30503 (abbreviated as Tafmer) was obtained from Mitsui Chemicals. The comonomer type and comonomer contents of all the samples are provided in the following chapters.

Solvents

Diethylene glycol methyl ether (DEGME) (99 %), Xylene (99%), 1,2,4-trichlorobenzene (≥ 99 %) and 1-decnaol were obtained from Sigma Aldrich and used as received. However, for the crystallization analysis fractionation (CRYSTAF) and high temperature-size exclusion chromatography (HT-SEC) experiments TCB reagent plus ® obtained from Sigma Aldrich was used. 1-decanol and TCB (≥ 99 %) were used as the primary mobile phase and the mobile phase in HT-HPLC, respectively.

3.2. Fourier-transform infrared spectroscopy

A Thermo Nicolet iS10 Spectrometer (Thermo Scientific, Waltham, MA) Fourier transform IR spectrometer employing an attenuated total reflectance (ATR) with a diamond crystal was used to determine the chemical composition of elastomer samples. The spectrometer was calibrated using narrowly distributed LLDPE samples with known comonomer contents in the range of 0.55 – 14.05 mol.%. The sample absorption spectra were measured at wavenumbers between

4000 to 650 cm^{-1}. The sample preparation method is similar to that employed by Soares et al.[3] FTIR measurements were done using 64 scans at a resolution of 8 cm^{-1}. A background scan was taken before each sample measurement. Thermo Scientific OMNIC software was used recording the data.

3.3. Size exclusion chromatography

A PL-GPC 220 high temperature chromatograph (Polymer Laboratories, now Agilent, Church Stretton, UK) was used to measure the molar mass and molar mass dispersity of the samples using differential refractive index as the detector. TCB with 0.025 w/v % butylated hydroxytoluene (BHT) as a stabilizer was used to dissolve the polymer samples. TCB with 0.0125 % w/v BHT was used as the mobile phase and its flow rate was set to 1 $mLmin^{-1}$. Three 300 × 7.5 mm^2 PLgel Olexis columns (Agilent Technologies, UK) were used together with a 50 × 7.5 mm^2 PLgel Olexis guard column, and 200 μL of each sample was injected. All experiments in HT-SEC were conducted at 150 °C. Narrowly distributed polystyrene (Agilent Technology, UK) was used as the standard for the instrument calibration.

3.4. Differential scanning calorimetry

TA Instruments Q100 DSC system calibrated with indium metal standard was used to investigate the thermal properties of the samples. The standard procedure was employed for the calibration step, and the same experimental conditions were used for measuring the melting and crystallization temperatures. These experimental conditions include a heating and cooling at a scanning rate of 10 °C/min between -50 and 150 °C temperature range. The samples were subjected to three temperature cycles, including first heating to remove the sample thermal history, first cooling to get crystallization and, second heating to get melting. All the crystallization and melting temperatures recorded were taken during the cooling cycle and the second heating cycle, respectively. After each cycle, the temperature was kept isothermally for 2 min. Nitrogen was used as a purge gas with a 50 mL/min flow rate.

3.5. Crystallization analysis fractionation

CRYSTAF experiments were conducted using a commercial CRYSTAF instrument (model 200 Polymer Char S.A, Valencia, Spain). Approximately 20 mg of each sample was dissolved in 35 mL of TCB. The crystallization fractionation analysis was conducted by simultaneously dissolving about 35 mg polymer sample in TCB in five stainless steel reactors equipped with automatic stirring and filtration devices. The dissolution time and temperature were 90 to150 minutes and 160 °C, respectively. After dissolution, the polymer solution temperature was decreased to 100 °C and kept for 1 hour to stabilize before it was slowly decreased again to 30 °C at a cooling rate of 0.1 °C/min. The concentration of the solution was determined automatically using an infrared detector operating at a fixed wavelength of 3.5 μm.

3.6. High-temperature high performance liquid chromatography

HT-SGIC made by Polymer Char (Valencia, Spain) was used as part of the high temperature chromatographic experiments. A high-pressure binary gradient pump (Agilent, Waldbronn, Germany) was utilized for solvent gradient elution in HPLC. The evaporative light scattering detector (ELSD, model PL-ELS 1000, Polymer Laboratories, Church Stretton, UK) was used with the following parameters: 1.5 SLM (gas flow rate), 160 °C nebuliser temperature and 270 °C (evaporative temperature). For all HT-HPLC experiments, a Hypercarb column (Hypercarb®, Thermo Scientific, Dreieich, Germany) with the following conditions was used: 100 × 4.6 mm^2 internal size, particle diameter of 5 μm (making a surface area of 120 m^2/g) and pore size of 250 Å. The HPLC oven temperature was kept constant at 160 °C analysis. In the first set of experiments, a linear gradient was applied from 100 % 1-decanol to 100 % TCB for 30 minutes after sample injection in order to achieve separation. Conditions were then re-established as shown in Fig. 3.1. For all HT-HPLC analyses, a concentration of 1 to 1.2 mg/mL were used (approximately 4 mg in 4 mL of 1-decanol) with 20 μL of each sample being injected.

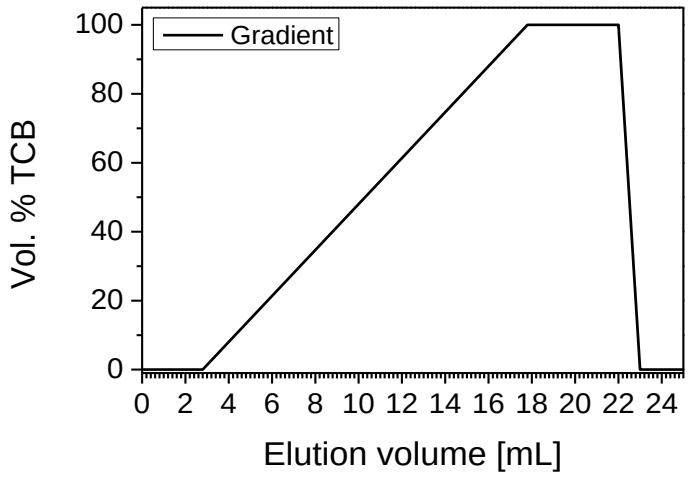

Figure 3.1. Solvent gradient profile (1-decanol→TCB_{30min}) used in HT-HPLC analysis of the LLDPE samples.

3.7. High-temperature two-dimensional liquid chromatography

HT-HPLC and HT-SEC were coupled with the aid of an electronically controlled eight-port valve system (VICI Valco instruments, Houston, Texas) equipped with two 100 μL sample loops. A 110/200 μL sample loop was used to carry out injection into the first dimension (HT-SGIC) and the flow rate was set at 0.05 $mLmin^{-1}$. The flow rate in the second dimension (HT-SEC) was set to 2.75 $mLmin^{-1}$ and ODCB was used as the mobile phase. A linear gradient was applied from 100% 1-decanol to 100% TCB within 15 mL (300 mins). In the second dimension, a PL Rapide H (Polymer Laboratories, Church Stretton, UK.) 100 × 10 mm^2 internal diameter column with a 10 μm particle diameter was used at 160 °C. The column temperature was kept constant at 160 °C for the duration of the analysis. The following parameters were used for the evaporative light scattering detector (ELSD, model PL-ELS 1000, Polymer Laboratories, Church Stretton, England): gas flow rate of 1.5 SLM, 160 °C nebulizer temperature and an evaporative temperature of 230 °C.

3.8. Preparative temperature rising elution fractionation.

p-TREF was carried out using an instrument developed and built in-house. About 3.0 g of the polymer sample was dissolved in 300 mL xylene in a glass reactor at 130- 140 °C in the presence of 2.0 wt.% Irganox 1010 (Ciba Specialty Chemicals, Switzerland) as the stabilizer.

After complete dissolution of the polymer sample, the reactor and its contents was put into a temperature-controlled preheated oil bath and filled with preheated sand (white quartz, Sigma-Aldrich, South Africa), used as a crystallization support. Both oil bath and sand were preheated to 130-140 °C.

In order to facilitate controlled crystallization of the polymer sample, the oil bath was cooled to room temperature at a cooling rate of 1 °C/hour. Thereafter, the crystallized mixture was packed into a stainless-steel column which was inserted into a modified gas chromatography oven for the elution step. Xylene (preheated) was used as the eluent in order to collect the fractions sequentially at 30, 40, 45, 50, 60, 90, 120, and 130 °C as the temperature of the oven was raised. The collected fractions were dried using a rotary evaporator followed by precipitation in acetone. The fractions were then dried to a constant weight in a vacuum oven.

This method was modified to form the second type of p-TREF method. In the second p-TREF method, the sample dissolution and crystallization step is the same, except that the dissolution was carried out using 400/100 mL of the ODCB/diethylene glycol monobutylether (DEGMBE) at 125 °C in a special glass column that is connected to a temperature regulating instrument. The polymer was allowed 4 h to dissolve completely. This instrument regulates the temperature of the fractionation glass column by circulating glycol in and out of the column under controlled temperature. In the crystallization step, the contents were cooled from 125 °C to -10 °C. The 80/20% ODCB/ DEGMBE mixture was used as the eluent. The fractions were collected at 0, 10, 25, 30, 35, 40, 60 and 125 °C and dried to a constant mass.

3.9. Preparative solution crystallization fractionation

3.0 g of the bulk polymer and 2.0 wt.% Irganox 1010 (Ciba Specialty Chemicals, Switzerland) was dissolved in 80/20% ODCB/ DEGMBE mixture at 125 °C for 3 h under constant stirring at 500 rpm. Thereafter, the dissolved polymer solution was cooled to 60, 40, 35, 30, 25, 10 and below 10 °C (soluble fraction), collecting the precipitated polymer at each temperature. The obtained fractions were washed with excess acetone and then dried to constant weight in a vacuum oven.

3.10. Preparative molar mass fractionation

p-MMF was conducted using a special glass column which has an oil inlet and outlet connecting the column to an external oil circulator. Approximately 3.0 – 5.0 g of polymer was dissolved in 200 mL of ODCB in the glass column in the presence of 2.0 wt.% Irganox 1010 (Ciba Specialty Chemicals, Switzerland) as a stabilizer. The sample dissolution was allowed to complete at 140 °C under constant stirring. Thereafter, 160 mL of DEGMBE was added as the non-solvent into the polymer solution to give a non-solvent/solvent ratio of 0.80. Then, after 45 min the temperature was dropped to 115 °C. The polymer solution was further given 30 min to equilibrate at 115 °C. The precipitated fraction was collected as the first fraction.

After the precipitated polymer had been completely isolated from the solution, aliquots of the DEGMBE were added to make 0.83, 0.85, 0.88, 0.93, 1.03 and 1.23 mL of the non-solvent while sequentially collecting the fractions at each non-solvent volume added. The polymer solution that remained in solution after the addition of 125 mL was collected as the eighth fraction (soluble fraction). All the collected fractions were washed in excess methanol and dried to a constant weight in a vacuum oven.

3.11. References

1. Ndiripo, A.; Albrecht, A.; Monrabal, B.; Wang, J.; Pasch, H. *Macromol. Rapid Commun.* **2018**, *39*, 1700703.
2. Arndt, J.-H.; Brüll, R.; Macko, T.; Garg, P.; Tacx, J. *Polymer* **2018**, *156*, 214–221.
3. Al-Khazaal, A. Z.; Soares, J. B. P. *Macromol. Chem. Phys.* **2017**, *218*, 1600332.

Chapter 4

Evaluation of preparative fractionation techniques for the fractionation of ethylene-co-1-octene copolymers

This is the first results chapter exploring various preparative fractionation techniques. The fractions obtained from the fractionation techniques are further analysed to give information on the sample microstructure as well as the usefulness of the type of fractionation technique.

4.1. Introduction

Preparative temperature rising elution fractionation (p-TREF) is already established as a fractionation technique of semicrystalline polyolefins. Recently, preparative molar mass fractionation has been used to fractionate low density polyethylene (LDPE) into several fractions irrespective of their branching. Since p-TREF is suitable for fractionating semi-crystalline polyolefins, its applicability for the fractionation of polyolefin elastomers would be of interest. Preparative-TREF can be modified to decrease the solubility of the elastomers. Another interesting temperature-based fractionating technique carried out in the absence of a support is preparative solution crystallization (p-SCF). A typical commercial elastomer (12.8 mol.%) supplied by Borealis was chosen and fractionated using p-TREF, p-MMF and p-SCF with minor modification to some of the techniques. It is worth to define the symbols that were used throughout chapters 4-6.

Definition of symbols

M_p peak molar mass
M_n average molar mass
M_w molar mass
Đ molar mass dispersity

4.2. Bulk analysis

Physical properties of LLDPEs, such as melt flow index (MFI), are mostly influenced by molar mass while chemical composition mainly affects solubility and, therefore, crystallinity.[1,2] Characterization of the bulk sample provides a first insight on the average chemical composition and molar mass of the sample. Bulk sample analysis, while informative, does not provide detailed information on the microstructure of the polyolefin sample. To do so, more information must be obtained by narrowing the regions of interest either by chemical composition (p-TREF) or by molar mass (p-MMF). Figure 4.1a-d show the SEC, CRYSTAF, DSC and HT-SGIC analysis results of LC-160 with a 1-octene content of 12.8 mol.%.

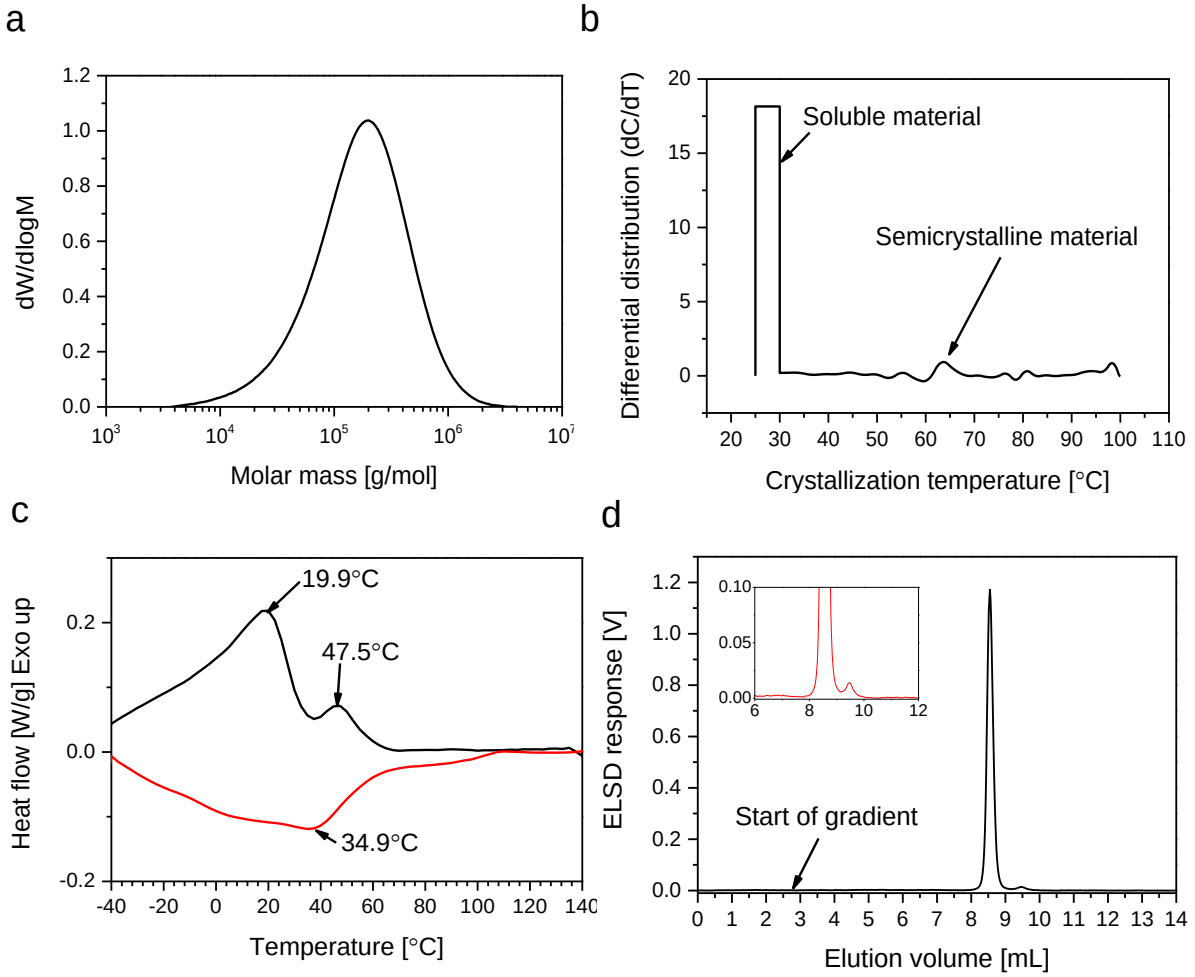

Figure 4. 1. Ethylene-co-1-octene sample (12.8 mol.%) molar mass distribution curve (a), CRYSTAF crystallization profile (b), DSC crystallization (black) and melting (red) in the temperature range between -50 and 150°C (c) and elution behaviour in HT-SGIC using a solvent gradient (d).

The SEC curve presented in Figure 4.1a shows that the bulk sample is unimodal in molar mass distribution. Typical metallocene-catalysed polyolefins have narrow molar mass distributions. However, conventional SEC analysis does not provide any information regarding the chemical composition unless coupled to FTIR online or offline. The chemical composition of the LLDPE elastomer was investigated using CRYSTAF. The crystallization behaviour in a TCB solution of the sample is illustrated in Figure 4.1b. The CRYSTAF region at or below 30 °C represents the soluble material (high 1-octene incorporated ethylene chains in the case of EO LLDPE) which does not crystallize out of the polymer solution.

Semicrystalline copolymer chains generally crystallize between 30 and approximately 80 °C, while the less branched PE homopolymer chains crystallize above 80 °C. This sample contains primarily soluble material at ambient temperature which can be seen as a rectangular peak in the region below 30 °C. This is indicative of high 1-octene contents incorporated in the molecular chains. Phiri et al.[43] used CRYSTAF to investigate the chemical composition of amorphous ethylene-propylene rubber (EPR). They discovered small portions of the samples crystallizing between 60 and 100 °C, which they attributed to presence of semicrystalline copolymer chains with relatively low comonomer incorporation. Similarly, the CRYSTAF results of the present LLDPE show small amounts of crystallisable material between 60 and 70 °C (see arrow in Fig. 4.1b). This suggests the presence of PE copolymer with intermediate 1-octene incorporation in the molecular backbone.

Differential scanning calorimetry has been widely used to study thermal properties, including crystallization and melting behaviour of complex polyolefins to ultimately gain information about chemical composition.[3-6] Fig. 4c shows the melting and crystallization thermograms of the bulk sample. Two distinct peaks at 19.9 and 47.5°C can be observed from the cooling curve, which may indicate chemical composition heterogeneity.

This could be due to the presence of molecular chains with varying degrees of comonomer contents exhibiting different distributions in crystallisable ethylene sequence lengths. Razavi-Nouri et al.[7] conducted a molecular structure characterization of two classes of LLDPE (m-LLDPE and m-VLDPE) using DSC, and attributed the two m-VLDPE crystallization peaks to compositional heterogeneity. Ndiripo et al.[8] demonstrated for the first time the suitability of HT-SGIC over HT-TGIC for the compositional analysis of ethylene-propylene elastomers with very high comonomer contents ranging between 26 – 100 mol% ethylene.

Furthermore, Arndt et al.[9] studied the chemical composition of bulk LLDPE elastomers with varying average comonomer contents ranging from 2.3 to 12.2 mol% and also confirmed the superiority of HT-SGIC for studying compositional heterogeneities of particularly low crystalline polyolefins. Herein, HT-SGIC was used as the method of choice for the investigation of the chemical composition distribution of the bulk LLDPE resins.

Figure 4.1d shows the HT-SGIC elution behaviour of the LLDPE on a Hypercarb® stationary phase. The separation mechanism is independent of the sample's crystallizability, but depends primarily on the adsorption-desorption interactive forces of the eluting components. It can be seen that this sample has material that elutes at 8.55 mL and a small fraction which elutes later at 9.50 mL. The later eluting components are typical of copolymer molecules with lower comonomer incorporation. These findings are in agreement with those reported by DSC and CRYSTAF and suggest that this elastomer exhibits chemical composition heterogeneity.

4.3. Preparative fractionation

The molecular structure of LLDPE is complex and may exhibit multiple distributions in CCD and MMD. These distributions influence the overall properties and behaviour of the samples on macroscopic scale. Preparative fractionation methods have proved to be invaluable for comprehensive molecular structure elucidation of complex polyolefins. Thus, it is necessary to fractionate these materials based on either CCD or MMD to comprehensively understand their molecular structure. Preparative-TREF and p-MMF techniques were employed for fractionating the LLDPE and their effectiveness was evaluated by comparing the results. The results of the bulk sample and the fractions obtained by these methods are presented and discussed below.

4.3.1. Chemical composition determination using FTIR

The determination of the SCB content for constructing the calibration curve used for the quantification of 1-octene in the elastomers is based on the knowledge that for high molar mass PEs, the CH_3 end groups provide a reliable measure of the ($-CH_3-$) content while the CH_2 provides the overall polymer chain concentration.[10] As such, the SCB content of EO LLDPE standards with known 1-octene content was determined by measuring the peak

absorbance/height of CH_3 ($Height_{CH_3}$) divided by the CH_2 peak area ($Area_{CH_2}$). This was plotted against the 1-octene content to give linear calibration from which 1-octene content of the samples used in this work was determined and its correlation is also shown on the graph, see Fig. 4.2.

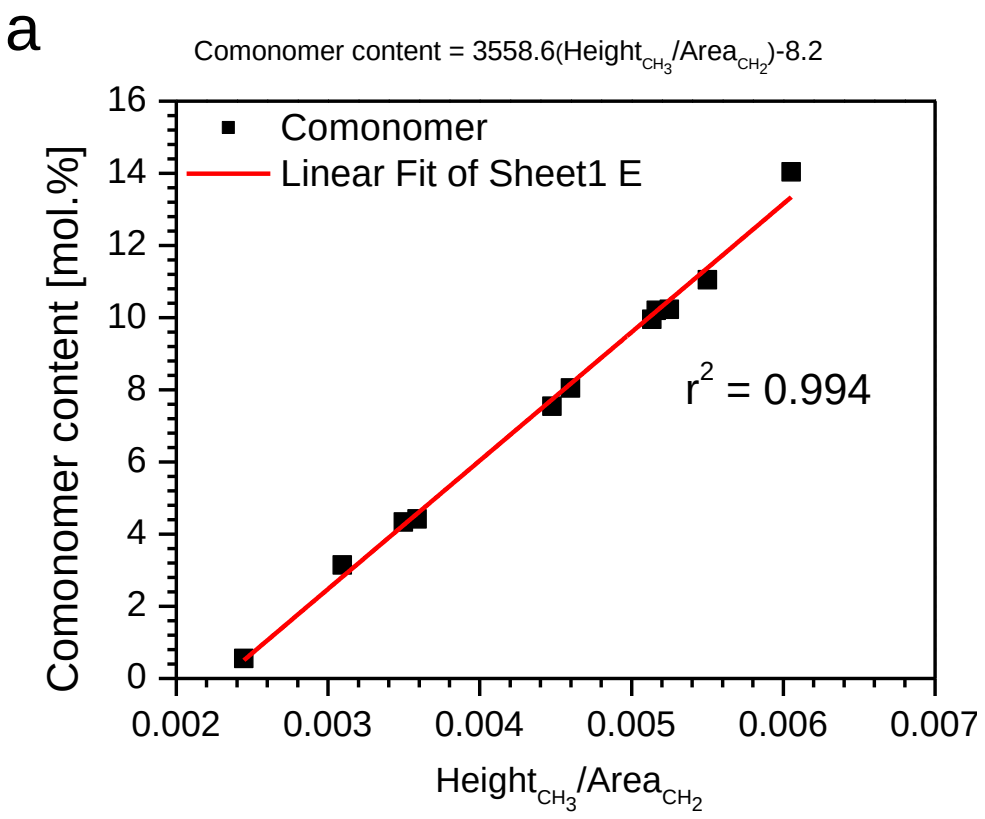

Figure 4. 2. Plot showing the calibration curve obtained from a series of ethylene-co-1-octene copolymers of known comonomer content in the range of 0.55 – 14.3 mol.%.

4.3.2. Fractionation using p-TREF and p-MMF.

The compositional heterogeneity of polyolefin copolymers has been widely studied using p-TREF method.[11-13] Preparative TREF is generally known for its superior separation ability and high sensitivity to varying degrees of SCB in semicrystalline copolymer chains. While the p-MMF method has been employed for preparative fractionation of a range of polyolefin materials including LDPE and semicrystalline LLDPE, it has not been applied in the fractionation of LLDPE elastomers.[14,15]

In contrast to p-TREF, p-MMF fractionates polymer chains based on their solubility in a non-solvent/solvent system, rather than crystallizability. The intermolecular structure heterogeneity of copolymer chains obtained from both fractionation methods can be comprehensively studied since in both techniques polymer molecules are physically separated. This section compares p-TREF fractionation to p-MMF fractionation for the molecular structure elucidation of elastomers. Thus, one LLDPE elastomer with a comonomer content of 12.8 mol% was subjected to different preparative fractionation techniques and the obtained fractions were subsequently analysed by other analytical techniques as mentioned in Chapter 3.

Table 4.1. Summary of molar mass data and comonomer content of p-TREF and p-MMF fractions as determined by HT-SEC and FTIR-ATR.

Fractions	**NS/SR[a] [mL]**	**Recovery wt.%**	**[C][b] mol.%**	**M_p[c] [kg/mol]**	**M_n[c] [kg/mol]**	**M_w[c] [kg/mol]**	**Đ[c]**
p-MMF fractions							
Fr 1	0.8	6.9	10.8	427.1	172.4	448.8	2.6
Fr 2	0.83	15.8	13.2	351.4	166.8	358.8	2.2
Fr 3	0.85	25.2	12.4	282.8	160.9	296.5	1.8
Fr 4	0.88	18.9	12.7	228.5	140.4	241.8	1.7
Fr 5	0.93	11.3	8.5	172.1	113.0	184.5	1.6
Fr 6	1.03	6.9	12.0	122.7	79.3	133.8	1.7
Fr 7	1.23	4.5	12.1	98.4	66.2	111.4	1.7
Fr 8	Soluble	10.4	12.3	91.1	46.0	99.3	2.2
Total recovery		**99.9**					
Fractions	**Temperature [°C]**	**Recovery wt.%**	**[C][b] mol.%**	**Mp[c] [kg/mol]**	**Mn[c] [kg/mol]**	**Mw[c] [kg/mol]**	**Đ[c]**
p-TREF (Xylene) fractions							
Fr 1	30	70.3	12.0	251.6	97.4	283.5	2.9
Fr 2	40	17.6	11.1	238.0	103.0	277.8	2.7
Fr 3	45	5.7	11.8	244.1	105.0	286.7	2.7
Fr 4	50	2.9	13.5	233.3	108.7	282.8	2.6
Fr 5	60	1.2	12.0	197.8	58.0	259.0	4.5
Fr 6	90	1.9	11.2	205.7	89.7	269.3	3.0
Fr 7	130	0.3	12.6	195.0	39.7	236.6	6.0
Total recovery		**99.9**					

[a] denotes non-solvent/solvent ratio, [b] comonomer content as determined by FTIR-ATR.
[c] molar mass properties as determined by HT-SEC

Figure 4.3a, b show the percentage recovery of fractions from p-TREF and p-MMF methods as well as their respective comonomer contents and dispersities. Fig. 4.3a shows an appreciably constant comonomer content as well as M_p across the fractions. After 60 °C, the fractions have broader Đ (2.9-6.0) which may be indicative of complex elastomer chain composition. However, these fractions are small in quantity and, therefore, do not contribute much to the properties of the bulk elastomer. Overlays of the fraction molar mass distribution curves clearly show the differences in the fractionation techniques, see Fig. 4.4. The constant M_p and Đ is expected for p-TREF fractions since this is not a molar mass sensitive fractionation method.

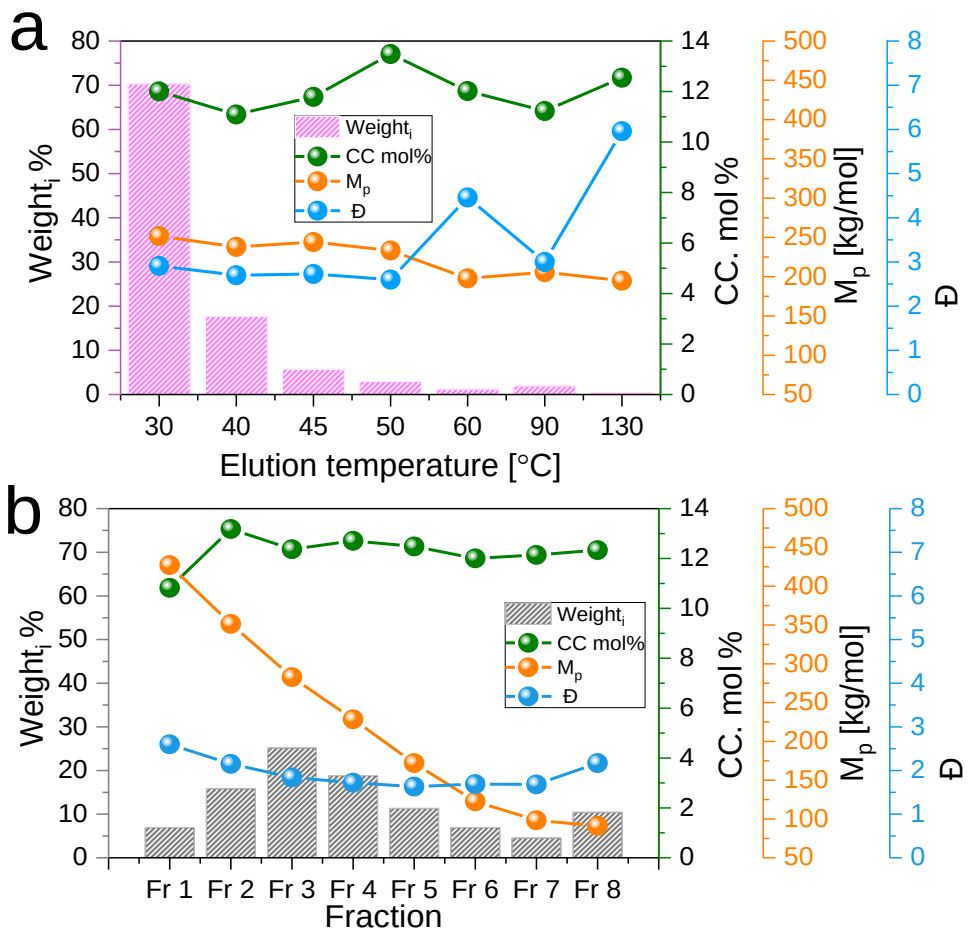

Figure 4.3. Plot showing the amounts of fraction material collected at each elution temperature from p-TREF fractionation and the respective molar mass properties (a); graph showing the amount of material collected at each non-solvent/solvent ratio from p-MMF fractionation (b). (also see Table 4.1).

Furthermore, the p-TREF graph in Figure 4.3a shows that more than 85% of the bulk sample components eluted in the first and second fractions at 30 and 40 °C, respectively. This means that some structural information can be lost from the p-TREF process since the majority of the material elutes as a single fraction. The molecular structure of the 30 °C fraction remains as complex as that of the bulk sample.

This is a common challenge for p-TREF fractionation of elastomers that have very low crystallinities.[16] In p-MMF, the decrease in M_p with increasing NS/SR (or fraction number) signifies the successful separation of the polymer chains based on their molar mass. The M_p for p-MMF fractions decreases from fraction 1 – 8 (91.1 – 427.1 kg/mol) and all fractions display narrow Đ (2.6 or below).

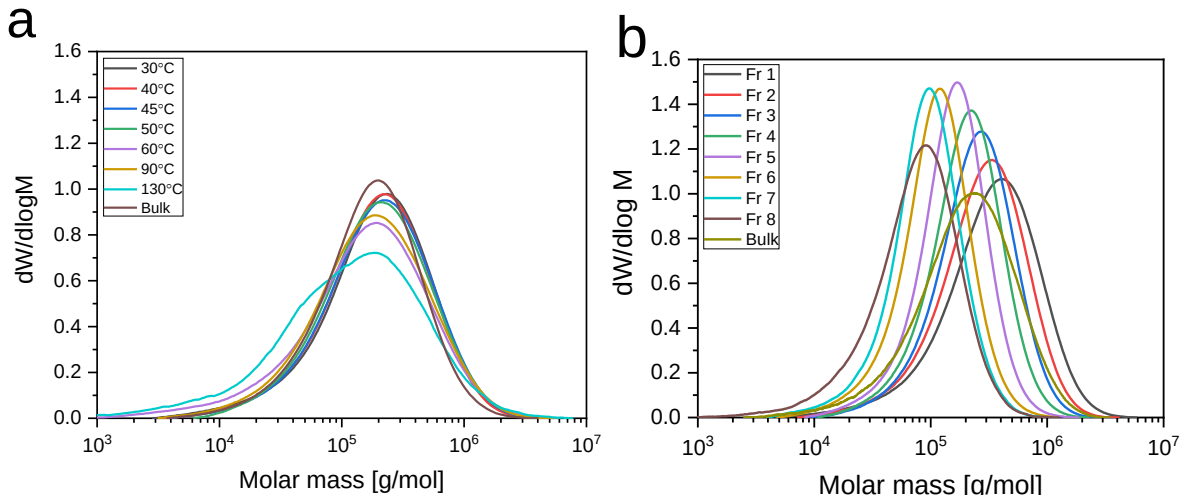

Figure 4. 4. Molar mass distribution profiles of (a) p-TREF fractions and (b) p-MMF fractions of sample LC 160 obtained by HT-SEC from a TCB solution.

The subsequent step to gaining in-depth knowledge of the molecular structure of the obtained fractions is to analyse them with various analytical methods. DSC provides preliminary information about the composition of polyolefins since the thermal behaviour of LLDPE copolymers can be correlated to their chemical structure. Figure 4.5 a, b show the results of the DSC analysis of the p-TREF and p-MMF fractions. The thermal behaviour was investigated at temperatures between -50 to 150 °C at 10 °C/min. The need for lower than ambient temperatures is due to the low crystallinity of the samples.

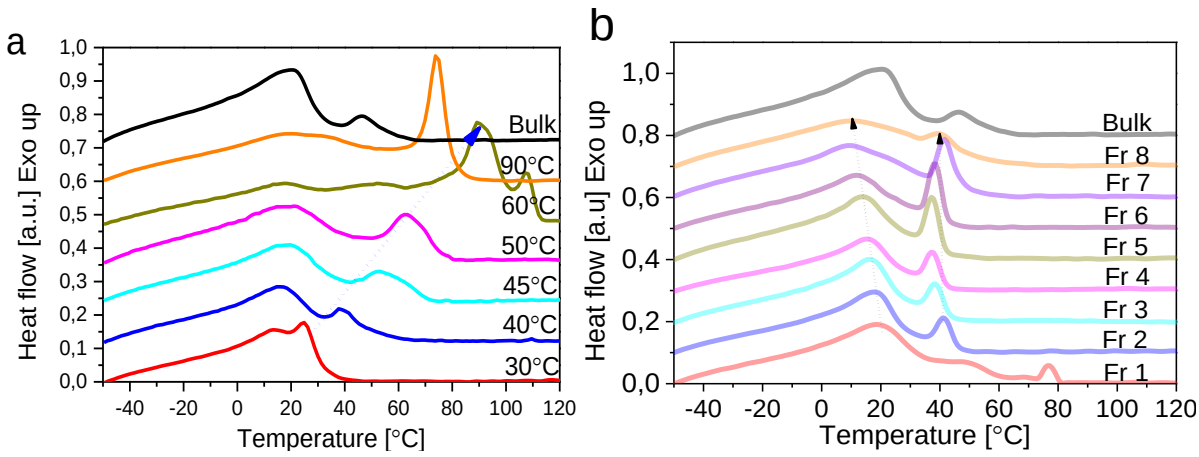

Figure 4. 5. DSC first crystallization curves of p-TREF (a) and p-MMF (b) fractions in comparison to their bulk elastomers, respectively.

Figure 4.5a presents the thermograms (cooling cycle) of the p-TREF fractions. Here, it can be seen that the fractions are heterogeneous in their crystallization behaviour. For LLDPE and PE materials, the crystallization thermograms give more information on the composition of the samples. However, the effects of cocrystallisation and chain entanglement still remain prevalent and affect the good resolution of component peaks. The 30 – 50 °C fractions have bimodal crystallization behaviours which indicate the presence of two main components in the fractions.

The second component has a crystallisation temperature that increases with TREF temperature which also implies a change in chemical composition (blue dotted arrow). The observed increase in the crystallization temperature of the fractions as the TREF temperature increase is only observed for the TREF fractions as expected. Furthermore, the 60 °C fraction shows a very complex distribution having components with the highest crystallization temperatures as well as being broad. Some of the components are not seen in the bulk crystallization profiles due to their small amounts.

Mirabella[17] proposed that PE copolymers crystallize in a stepwise manner starting with the polymer chains that exhibit the thickest lamellar then followed by the thinner lamellar. On the other hand, p-MMF fractions show complex crystallization behaviour as well, indicating complex chemical compositions of this sample. The fractions mainly consist of a low

crystallizing broad peak and a higher crystallizing narrower peak. There is no significant difference between the bulk sample and fractions, and this is attributed to the insensitivity of p-MMF to chemical composition. The cooling thermograms of the p-TREF fractions resemble that of the p-MMF fractions, but show broad peaks at temperatures around 22 °C, attributed to the low temperature crystallizing components. The significant differences in the overall shapes of the thermograms can be attributed to the sensitivity of p-TREF to chemical composition which p-MMF is sensitive to molar mass. Gabriel et al.[18] attributed the different crystallization peaks to the presence of block-like structures of high 1-octene and low 1-octene content within the molecular chains of m-LLDPE samples.

Consequently, these blocks presumably crystallize independently at different temperatures as a function of their comonomer content. For the LLDPE copolymers with comparable M_p values (within one fraction), the differences in the peak melting and crystallization temperatures may be attributed to chemical heterogeneity amongst the polymer chains.[19] It is also proposed that, since xylene promotes co-crystallization as has been previously reported[20], the blocks with low SCB co-crystallizes with the block that has higher SCB. However, in DSC these different blocks with different SCB content can be identified by their different heat flows and/or crystallization temperatures.[18]

Leone[21] showed that different conditions for copolymerization of LLDPE could affect the crystallization behaviour of polymers even if they have similar SBC content. Since this is a random copolymer and has similar average comonomer content and comparable molar mass values (see Table 4.1), the observed trend in the cooling thermograms of p-TREF fractions could not be explained conclusively by DSC. HT-SGIC is an excellent chemical composition sensitive method that separates polymer chains irrespective of their degree of crystallinity. Hence HT-SGIC could provide a more detailed compositional information for both the p-TREF and p-MMF fractions.

This technique can separate polyolefin macromolecules with complex chemical composition distributions. The basis of separation is the interaction of the uninterrupted methylene sequences in samples derived from ethylene as a monomer. The longer these sequences are, the stronger the interactions. Therefore, more of TCB is required to desorb the polyolefin chains from the stationary porous graphitic carbon stationary phase. Fig. 4.6 illustrates the

elution behaviour of the p-TREF fractions in comparison to the bulk sample. The fractions elute in the same region as the bulk which is as expected.

However, the fractions have different elution behaviour owing to their different chemical compositions. The differences are not significant, although some can be highlighted. Unlike the bulk sample, the 30 °C fraction is narrower in its elution behaviour indicating a less complex chemical composition.

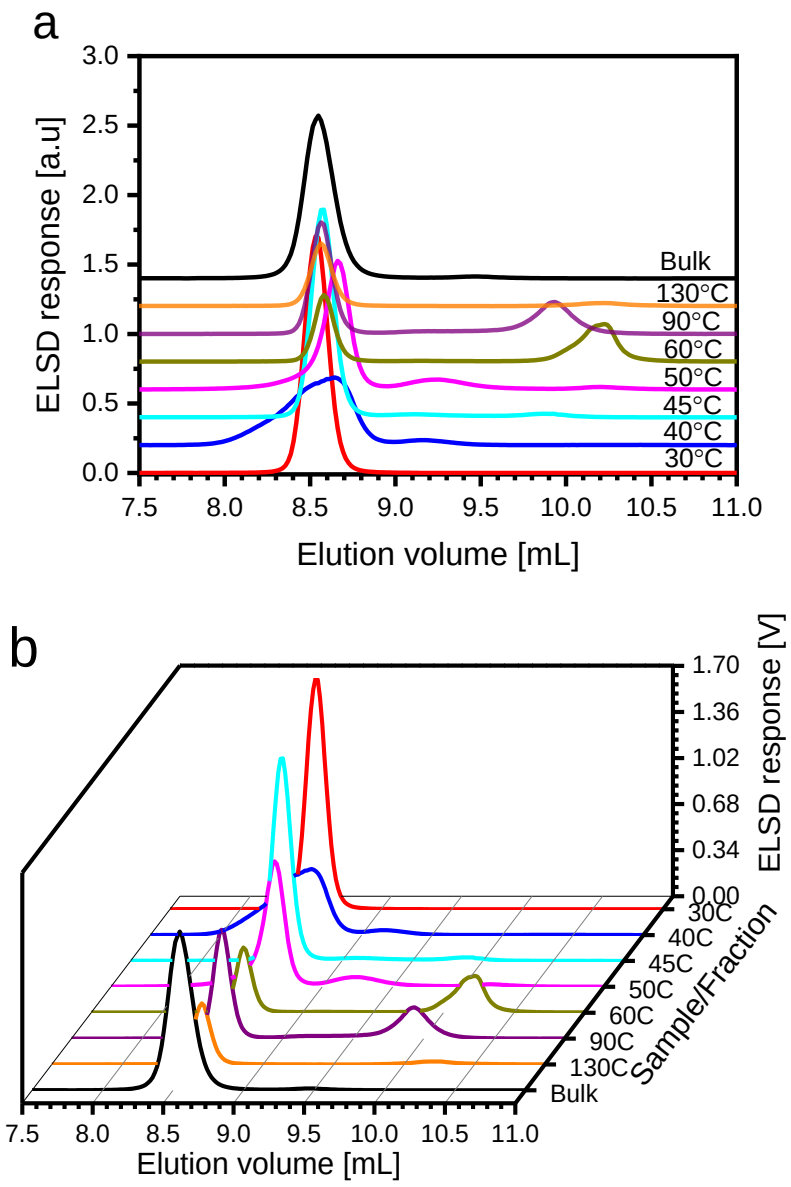

Figure 4.6. Elution behaviour of p-TREF fractions obtained using a 1-decanol→TCB_{30min} on porous graphic carbon as illustrated in a stack plot (a) and a water fall plot (b).

The 40 °C fraction, however, exhibits the broadest elution profile that is indicative of a very complex chemical composition make up. The 45 – 90 °C fractions elute in a bimodal manner with a smaller fraction eluting between 9.0 – 10.5 mL. This fraction most probably has longer ethylene sequences or a larger molar mass. Comparing the 60 °C and 90 °C fractions, similar trends as seen in DSC are observed. The 60 °C elutes (HT-SGIC) and crystallizes (DSC) in broader profiles which indicates a complex chemical composition distribution.

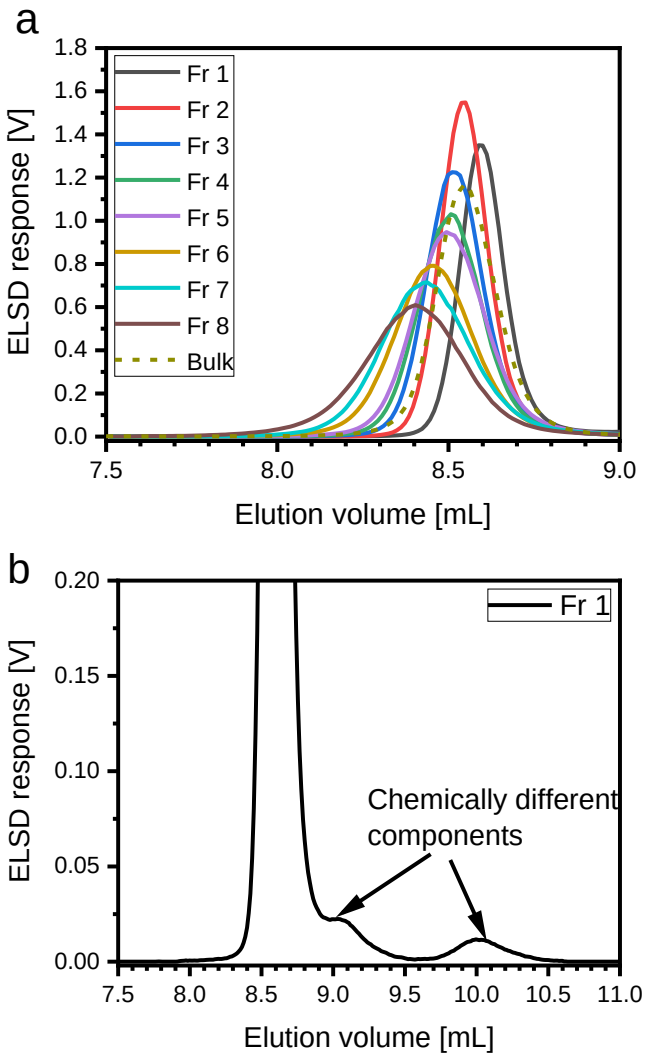

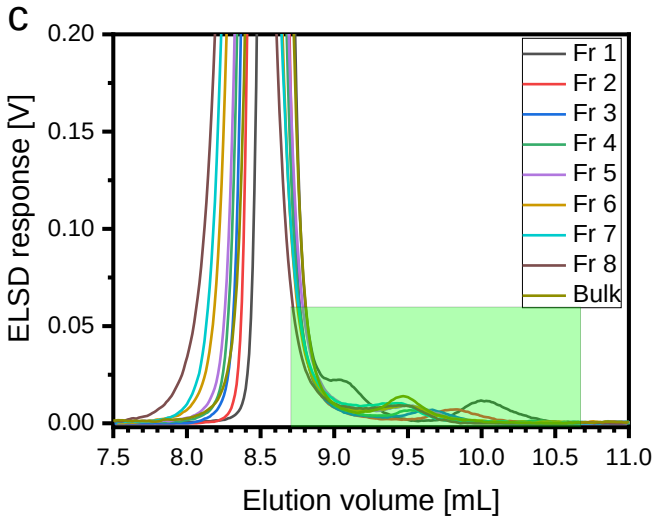

Figure 4.7. Elution behaviour of p-MMF fractions under a 1-decanol→TCB_{30min} gradient. Overlays of the elution profiles are shown in (a). Fraction 1 elution behaviour shown in (b), illustrating the presence of chemically different elastomer chains. The zoomed in plot of the fractions and the bulk are shown in (c). Region where chemically different small refractions elute is highlighted by the green rectangle.

When sample LC-160 is fractionated using p-MMF, the resulting fractions show interesting elution behaviour in HT-SGIC as illustrated in Fig. 4.7 a-c. Similar to the bulk, the fractions elute with smaller components at higher volumes. Fig. 4.7b, c illustrate this observation. These components suggest chemical heterogeneity, having lower SCB content. The elution behaviour of the main component of each fraction (more clearly illustrated in Fig. 4.7a) shows that the elution volume decreases with increasing fraction number or decreasing molar mass.

In addition, the peak onset of each fraction decreases making the peaks rather broad as the fraction number increases. When the full width at half maximum (FWHM) is compared to the dispersities (Fig. 4.7a), it can be seen that the fractions have rather similar dispersities but different FWHM. This implies that the fraction chemical composition becomes more complex with decreasing molar mass. The decrease in the peak elution volume can be explained by the change in either molar mass or chemical composition. FTIR was used to determine the chemical composition of the fractions. Although the technique is not as sensitive as ^{13}C-NMR, estimates of the comonomer content can be obtained from the calibration equation. Figure 4. 8b shows both the fraction comonomer content and HT-SGIC elution volume as function of their respective molar mass.

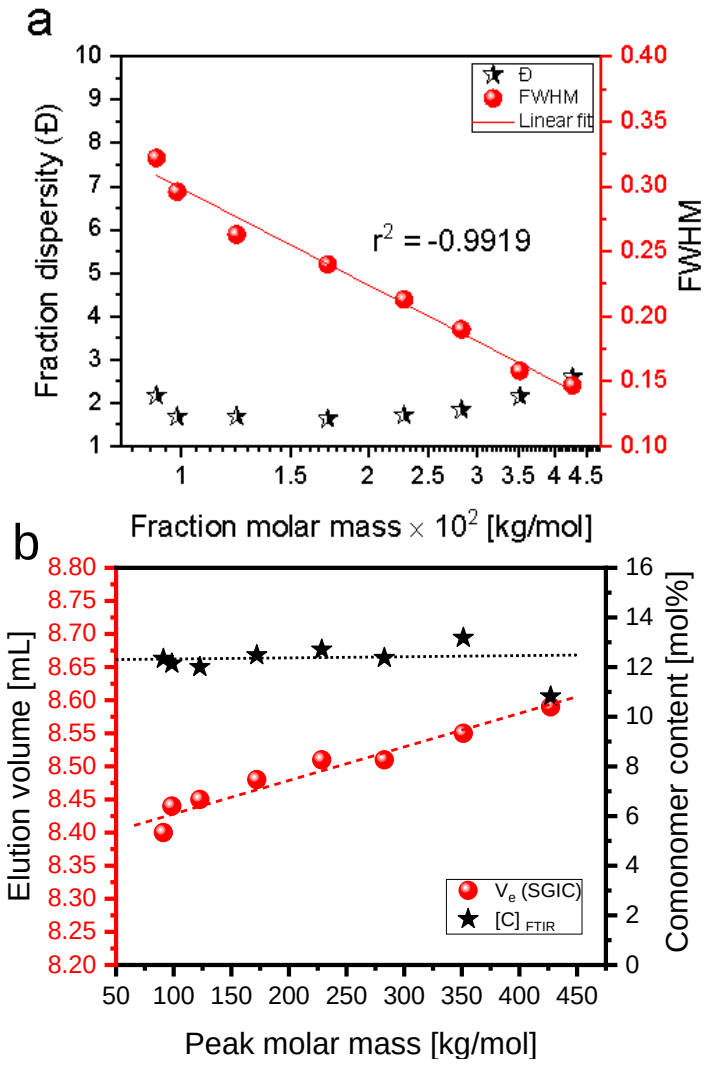

Figure 4. 8. Plot showing p-MMF fraction dispersity (Đ) and the peak full width at half maximum (FWHM) as a function of fraction peak molar mass(a); comonomer content and SGIC elution volume as a function of fraction peak molar mass (b).

The peak broadening with decreasing molar mass/ chain length can also be attributed to symmetrical axial dispersion which could be correlated to α-olefin incorporation at critical polymer chain lengths.[22] Furthermore, the p-MMF fractions have rather similar average comonomer contents (from FTIR), hence their elution behaviour can be mainly accounted for by the molar mass differences among the fractions. In a recent work on EO LLDPE elastomers with molar masses of 14 kg/mol and above, Arndt et al.[9] demonstrated using HT-SGIC that the elution behaviour was more dependent on the average 1-octene content.

However, this does not apply to this study since the average comonomer content is similar. At constant comonomer content but varying molar mass, the lowest molar mass chains would have the shortest ethylene sequence length, as a result be the least retained on porous graphitic carbon. Similar elution behaviour was observed by Al-khazaal et al.[22] on the TGIC of a series of EO LLDPE elastomers with constant comonomer content between 0-13 mol.% per series, but varying chain lengths.

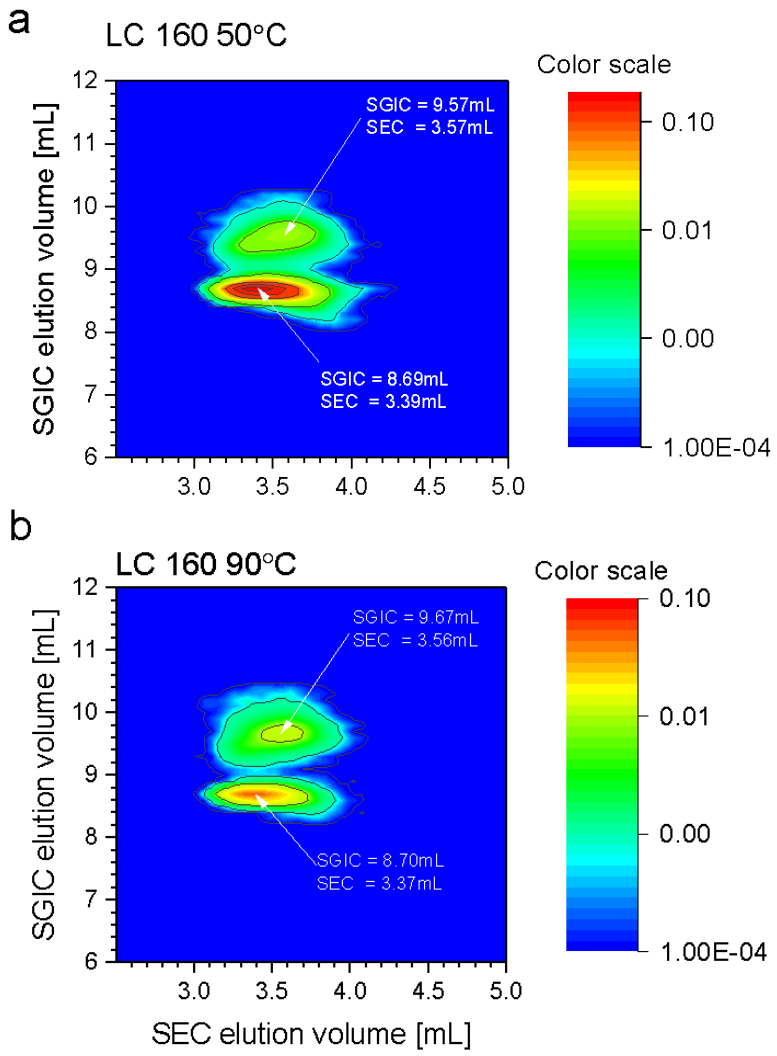

Figure 4.9. HT-2D-LC contour plots for the 50 and 90 ºC p-TREF fractions. A Hypercarb® column with 100 × 4.6 mm^2 was used in the first dimension with a flow rate of 0.05 mL/min at 160 °C. A Rapide H HT-SEC column was used in the second dimension with an ODCB flow rate of 2.75 mL/min. 100 µL of a 3 mg/mL solution was injected for each sample.

Monrabal[23] proposed that the interaction strength between copolymer chain and the Hypercarb® porous graphitic carbon stationary phase is dependent on the contact surface area of the macromolecule. As such, low molar mass chains have smaller contact surface area with the stationary phase. Thus, smaller macromolecules have comparably weaker stationary phase-polymer interactions and, therefore, will elute faster than the high molar mass chains.

Two dimensional-liquid chromatography separates components based on both chemical composition (first dimension) and molar mass (second dimension). Consequently, both the MMD and CCD can be correlated simultaneously. Two p-TREF fractions that showed chemical heterogeneity in SGIC were chosen for analysis in 2D-LC (fractions with insufficient amounts could not be analysed further). As seen from Fig. 4.9 both HT-2D-LC contour plots show two eluting components. The first component for both fractions elutes in a rather narrow SGIC elution volume while the second is broader.

The 2D-LC contour plot for the 50 ºC fraction shows presence of components with significantly different compositions (SGIC dimension, 8.59 and 9.57 mL). Similar observation was made for the 90 ºC fraction. The later eluting component in both cases has lower molar mass (high elution volume in the HT-SEC dimension) as compared to the first component. The late elution behaviour which signifies stronger retention can, therefore, be attributed to the lower comonomer content of the second eluting component.

The fractions can be compared in several ways. One way is to subtract matrices and plot the residual data in a new contour plot. However, the main drawback is encountered when samples with different molar masses are to be compared. The detector response is dissimilar even when the same conditions for detection are used. Another way of comparing the fractions is to obtain profiles from the contour plots as illustrated in Fig. 4.10.

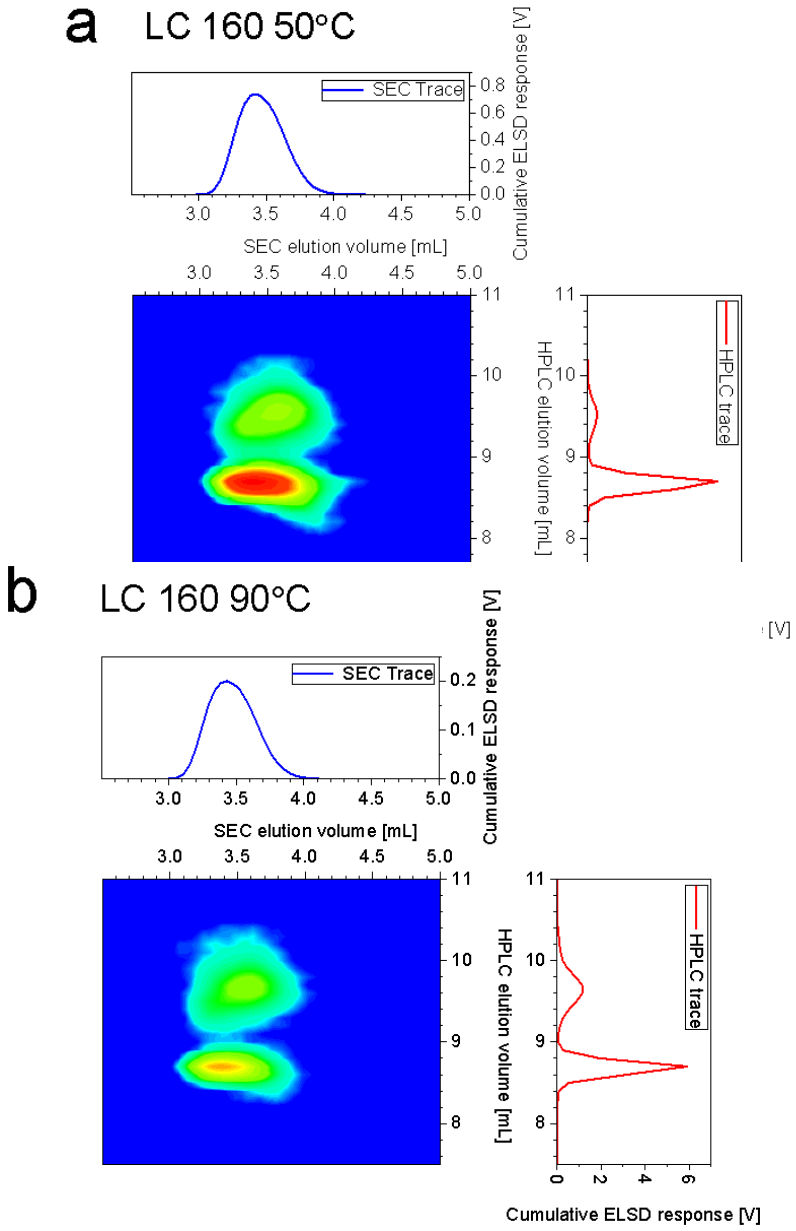

Figure 4.10. HT-2D-LC contour plot for the 50 and 90 ºC p-TREF fractions showing the cumulative SEC and HPLC profiles.

From the traces, it is clear that the molar mass distribution curves of the fractions are monomodal. The HPLC dimension shows the multimodal behaviour of the fractions in both instances. This section discusses the results obtained by p-SCF and p-TREF fractionation. In the present discussion, the p-SCF and p-TREF methods were modified by using a solvent mixture to help decrease the solvating power of ODCB.

In contrast to the normal TREF that employs only a good solvent such as xylene, the modified TREF employs two solvents, a good solvent and a non-solvent. The main role of the non-solvent is to minimize the effect of coelution, especially of the components that contain very high 1-octene content and therefore soluble at room temperature. The LC-160 elastomer was dissolved in ODCB followed by addition of DEGMBE to make 4:1 v/v ODCB/DEGMBE mixture.

4.3.3. Characterization and comparison of the fractions obtained by p-TREF and p-SCF.

The LC 160 sample was fractionated using p-TREF and p-SCF and the results of the obtained fractions are presented and discussed in this section. Figure 4.11 (a) shows the four fractions that were collected from the p-SCF method at temperatures between 35 ºC and 10 °C.

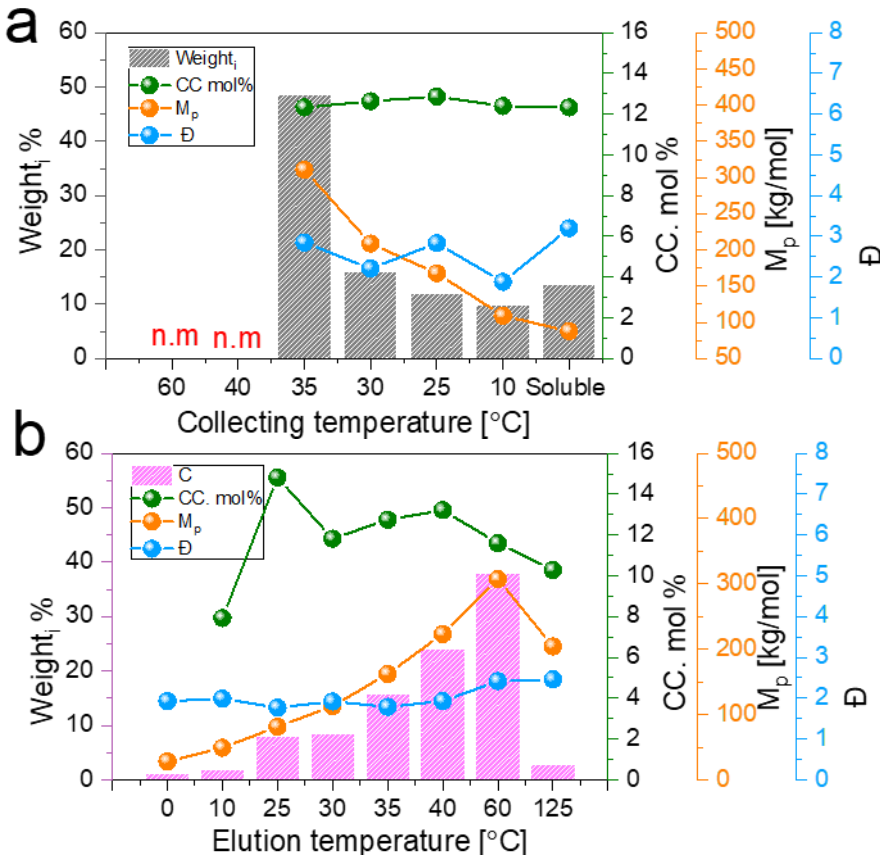

Figure 4.11. Plots of the p-SCF (a) and p-TREF (b) fractions showing the recovered weight percentage of the fractions and their respective peak molar mass, dispersities and comonomer content. In both sets of fractionation experiments a mixture of ODCB and DEGMBE (80/20%) was used as the solvent/eluent.

Here, a solution of the dissolved polymer was cooled with constant stirring and fractions were collected at the mentioned temperatures. The fifth fraction was the material that failed to crystallize at 10 °C and is classified as the soluble fraction. To achieve lower temperatures, a cooling device was used to circulate a cooling liquid around the column. ODCB was chosen as solvent of choice due to its low melting point. No fraction was collected at 60 and 40 °C and this confirms that this sample has low crystallizability even when small amounts of a non-solvent are added.

Table 4.2. Summary of the molar mass properties of the p-SCF and p-TREF fractions as determined by HT-SEC.

Sample	**Fraction [°C]**	**Recovery Wt %**	**[C][a] Mol%**	**M_p[b] [kg/mol]**	**M_n[b] [kg/mol]**	**M_w[b] [kg/mol]**	**Đ[b]**
p-SCF fractions							
Fr 1	60	n.m	n.m	n.m	n.m	n.m	n.m
Fr 2	40	n.m	n.m	n.m	n.m	n.m	n.m
Fr 3	35	48.5	12.3	310.7	109.7	312.9	2.9
Fr 4	30	16.1	12.6	208.7	93.9	207.6	2.2
Fr 5	25	12.1	12.9	167.8	64.8	183.8	2.8
Fr 6	10	9.7	12.4	108.9	57.7	108.4	1.9
Fr 7	Soluble	13.6	12.3	87.6	28.8	92.2	3.2
Total recovery		**100.0**					
p-TREF fractions							
Fr 1	0	1.3	n.m	28.4	16.1	31.1	1.9
Fr 2	10	1.8	7.9	49.2	28.8	57.3	2.0
Fr 3	25	7.9	14.8	81.4	46.0	81.7	1.8
Fr 4	30	8.4	11.8	113.0	57.2	109.6	1.9
Fr 5	35	15.7	12.7	162.3	89.7	160.8	1.8
Fr 6	40	24.1	13.2	223.4	122.7	236.8	1.9
Fr 7	60	38.0	11.6	307.4	132.7	320.7	2.4
Fr 8	125	2.8	10.3	204.5	97.0	238.3	2.5
Total recovery		**100.0**					

[a] comonomer content as determined by FTIR, [b] molar mass properties as determined by HT-SEC
[c] n.m denotes no material obtained

The fractions collected at 35 °C and below have broad dispersities indicating molar mass heterogeneity. The peak molar masses of the fractions decrease with decreasing elution temperature. The 35 °C fraction constitutes the majority of the sample by weight. Interestingly, a significant amount of material was collected at a temperature below 10 °C. However, it is suspected that the fractionation mechanism was influenced by both molar mass and chemical composition. This shall be further evaluated using more comprehensive compositional analytical techniques.

Eight fractions with relatively narrower molar mass dispersities were obtained by p-TREF in a ODCB: DEGMBE (80/20%) mixture at varying fractionation temperatures as shown in Fig. 4.11b (see also Table 4.2). It is evident that the weight percentages of the collected fractions increase with increasing elution temperature and fraction 7 being the largest. Interestingly, the molar masses of the fractions also increase with elution temperature. This was however not expected in p-TREF.

It is expected that the crystallinity of the collected fractions increases with increasing temperature since the process is dependent on crystallizability and molar mass is not expected to play a major role.[6,18] Since in the present case a solvent and non-solvent mixture was used, phase separations which are molar mass dependent may influence fraction collection. The SEC curves for fractions from both p-SCF and p-TREF are shown in Figure 4.12 a, b, respectively.

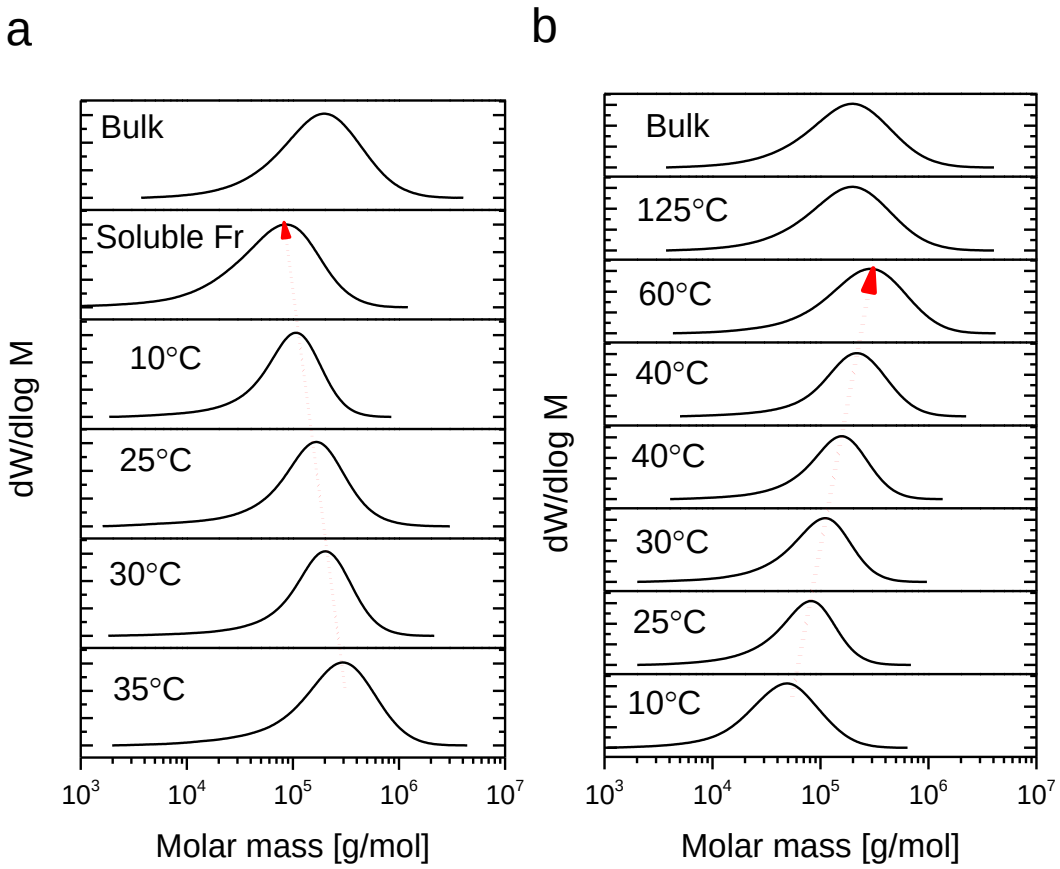

Figure 4.12. Molar mass distribution curves of p-SCF (a) and p-TREF fractions (b) as determined by HT-SEC from a TCB solution at 150 °C.

Preparative-SCF and preparative-TREF fractions that were recovered are narrow and monomodal. Both fractionation techniques (p-SCF and p-TREF) showed that the molar mass of the obtained fractions increases with increasing fractionation temperature. Since the purpose of the solvent mixture was to optimize the fractionation by suppressing the solubility of the highly soluble materials, it was expected that the fractionation mechanism will be mainly influenced by SCB content as usual.

To the best of our knowledge, no p-TREF method using the conditions employed here has been reported for fractionating EO elastomers, thus, it would be interesting to gain in-depth information about the chemical structure of the obtained fractions and relate it to its molar mass to establish the mode of separation.

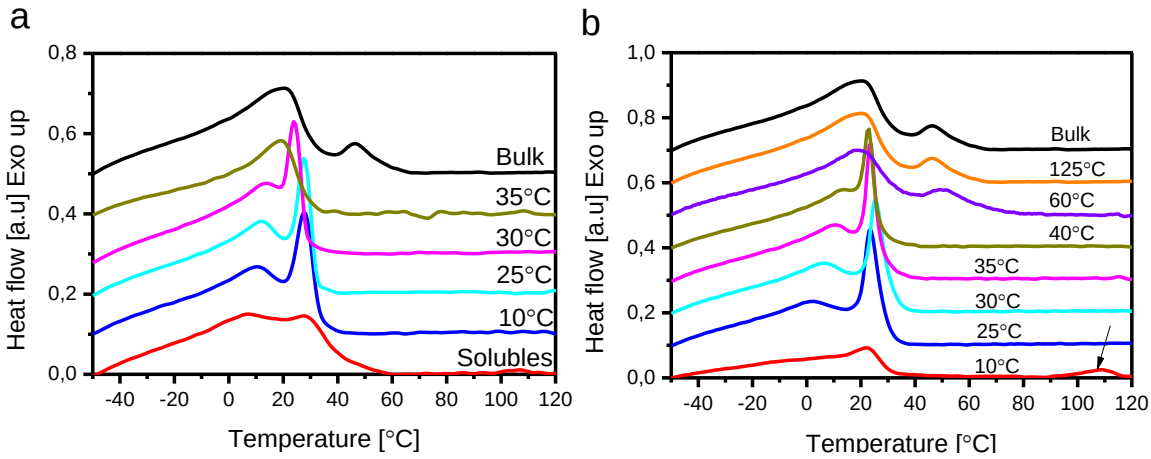

Figure 4.13. Crystallization curves of p-SCF (a) and p-TREF (b) fractions. The arrow in (b) indicates material crystallizing between 90 – 120 °C.

Figure 4.13a and b show the thermal behaviour of the fractions obtained by p-SCF and p-TREF, respectively. The soluble fraction for p-SCF fraction shows a broad cooling thermogram with two identifiable ill-defined peaks which can be attributed to chains that are chemically heterogeneous. Similar to the bulk, the fractions have very low crystallization temperature which stretch into sub-ambient regions.

Generally, both sets of fractions behave in a similar manner. The low temperature/ soluble fraction is broad and contains a small fraction crystallizing at high temperatures (see Fig. 4.13.). The middle fractions (10 – 30 °C in p-SCF and 25 – 40 °C in p-TREF) have similar crystallization behaviour. These peaks consist of a broad low crystallizing peak and a sharp higher temperature peak (20 – 40 °C). Fractions recovered at 60 and 125 °C in p-TREF show the presence of components also seen in the bulk which crystallize between 40 – 60 °C.

Since the molar mass distribution curves are quite narrow and unimodal, the broad thermal behaviour of individual fractions is most likely to be influenced by the inter- and intrachain short chain branch heterogeneity. The thermal behaviour of these fractions are testimonial of the complex composition nature of the fractions and the bulk resin.

HT-SGIC can separate the samples into chemically different components. Unlike in DSC, the technique does not rely on the thermal response which is heavily influenced by the chemical composition. Here, the evaporative light scattering detector is used. The detector is known to be non-linear in its response. However, within certain limits, the detector can be linear and used

for quantification. Instead, the separated macromolecules give a detector response proportional to their quantity provided that the sample concentration is within the limits of the required injected mass. Figure 4.14 shows the elution behaviour of the p-SCF and p-TREF fractions. Although both sets of fractions elute in a very narrow range, some information can be obtained from the elugrams regarding their chemical composition. The p-SCF fractions elugrams become broader as the temperature decreases, indicating that the extent of molecular structure complexity increases with decreasing crystallinity.

This trend in peak broadness may indicate decreasing sensitivity to chemical composition or fractionation efficiency as the temperature decreases. In addition, the soluble fraction constitutes all the material that did not crystallize out of solution below 10 ºC irrespective of their microstructure, thus it is the most heterogeneous fraction.

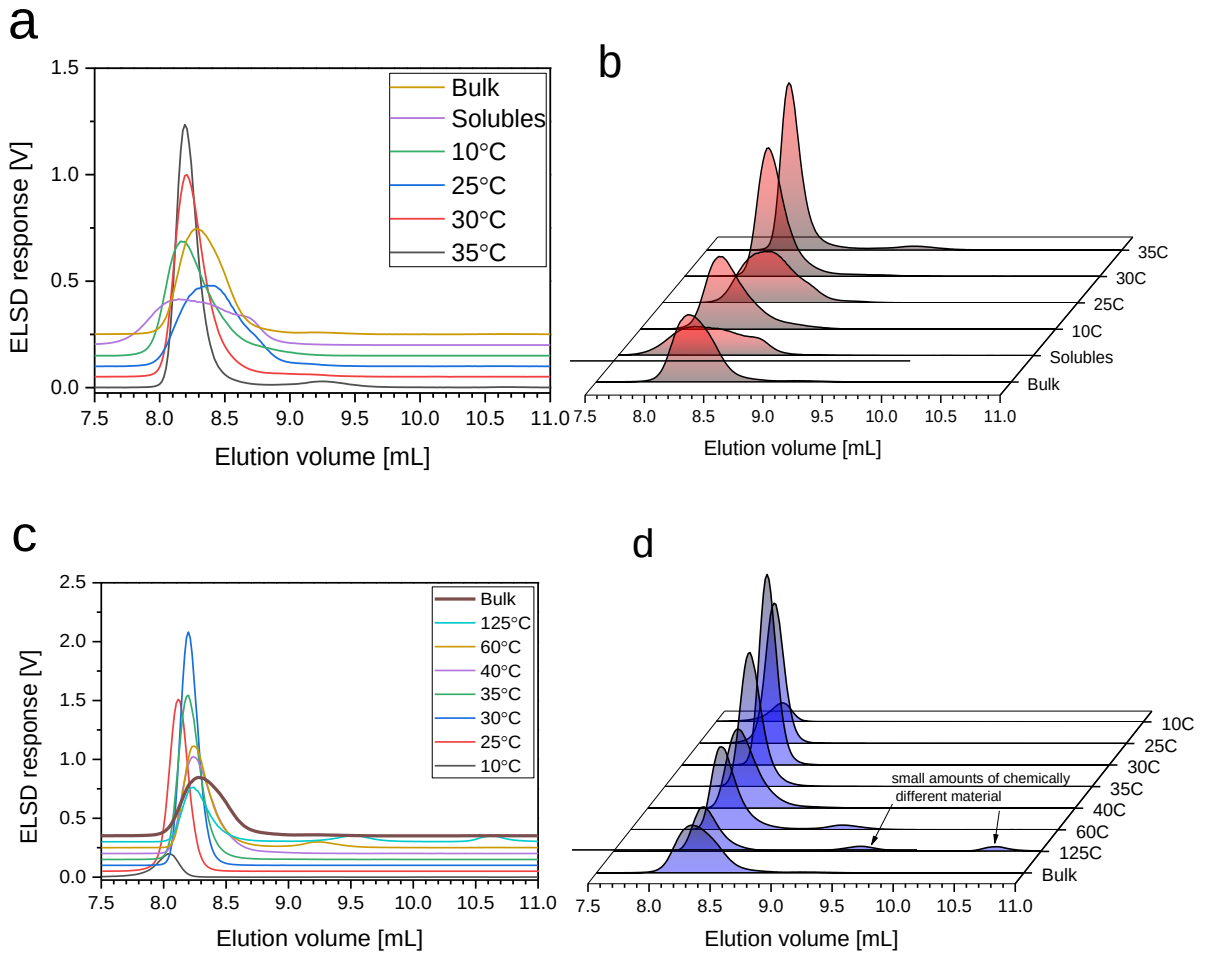

Figure 4.14. Elution behaviour of p-SCF (a, b) and p-TREF fractions (c, d) on porous graphitic carbon (Hypercarb®|) under a 1-decanol→TCB_{30min} solvent gradient at 160°C (b).

The p-TREF fractions elute at roughly the same elution volume, although very minor differences are seen. The 60 and 125 ºC fractions show bimodal elution behaviour suggesting chemical composition heterogeneity in the fractions. While some differences are clear, they are minute. When the fraction elution volume is related to the TREF elution temperature, (Fig. 4.15), it can be seen that the elution volume increases with the TREF elution temperature (as shown by the dotted arrow) up to the 35 °C fraction where it remains constant. However, trend towards lower comonomer contents is also seen in Table 4.2.

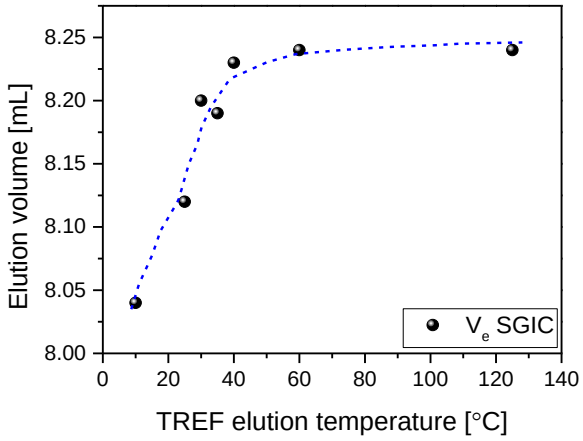

Figure 4.15. Correlation of p-TREF fraction elution volume in HT-SGIC with p-TREF collection temperature.

In order to investigate the relationship between the early and late eluting components of the multimodal 40 and 125 °C p-TREF fractions, HT-2D-LC was used. Fig. 4.16 shows the contour plots of the 40 and 125 °C fractions obtained from HT-2D-LC with ODCB as the second-dimension solvent. Here it is clearly shown that the 40 °C fraction has one visible component tailing towards lower molar masses with increasing SGIC elution. This means the later eluting component seen in the first dimension has lower molar mass as compared to the early eluting one.

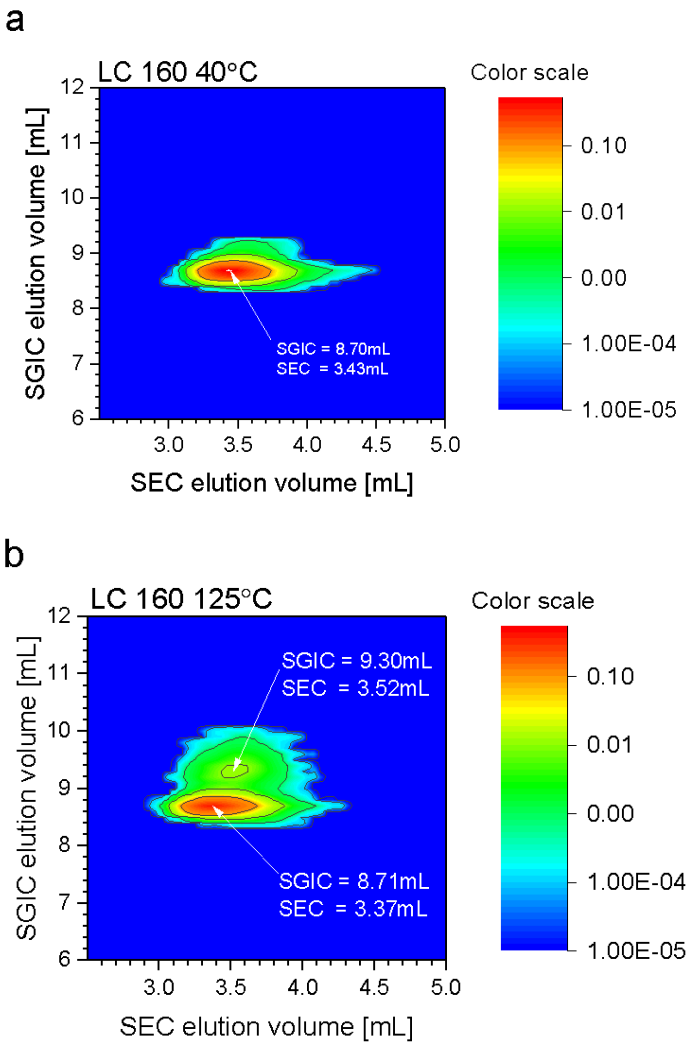

Figure 4.16. HT-2D-LC contour plots showing the elution behaviour of the 50 °C (a) and 125 °C (b) p-TREF fractions.

The same is observed with the 125 °C fraction, see Fig. 4.16b. The late elution behaviour which signifies stronger retention can, therefore, be attributed to the lower comonomer content of the second eluting component. Fig. 4.17a, b shows the same analyses with traces of the first and second dimensions showing both the chemical composition and molar mass profiles. The late fractions are small in their quantity can go undetected (Figs. 4.16a and 17a). The high flow of the solvent in the second dimension also contributes to the poor detection since this large amount of solvent has to vaporized to leave sample polymer chains which then scatter the light.

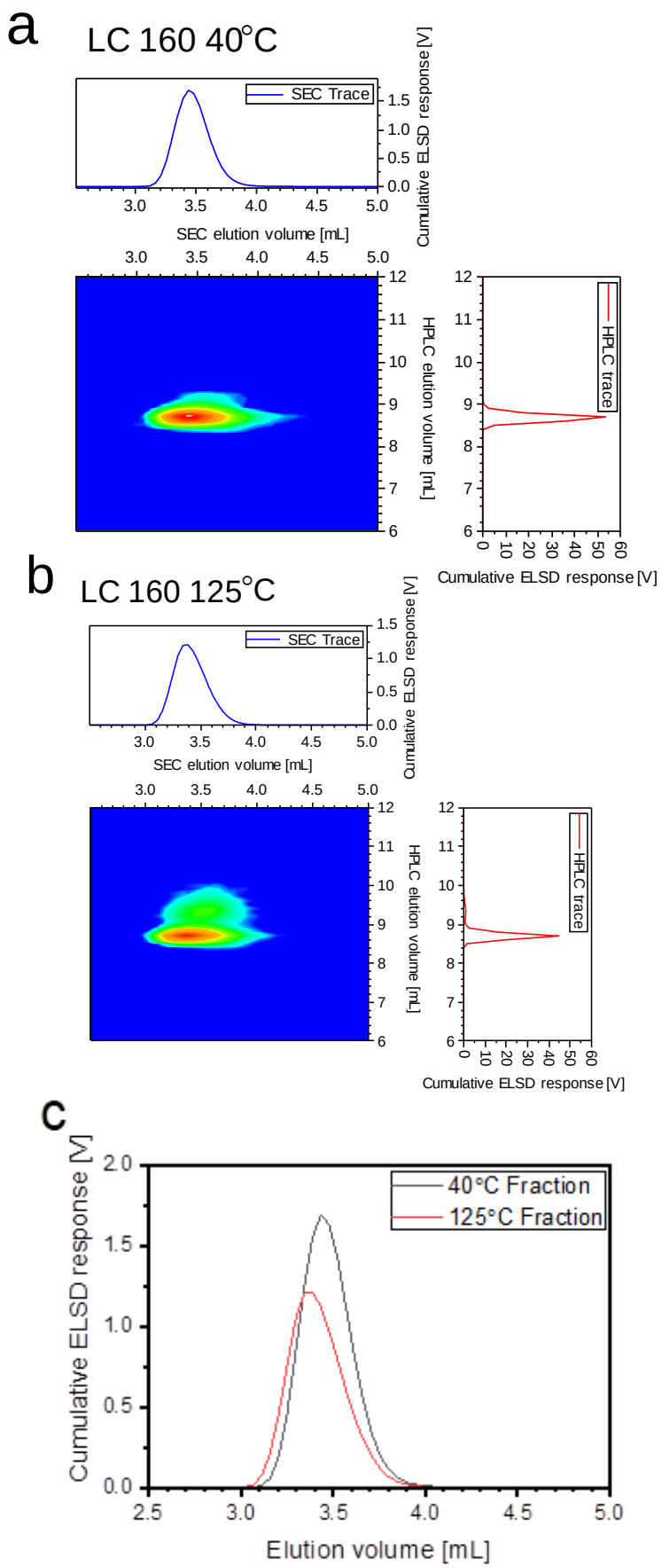
a
LC 160 40°C
SEC Trace
SEC elution volume [mL]
Cumulative ELSD response [V]
HPLC elution volume [mL]
HPLC trace
Cumulative ELSD response [V]
b
LC 160 125°C
SEC Trace
SEC elution volume [mL]
Cumulative ELSD response [V]
HPLC elution volume [mL]
HPLC trace
Cumulative ELSD response [V]
c
40°C Fraction
125°C Fraction
Cumulative ELSD response [V]
Elution volume [mL]

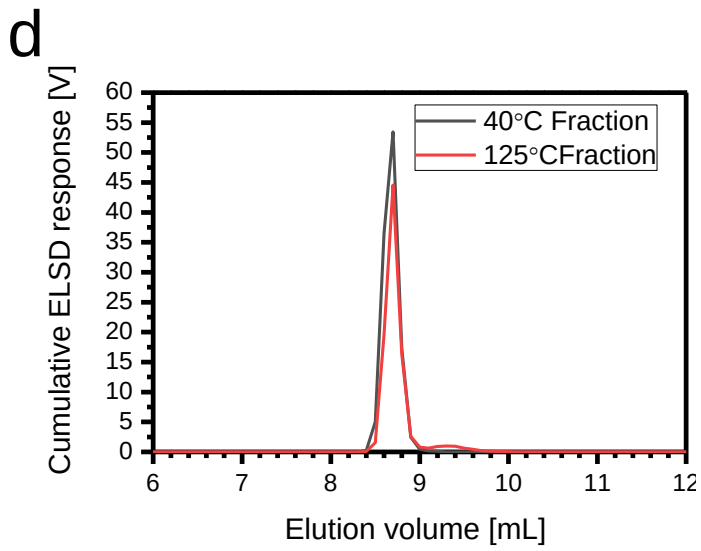

Figure 4.17. HT-2D-LC contour profiles of the 40 and 120 °C p-TREF fractions in (a) and (b) respectively; overlays of SEC and HPLC traces obtained from the HT-2D-LC analyses (c and d) respectively.

4.4. Conclusions

The analysis of elastomer materials is a challenging task. More so, established crystallization-based techniques for preparative fractionation of polyolefins fail at fractionating elastomer material into several fractions over the crystallisable temperature range. Various preparative fractionation methods have been tested herein. While the use of preparative TREF is limited due to the elution of the majority of material at ambient temperatures, preparative molar mass fractionation is shown to produce fractions with narrow molar mass distributions in sufficient quantities for further analysis. Despite this drawback, it was seen that both techniques provide information on the complex nature of the LC 160 sample.

In the second part of the chapter, crystallization-based techniques are modified by using a binary solvent mixture of a solvent and non-solvent. This was intended to increase the solution crystallization temperature. However, in both the preparative TREF and solution crystallization techniques, the fraction molar masses showed a trend which illustrates that the fractionation was rather molar mass-based. These techniques can be studied further and can form part of a more detailed study later on.

4.5. References

1. Hosoda, S. *Polym. J.* **1988**, *20*, 383–397.
2. Macko, T.; Pasch, H.; Kazakevich, Y.; Fadeev, A. *J. Chromatogr. A* **2003**, *988*, 69–76.
3. Schick, C. *Anal. Bioanal.Chem.* **2009**, *395*, 1589–1611.
4. Balbontin, G.; Camurati, I.; Dall'Occo, T.; Finotti, A.; Franzese, R.; Vecellio, G. *Angew. Makromol. Chem.* **1994**, *219*, 139–160.
5. Menczel, J. D.; Judovits, L.; Prime, R. B.; Bair, H. E.; Reading, M.; Swier, S. *Thermal Analysis of Polymers;* John Wiley & Sons: New Jersey, 2009, p 7–240.
6. Zhang, M.; Lynch, D. T.; Wanke, S. E. *J. Appl. Polym. Sci.* **2000**, *75*, 960–967.
7. Razavi-Nouri, M. *Polym. Test.* **2006**, *25*, 1052–1058.
8. Ndiripo, A.; Albrecht, A.; Monrabal, B.; Wang, J.; Pasch, H. *Macromol. Rapid Commun.* **2018**, *39*, 1700703.
9. Arndt, J.-H.; Brüll, R.; Macko, T.; Garg, P.; Tacx, J. *Polymer* **2018**, *156*, 214-221.
10. Pasch, H.; Malik, M. I. *Advanced separation techniques for polyolefins*; Springer: New York, 2014.
11. Karbashewski, E.; Kale, L.; Rudin, A.; Tchir, W. J.; Cook, D. G.; Pronovost, J. O. *J. Appl. Polym. Sci.* **1992**, *44*, 425–434.
12. Zhou, X.; Hay, J. N. *Eur. Polym. J.* **1993**, *29*, 291–300.
13. De Goede, E.; Mallon, P.; Pasch, H. *Macromol. Mater. Eng.* **2010**, *295*, 366–373.
14. Jørgensen, J. K.; Larsen, A.; Helland, I. *e-Polymers* **2010**, *10*, 1596–1612.
15. Ndiripo, A.; Bungu, E.; Pasch, H. *Polym. Int.* **2018**, *68*, 206–217.
16. Phiri, M. J.; Cheruthazhekatt, S.; Dimeska, A.; Pasch, H. *J. Polym. Sci., Part A: Polym. Chem.* **2015**, *53*, 863–874.
17. Mirabella, F. M. *Journal of Applied Polymer Science* **2008**, *108*, 987–994.
18. Gabriel, C.; Lilge, D. *Polymer* **2001**, *42*, 297–303.
19. Eselem Bungu, P.; Pasch, H. *Polym. Chem.* **2017**, *31*, 4565–4575.
20. Cheruthazhekatt, S.; Pasch, H. *Anal. Bioanal.Chem.* **2014**, *406*, 2999–3007.
21. Leone, G.; Mauri, M.; Pierro, I.; Ricci, G.; Canetti, M.; Bertini, F. *Polymer* **2016**, *100*, 37-44.

22. Al-Khazaal, A. Z.; Soares, J. B. P. *Macromol. Chem. Phys.* **2017**, *218*, 1600332.

23. Monrabal, B. *Macromol. Symp.* **2015**, *356*, 147–166.

Chapter 5

Effect of chemical composition on preparative molar mass fractionation

In the present chapter, four linear low-density copolymers with increasing 1-octene contents were fractionated using preparative molar mass fractionation in order to evaluate the effect of comonomer content on the fractionation technique. The fractions of the samples were further analysed with an array of analytical techniques.

5.1. Introduction

The complexity of LLDPEs is influenced by several parameters including catalyst-type, reactor and reaction conditions, to name few. Thus, the suitability of a characterization method for molecular structure determination of complex copolymers such as LLDPE elastomers requires to be evaluated in different samples. The behaviour of ethylene-co-α-olefin copolymers with increasing comonomer content in p-TREF is well documented. It is of interest to investigate the behaviour of ethylene-co-1-octene copolymers with comparable molar masses but different comonomer contents in p-MMF. The first section of this chapter introduces the four samples and briefly discusses the results thereof.

5.2. Bulk analysis

Table 5.1. Molar mass and average chemical composition information of the bulk samples as determined by HT-SEC and FTIR, respectively.

Supplier	Sample	[C][a] [mol.%]	M_p [kg/mol]	M_n [kg/mol]	M_w [kg/mol]	Đ
Borealis	**Sample 1**	4.4	140.5	58.1	175.2	3.0
Borealis	**Sample 2**	7.5	155.3	66.9	189.0	2.8
Borealis	**Sample 3**	10.0	162.5	69.2	192.2	2.8
Borealis	**Sample 4**	11.1	202.4	95.9	244.2	2.6

a Determined by ^{13}C-NMR, **b** molar mass properties as determined by HT-SEC
c n.m denotes no material obtained

The molar mass distribution profiles of the four samples are shown in Fig. 5.1a. All four samples possess unimodal molar mass distributions. While the molar masses of samples 1-3 are comparable, the molar mass of sample 4 is appreciably larger. In an attempt to obtain the chemical composition distribution profiles of the samples, CRYSTAF analyses were carried out. Fig. 5.1b shows the profiles obtained for the four samples.

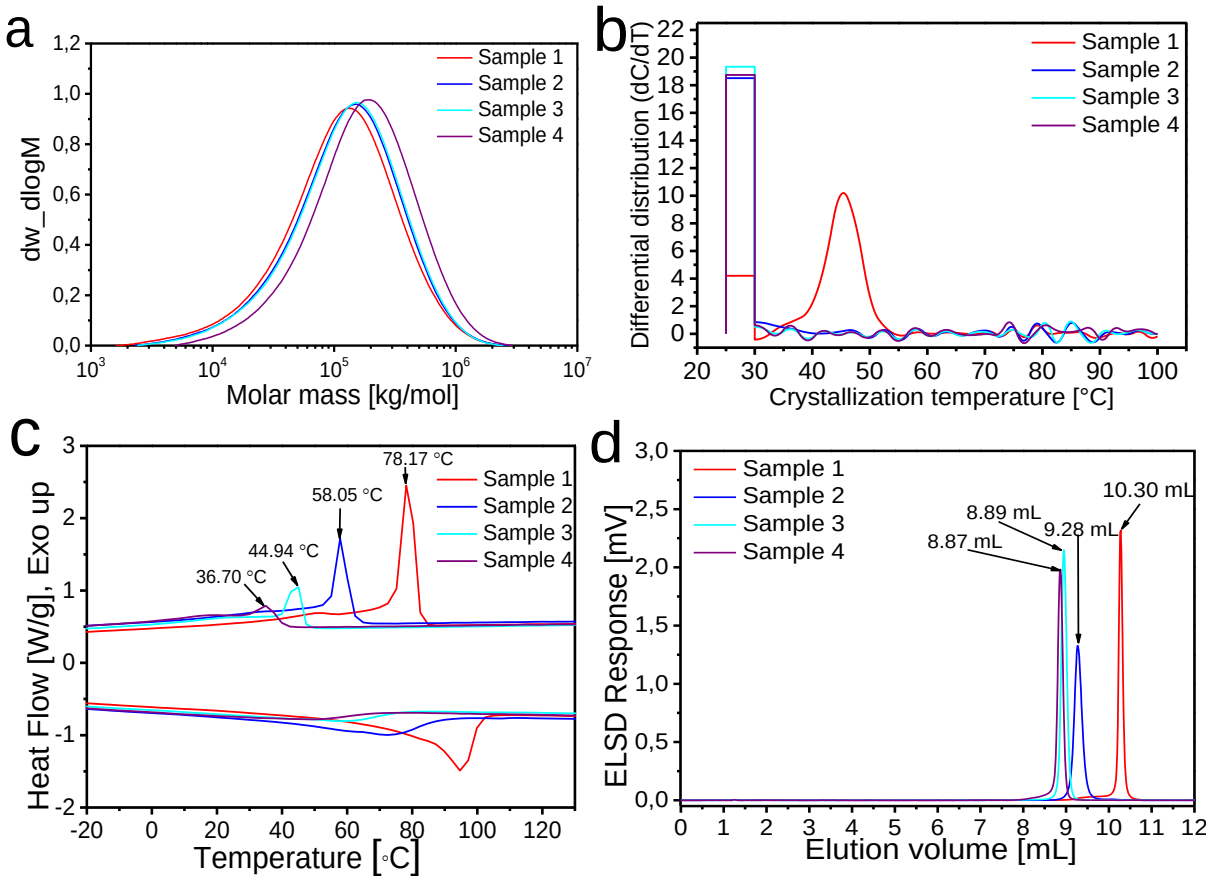

Figure 5.1. MMD profiles of the four ethylene-co-1-octene samples as determined by HT-SEC (a); CRYSTAF crystallization profiles obtained from a TCB solution (b); crystallization exotherms and melting endotherms recorded between -50 – 150 ºC showing the thermal behaviour of the four samples in DSC (c); elution behaviour of the four samples on a 10×4.6mm^2 Hypercarb® column under a 1-decanol→TCB$_{30min}$ gradient (d).

It is evident that only sample 1 (4.4 mol.%) has a significant amount of semicrystalline components characterized by the crystallization peak at about 45 °C. Furthermore, while sample 1 also shows presence of soluble material (below 30 °C), sample 2-4 appear to consist mainly of soluble components which appear at 30 °C and below. The soluble nature is attributed to the high 1-octene incorporation on polyolefin backbone.

DSC, on the other hand is generally sensitive to the lamella thickness of LLDPE copolymers which is dictated by their SCB (or comonomer) and SCBD (comonomer distribution). Thermal analysis of the samples is shown in Fig. 5.1c. Accordingly, the lamella thickness of these samples is expected to increase with decreasing SCB content, hence sample 1 has the highest peak crystallization temperature and sample 4 the lowest. Crystallisation peaks show distinct crystallization patterns as compared to the melting endotherms. The sensitivity of the chain rearrangement that the crystallization peaks provide has been shown previously.[1,2]

HT-HPLC using solvent gradient was employed to further probe the chemical structure of these samples since the adsorption-desorption mechanism in Hypercarb® stationary phase is a function of ethylene sequence length of copolymers. Consequently, the chemical composition of copolymers can be deduced from their elution behaviour. Figure 5.1d shows the elution order of the samples with the highest 1-octene incorporated sample 4 eluting last, followed by sample 3, 2 and lastly sample 1. The observed elution behaviour is in agreement with the DSC results. However, for more detailed information with regards to the overall molecular structure of these four LLDPEs, fractionation is necessary.

5.3. Analysis of fractions

The four LLDPE samples were fractionated by the p-MMF method as already highlighted in Chapter 3 Section 3.6. The molar mass properties of the fractions were studied using HT-SEC under similar conditions used for the bulk samples. The molar mass values are shown in Table 5.2. Figure 5.2 shows the relationship between the recovered fraction wt.% of the collected fractions and their respective molar mass and average chemical composition properties.

For samples 1-3, the majority of the sample by wt.% precipitates out of solution as the first fraction at the 0.8 (200/160 mL) NS/SR ratio, see Fig. 5.2. Eight fractions were collected for each sample in sufficient amounts to enable subsequent offline analyses, see Table 5.2. The last fraction was the soluble fraction which constitutes mainly material that could not precipitate out of solution between 0.8 and 1.23 NS/SR. The fraction was recovered by addition of excess methanol. The majority of the fractions exhibit very low dispersities with the highest being 2.3-2.4 (the last fractions of samples 2 and 3).

Table 5. 2. Molar mass and average chemical composition information of the bulk samples as determined by HT-SEC and FTIR, respectively.

Fractions	NS/SR[a] [mL]	Recovery Wt.%	[C][b] mol%	M_p[c] [kg/mol]	M_n[c] [kg/mol]	M_w[c] [kg/mol]	Đ[c]
			Sample 1				
Fr 1	0.8	45.2	4.2	185.6	126.5	213.9	1.7
Fr 2	0.83	20.2	2.9	123.8	88.1	136.8	1.6
Fr 3	0.85	5.8	2.6	106.9	73.1	120.2	1.7
Fr 4	0.88	6.3	4.7	94.8	68.5	107.0	1.6
Fr 5	0.93	2.6	3.5	82.0	58.1	90.6	1.6
Fr 6	1.03	8.6	4.5	64.6	48.5	71.5	1.5
Fr 7	1.23	4.2	4.5	48.1	36.5	56.5	1.6
Fr 8	Soluble	6.9	2.8	38.2	25.6	43.1	1.7
Total recovery		**99.6**					
			Sample 2				
Fr 1	0.8	62.9	8.5	200.1	130.0	247.4	1.9
Fr 2	0.83	3.3	7.8	151.5	110.5	181.3	1.6
Fr 3	0.85	2.8	7.1	132.6	99.1	148.4	1.5
Fr 4	0.88	5.1	7.4	114.1	78.6	125.1	1.5
Fr 5	0.93	3.7	8.5	101.1	66.9	110.9	1.7
Fr 6	1.03	5.2	7.8	73.6	51.5	85.2	1.7
Fr 7	1.23	11.0	78	66.1	46.5	74.7	1.6
Fr 8	Soluble	5.8	6.8	22.2	10.9	26.6	2.4
Total recovery		**99.8**					
			Sample 3				
Fr 1	0.8	45.4	9.5	248.3	144.1	287.7	2.0
Fr 2	0.83	10.2	10.0	177.7	115.3	198.2	1.7
Fr 3	0.85	4.8	9.9	164.2	113.9	176.2	1.6
Fr 4	0.88	4.9	9.3	142.2	100.4	151.1	1.5
Fr 5	0.93	5.6	10.4	122.2	89.8	130.5	1.5
Fr 6	1.03	14.5	9.8	91.4	69.2	101.1	1.5
Fr 7	1.23	5.7	9.5	62.1	46.0	73.4	1.6
Fr 8	Soluble	7.5	9.0	29.8	16.9	38.1	2.3
Total recovery		**98.6**					
			Sample 4				
Fr 1	0.8	18.1	11.3	368.4	200.0	391.8	2.0
Fr 2	0.83	17.1	10.2	287.8	179.0	304.0	1.7
Fr 3	0.85	17.5	10.7	239.3	158.3	266.7	1.7
Fr 4	0.88	12.7	11.0	197.4	134.4	224.3	1.7
Fr 5	0.93	13.8	12.2	157.0	111.0	180.7	1.6
Fr 6	1.03	11.2	10.9	108.1	75.9	125.4	1.7
Fr 7	1.23	6.6	10.9	77.9	59.5	96.1	1.6
Fr 8	Soluble	1.9	9.4	59.5	40.7	73.0	1.8
Total recovery		**98.9**					

[a] denotes non-solvent/solvent ratio, [b] comonomer content as determined by FTIR,

[c] determined from HT-SEC

Therefore, from a molar mass distribution point of view, the samples are homogenous, and this is typical of m-LLDPEs. From Fig. 5.2, it is evident that the M_p decreases with fraction number (increasing non-solvent in solvent mixture). This indicates the selective sensitivity of the p-MMF method towards molar mass. Consequently, the uniformity (characterized by low Đ) of the molar masses of the polymer chains in each fraction is not compromised by the amount of fraction collected. Although the determination of the average chemical composition of polyolefins with FTIR is known to be not as accurate as that obtained by 13C-NMR, the analysis provided some useful information on the fractions. Generally, the fractions have similar average chemical compositions. We attribute the noticeable variations to experimental error.

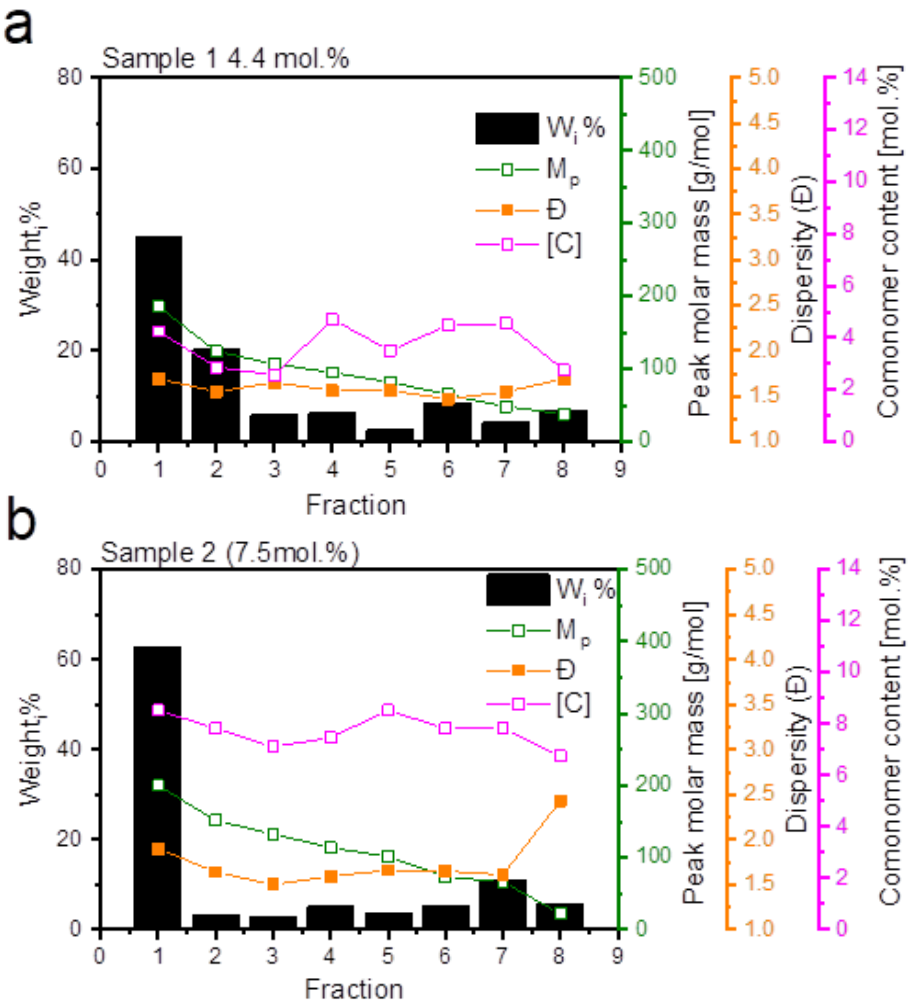

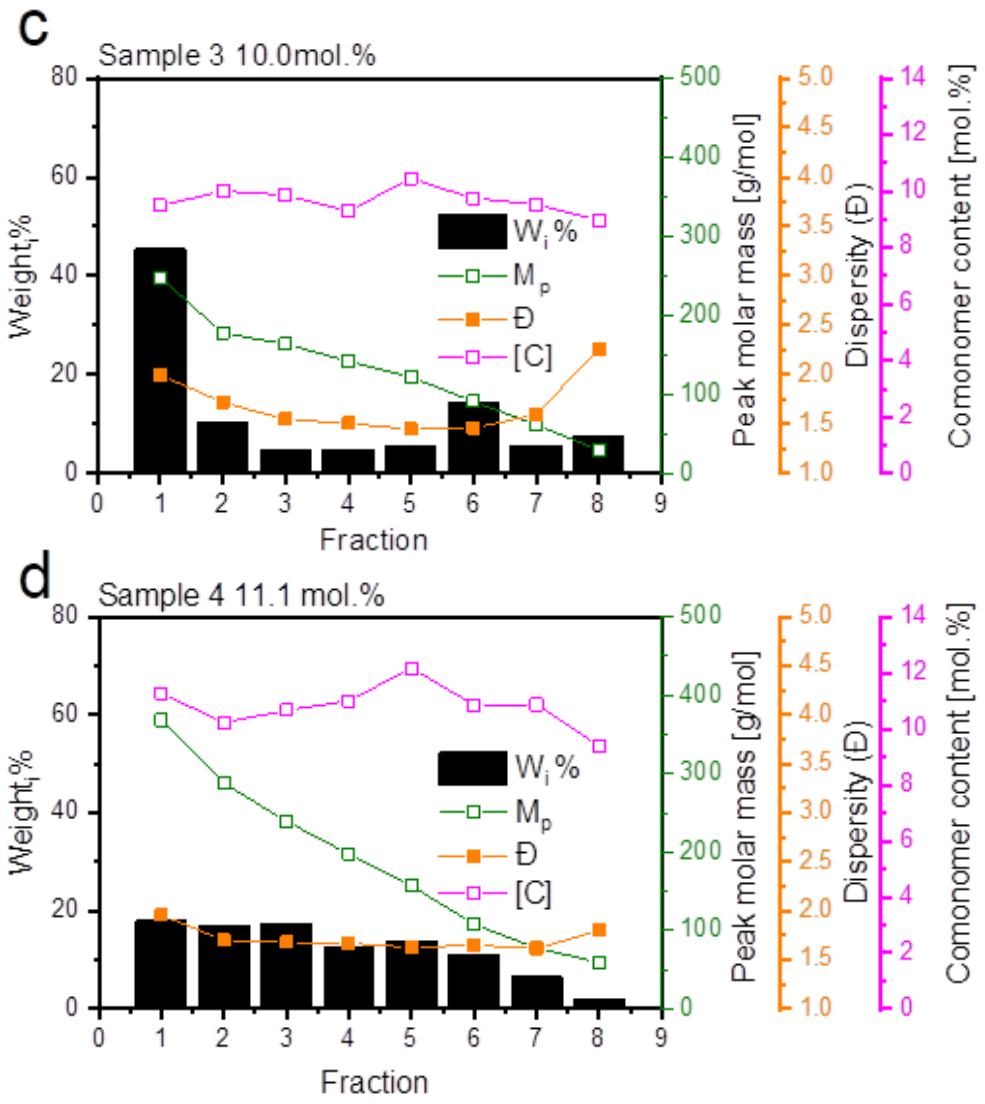

Figure 5. 2. Plots showing the percentage weight recoveries, peak molar mass from and dispersity as obtained from HT-SEC and comonomer content of the fractions for samples1-4 in (a-d) respectively.

Generally, chemical composition does not play a significant role in molar mass fractionation. To evaluate this, fraction properties were compared from the four samples. Fig. 5.3 compares the peak molar mass, dispersities and comonomer content for the fractions obtained from different samples. It is evident that as the comonomer content of the bulk samples increases the peak molar mass of the fractions collected at similar volumes also increases, see Fig. 5.3a. The differences in the peak molar mass are pronounced in the first fraction and decrease with fraction number.

The separations in HT-SEC are based on hydrodynamic volume (V_h) while those in p-MMF are assumed to be according to absolute molar mass. However, it would be speculative to assume that the fractions collected at the same solvent/non-solvent ratio have similar absolute molar mass. To prove this, the HT-SEC would have to be coupled to the multi-angle laser light scattering (MALLS) detector to obtain information on the hydrodynamic radii (R_h) and absolute molar mass.

The dispersities of all the fractions are rather narrow as already discussed earlier, see Fig.5.3a. The average comonomer contents of the fractions mimic those of their respective bulk samples. From Fig. 5.3c it is evident that the fractions have rather similar chemical compositions as discussed in the previous sections. When the fraction comonomer contents are plotted as a function of their peak molar mass, small differences are seen in the behaviour of samples 2 and 3 which suggests that the low molar mass fractions have slightly lower comonomer contents, see Fig. 5.3d.

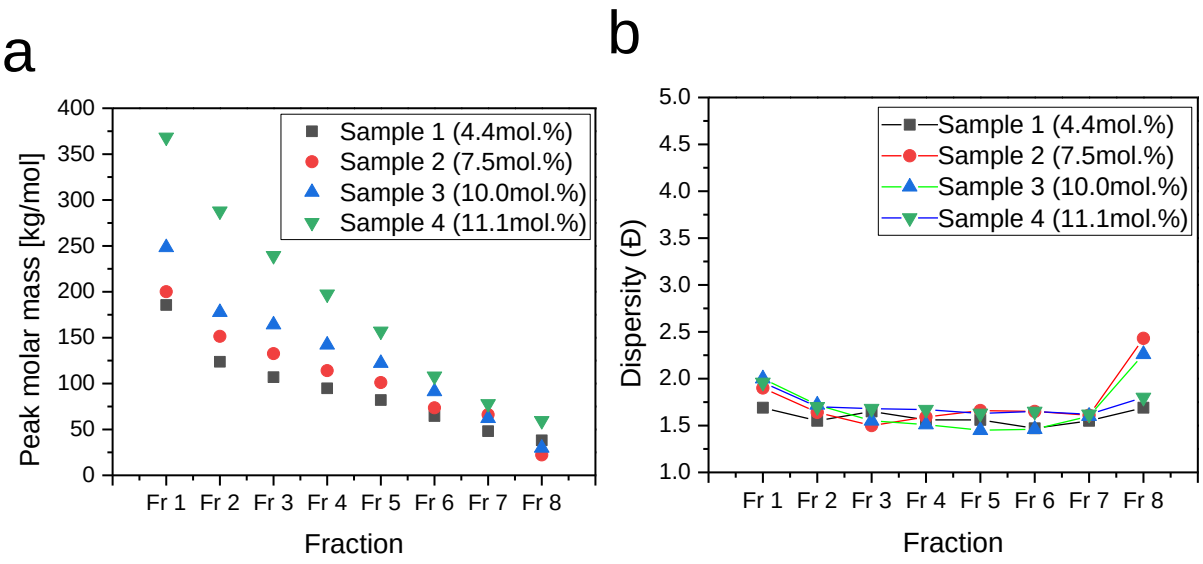

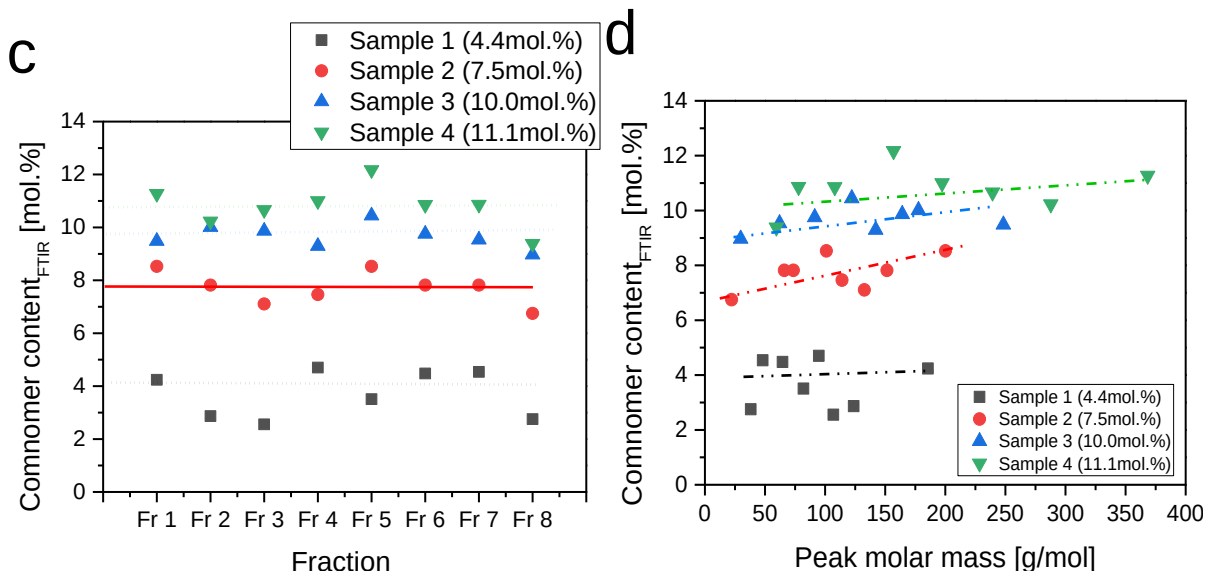

Figure 5.3. Fraction peak molar mass (a), dispersity (b) and comonomer content (c) as a function of fraction number for the fractions obtained from samples 1-4; comonomer content as a function of peak molar mass (d).

Fig. 5.4 shows the molar mass distribution curves of the fractions and their respective bulk samples. The molar mass distribution curves indicate visually what has been discussed in the previous sections. The peak molar masses are distinctly isolated from the other and the distributions are quite narrow. These are all indications of a successful fractionation according to molar mass. The thermal properties of the fractions were obtained using DSC and compared to their respective bulks as illustrated in Fig. 5.5a-d.

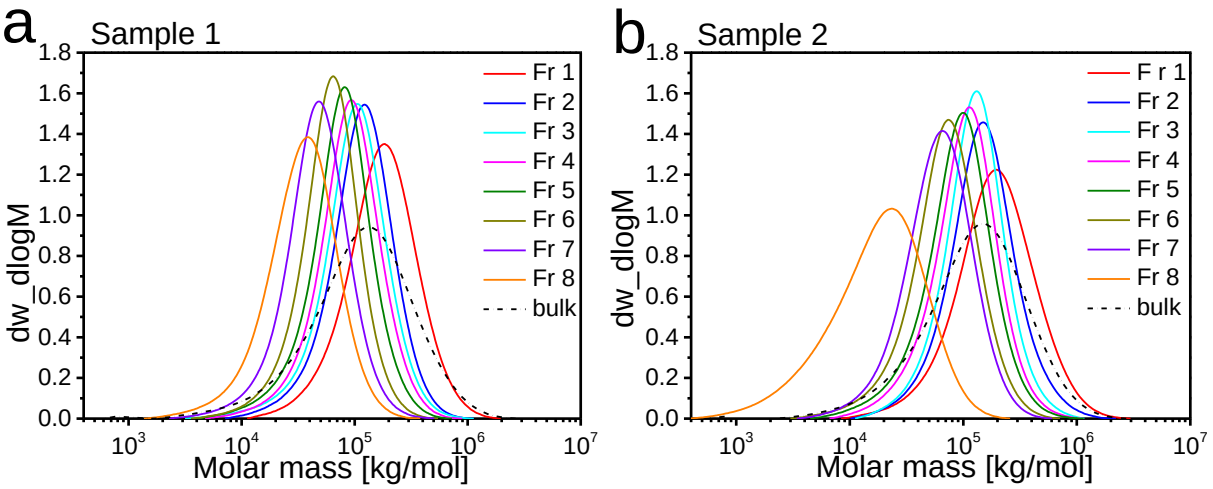

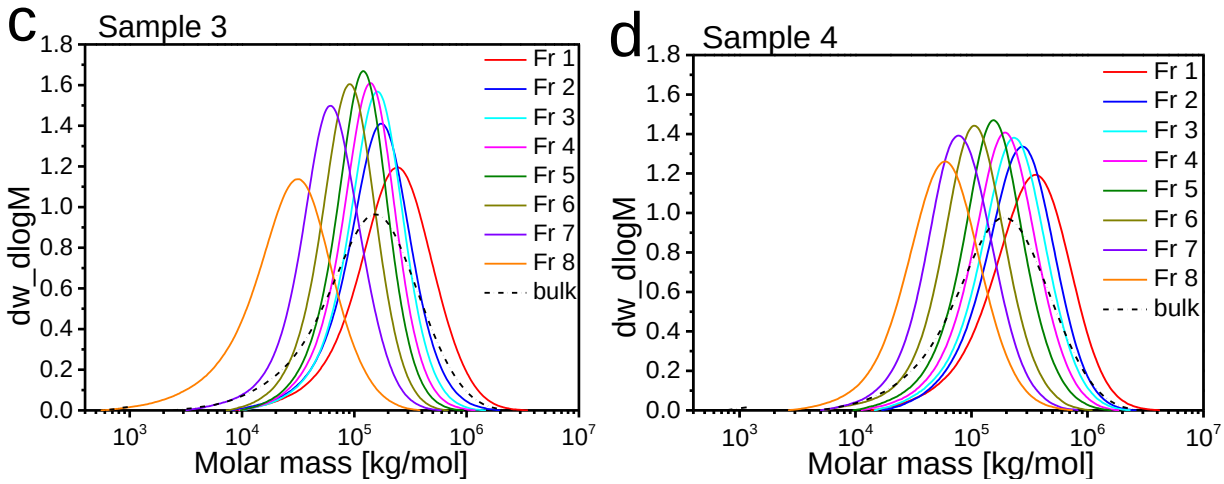

Figure 5.4. Molar mass distribution curves for samples 1-4 p-MMF fractions.

The fractions behave quite similar to the bulk materials although small differences can be seen. The cooling thermograms show two peak temperatures, one intense peak and a broader less visible peak; this is typical of m-LLDPE elastomers.[3-6] Furthermore, since the shape of the exotherms is similar for the fractions, the difference in the cooling peak temperature could be a result of intrachain distribution rather than intermolecular chain distribution.

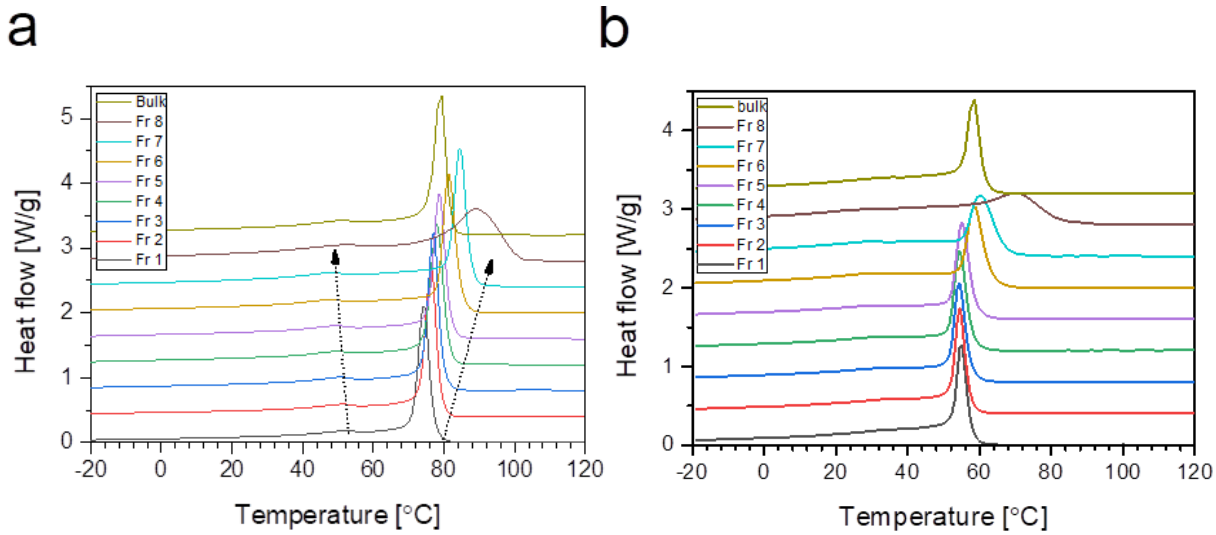

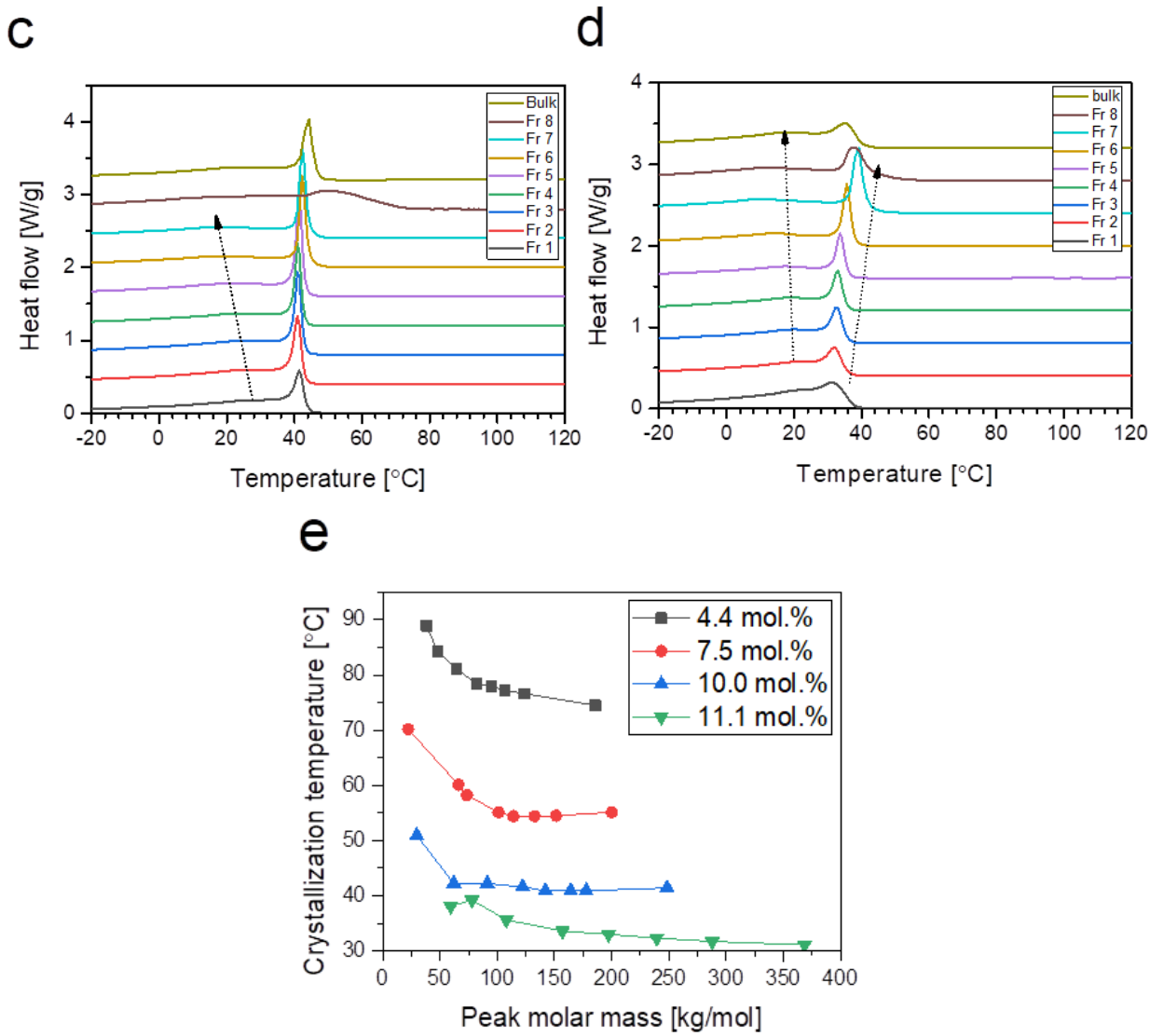

Figure 5.5. DSC crystallization exotherms of samples 1-4 p-MMF fractions (a-d). The dotted arrows show trends in the crystallization behaviour of the peaks; fraction crystallization temperature as a function of peak molar mass for the four samples (e).

Fractions from samples 1,2 and 4 show an increase in the crystallization temperature with decrease in molar mass or increase in fraction number. This can be attributed to the rapid rearrangement of smaller chains as compared to the larger chains. Since the comonomer content is rather similar, it can be assumed that it plays an insignificant role across a fraction set. The increase in the crystallization temperature of the fractions is rather surprising since the fractions have similar comonomer contents as shown in Table 5.2. Hosoda[7] demonstrated that the crystallization behaviour of LLDPE copolymers with molar masses greater than 100 kg/mol

is mainly influenced by SCB content. The eighth fraction in each of the samples has a broad crystallization temperature which indicates broad chemical composition. This is derived from the fact that the molar mases of the fractions are quite narrow as already highlighted in the above discussion.

HT-SGIC separates polyolefin chains based on the selective interactions with the Hypercarb® stationary phase, irrespective of their crystallinity, as previously discussed in the preceding chapter. Figure 5.6 shows the elution behaviour of samples 1-4(a-d) p-MMF fractions at a 30 min 1-decanol→TCB gradient. The p-MMF technique fractionates polymers based on their molar mass, therefore, all the fractions were expected to elute in a similar elution volume in HT-SGIC since they have similar chemical compositions. There were no unretained components (below 1.50 mL) in all of the elugrams of the respective samples. This suggests that all the copolymer chains exhibit long ethylene sequence lengths.

The elugrams of sample 1 fractions (Figure 5.6a) show bimodal elution peaks which indicate the molecular structure complexity as a result of chemical structure heterogeneity within each faction. This is a typical characteristic of LLDPE copolymers synthesized by ZN-catalyst. However, such behaviour is observable from the bulk elugram. The early eluting peak shows a slight decrease in its elution volume, which indicates a change in interaction behaviour and is suspected to be due to PE copolymers. This in turn could be influenced by the decrease in fraction molar mass.

A second sharper peak elutes at relatively the same position in the fractions. The differences in the first and second peaks can be due to differences in chemical composition. The late eluting peak could be a PE homopolymer. The second peak disappears with decreasing molar mass. Sample 1 has the least comonomer content of the investigated samples. At such a low comonomer content, it is highly likely that interchain heterogeneity exits due to the limited availability of the comonomer in the reaction mixture as the polymerization progresses. However, the exact polymerisation conditions have to be known. Therefore, fractions of the copolymer with less comonomer incorporation will exist as the reaction progresses.

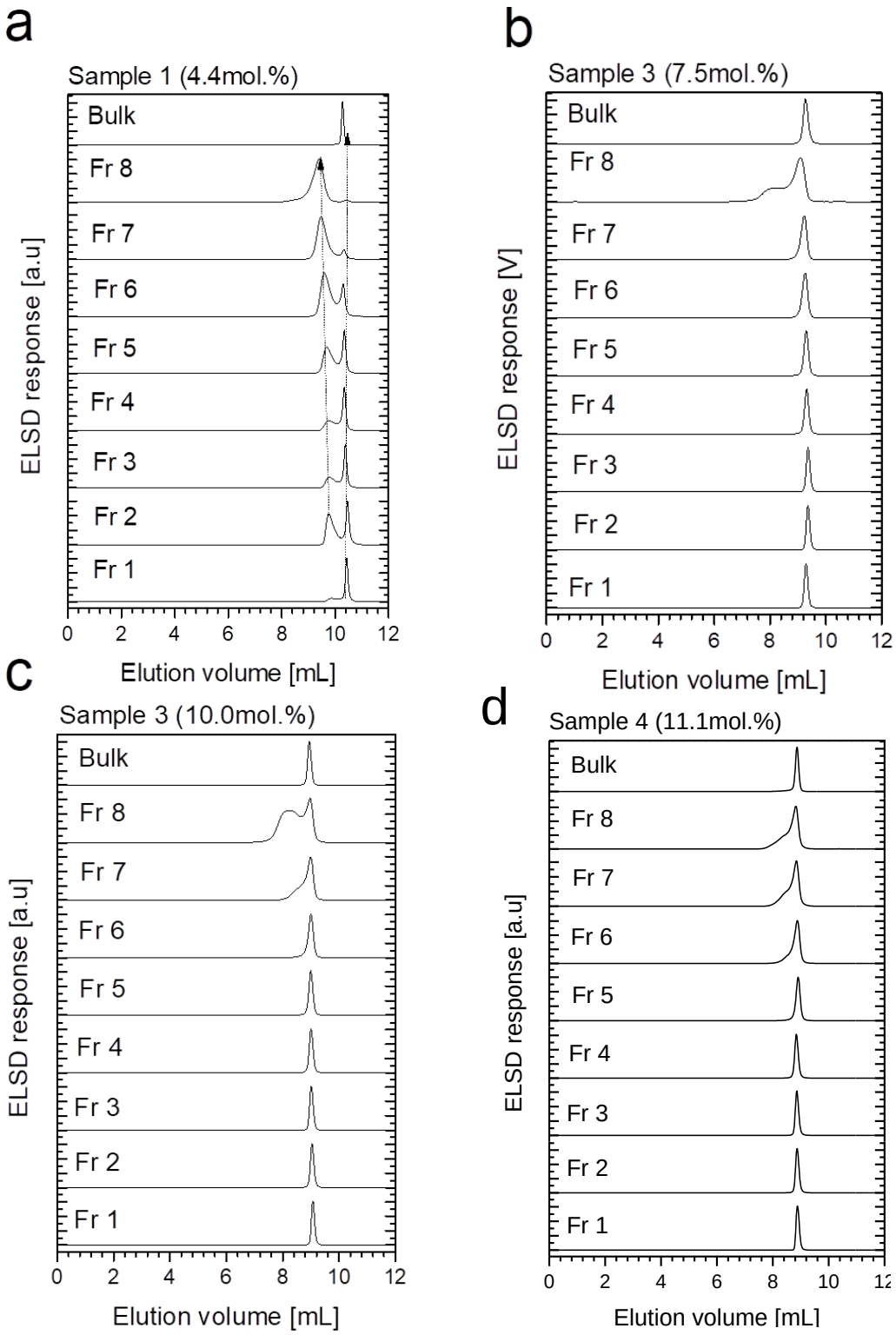

Figure 5.6. Elution behaviour of sample 1-4(a-d) p-MMF fractions on porous graphitic carbon stationary phase of under a 1-decanol→$TCB_{30\ min}$ solvent gradient.

With regards to samples 2-4, there is no observable presence of homopolymers. Their respective fractions are rather homogenous in their elution behaviour with the exception of fraction 6-8 for each sample. This homogeneous elution behaviour confirms the p-MMF process separated polymer molecules according to molar mass rather than chemical composition. Fig. 5.7 shows the overlays of the elugrams for better comparison. The observed broad elution in the fractions 6-8 for samples 2-4 can be attributed to the relatively lower molar mass of the fractions as compared to the fractions 1-5.

It is speculated that as the comonomer feed is increased to target a higher comonomer end product, the polymerization reactions produce more uniform polymer chains as compared to when the comonomer feed is restricted. Al-Khazaal et al.[8] recently reported a similar elution behaviour of LLDPE elastomers and demonstrated that longest ethylene sequence length distribution (LESLD) and overall ethylene sequence distribution (OESD) decreased with chain length. However, neither the LESD nor OESD could account for the elution behaviour of the EO molecules in TGIC.

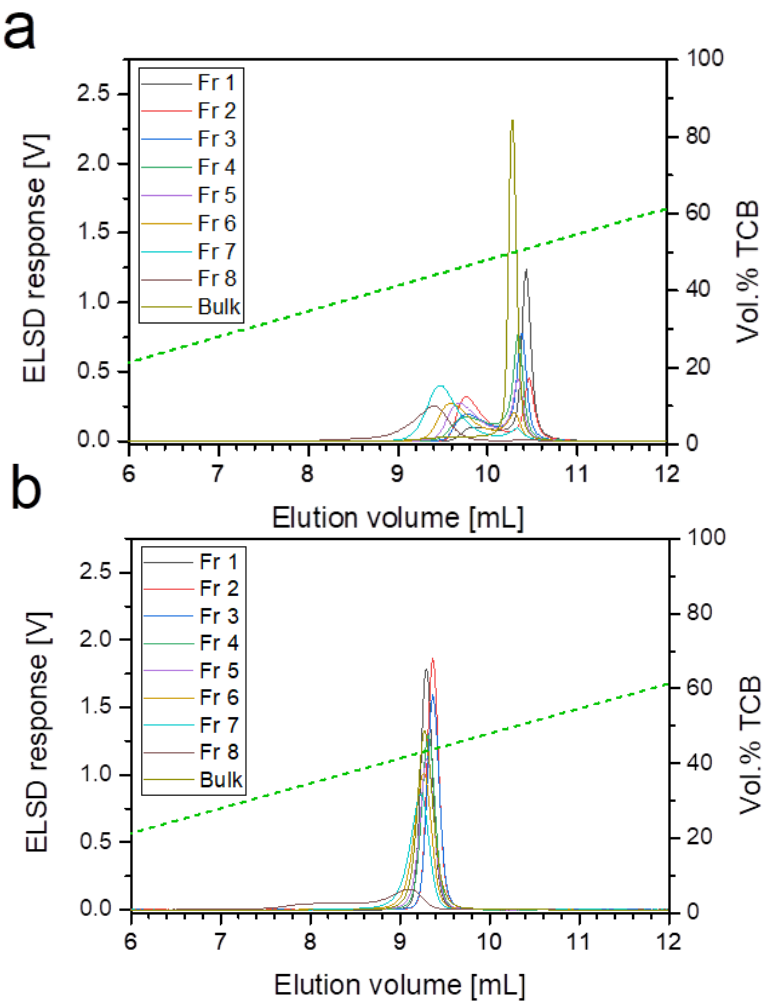

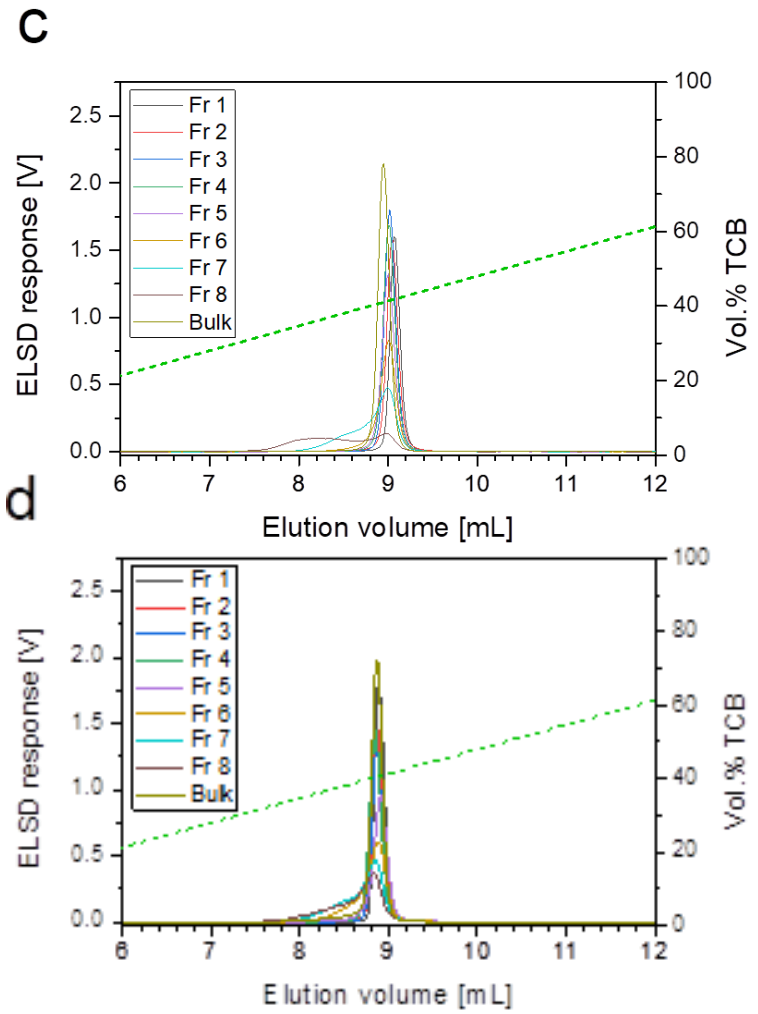

Figure 5.7. Overlays of elugrams of sample 1-4(a-d) p-MMF fractions on porous graphitic carbon stationary phase of under a 1-decanol→$TCB_{30\ min}$ solvent gradient.

To compare the elution behaviour of the fractions across the bulk samples, Fig. 5.8 was constructed. Here it can be seen that the fraction elution volume is influenced by the chemical composition of the bulk. The three last fractions elute in rather lower elution volume as compared to the first five. Apart from this, the rest of the samples show that the fractions elute at similar elution volumes. The fractionation produces fractions with similar chemical composition/comonomer content, which is expected. As the comonomer content increases, the polymer chains across all fractions are expected to have uniformly distributed comonomer.

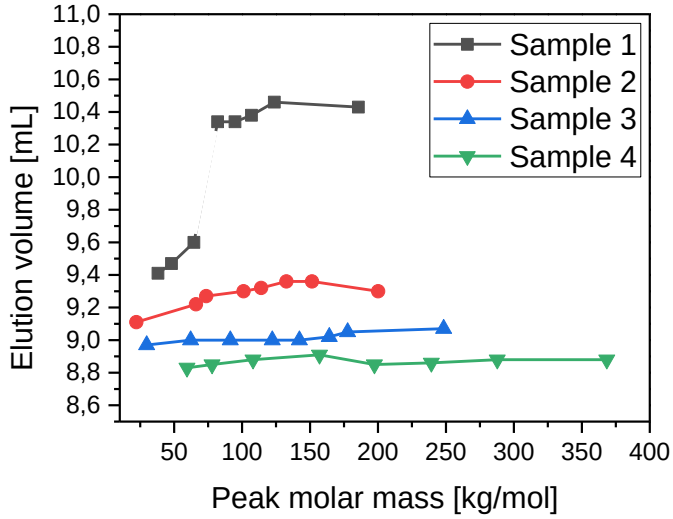

Figure 5.8. Relationship between elution volume and the peak molar mass of the factions obtained from four LLDPE samples depicting their molecular structure complexity.

The sampling volume from the first dimension is 100 µL. Therefore, some material from different peaks can be co-sampled into the second dimension.

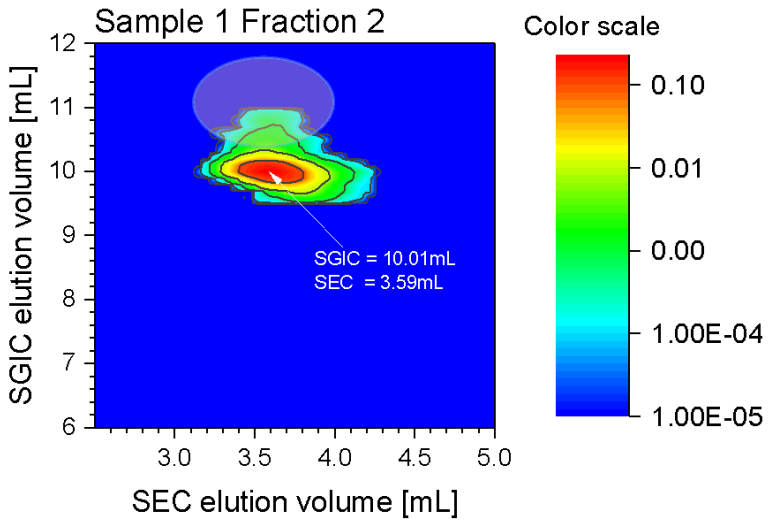

Figure 5.9. 2D-LC contour plot for the sample 1 p-MMF fraction 2. Porous graphitic carbon was used in the first dimension with a flow rate of 0.05 mL/min at 160 °C. A 1-decanol→TCB_{300min} gradient was used in the first dimension. In the second dimension, a Rapide H SEC column was used at 160 °C with a flow rate of ODCB of 2.75 mL/min. 110 µL of the sample was injected.

However, it can be seen that the early eluting components have lower molar mass as compared to the late eluting ones. To better illustrate this, the SEC elugrams obtained in the second dimension are plotted in Fig. 5.10. The molar mass of the eluting components increases up to 10.1 mL as the SGIC elution volume decreases, suggesting molar mass dependence of the elution behaviour of fraction 2 polymer chains.

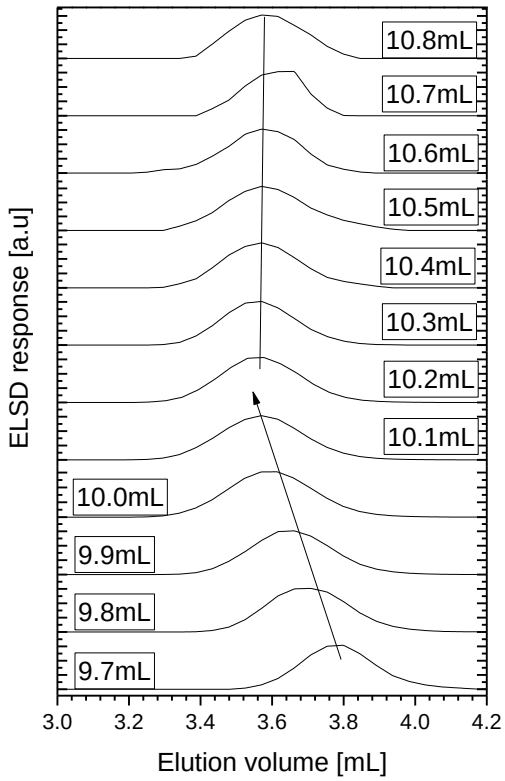

Figure 5.10. HT-SEC traces obtained from the second dimension during the two-dimensional analysis of Sample 1 Fr 2.

5.4. Conclusions

Higher comonomer contents prevent LLDPE to be fractionated using preparative temperature rising elution fractionation (p-TREF) and other crystallization-based techniques. Preparative molar mass fractionation (p-MMF) is an alternative that can simplify the complexity of the bulk sample to produce fractions for offline analysis. Four samples with increasing comonomer contents but comparable molar masses were the subject of study in order to determine the influence of chemical composition on the p-MMF process. Eight fractions were recovered from each of the samples that were investigated. The findings show that fractions collected at similar

solvent/non-solvent ratios have dissimilar molar masses. However, the fraction chemical composition was independent of the fraction number and was influenced by the average chemical composition of the respective bulk sample. Sample 1 fractions showed presence of both PE copolymer and homopolymer in their SGIC elution profile. Three low molar mass fractions of this sample were observed to have different elution behaviour in SGIC which were attributed to presence of PE homopolymer. A decrease in the chemical composition heterogeneity with an increase in the bulk sample comonomer content was also observed. This was attributed to the uniformity in the comonomer distribution across the fractions as the comonomer content was increased.

5.5. References

1. Ndiripo, A.; Joubert, D.; Pasch, H. *J. Polym. Sci., Part A: Polym. Chem.* **2016**, *54*, 962–975.
2. Ndiripo, A.; Pasch, H. *Anal. Bioanal.Chem.* **2015**, *407*, 6493–6503.
3. Tarasova, E.; Poltimäe, T.; Krumme, A.; Lehtinen, A.; Viikna, A. *Macromol. Symp.* **2009**, *282*, 175–184.
4. Leone, G.; Mauri, M.; Pierro, I.; Ricci, G.; Canetti, M.; Bertini, F. *Polymer* **2016**, *100*, 37-44.
5. (5) Razavi-Nouri, M. *Polym. Test.* **2006**, *25*, 1052–1058.
6. Liu, W.; Wang, W.-J.; Fan, H.; Yu, L.; Li, B.-G.; Zhu, S. *Eur. Polym. J.* **2014**, *54*, 160–171.
7. Hosoda, S. *Polym. J.* **1988**, *20*, 383–397.
8. Al-Khazaal, A. Z.; Soares, J. B. *Macromol. Chem. Phys.* **2017**, *218*, 1600332.

Chapter 6

Comprehensive microstructural analysis of ethylene-co-1-octene elastomers by preparative fractionation and high temperature chromatography

In the present chapter, three commercial polyolefin elastomers with comparable bulk comonomer contents are fractionated and analysed using offline advanced analytical techniques.

6.1. Introduction

It has been shown in Chapter 5 that p-MMF fractionation provides useful information regarding the molecular structure of non-crystalline and crystalline LLDPEs. The elastomers, although non-crystalline, have unique properties which make them useful in particular applications such as films for packaging. The characterization of non-crystalline LLDPEs by preparative fractionation methods has not been extensively conducted. This chapter focuses mainly on the characterization of three commercial elastomers with high 1-octene contents which were fractionated according to molar mass using the p-MMF method.

6.2. Bulk analysis

The three commercial samples under investigation were obtain from different suppliers and their bulk properties are given in table 6.1.

Table 6.1. Molar mass and average chemical composition information of three elastomer bulk samples as determined by HT-SEC and FTIR, respectively.

Supplier	Sample	[C][a] [mol%]	M_p[b] [kg/mol]	M_n[b] [kg/mol]	M_w[b] [kg/mol]	Đ[b]
Dow Chemicals	**ENGAGE 8842**	13.3	211.0	99.1	250.7	2.5
Dow Chemicals	**ENGAGE 8100**	10.4	176.2	79.9	212.1	2.7
Mitsui Chemicals	**TAFMER**	10.1	134.9	57.7	152.4	2.6

[a] comonomer content as determined by ^{13}C-NMR. [b] determined by HT-SEC, polystyrene equivalent molar mass.

The molar mass properties of the three LLDPE elastomers were obtained by HT-SEC using a polystyrene calibration, see Table 6.1. The bulk samples have narrow dispersities which are characteristic of LLDPEs produced by metallocene catalyst. In addition to having narrow molar mass distributions, the samples are expected to have narrow chemical composition distributions.

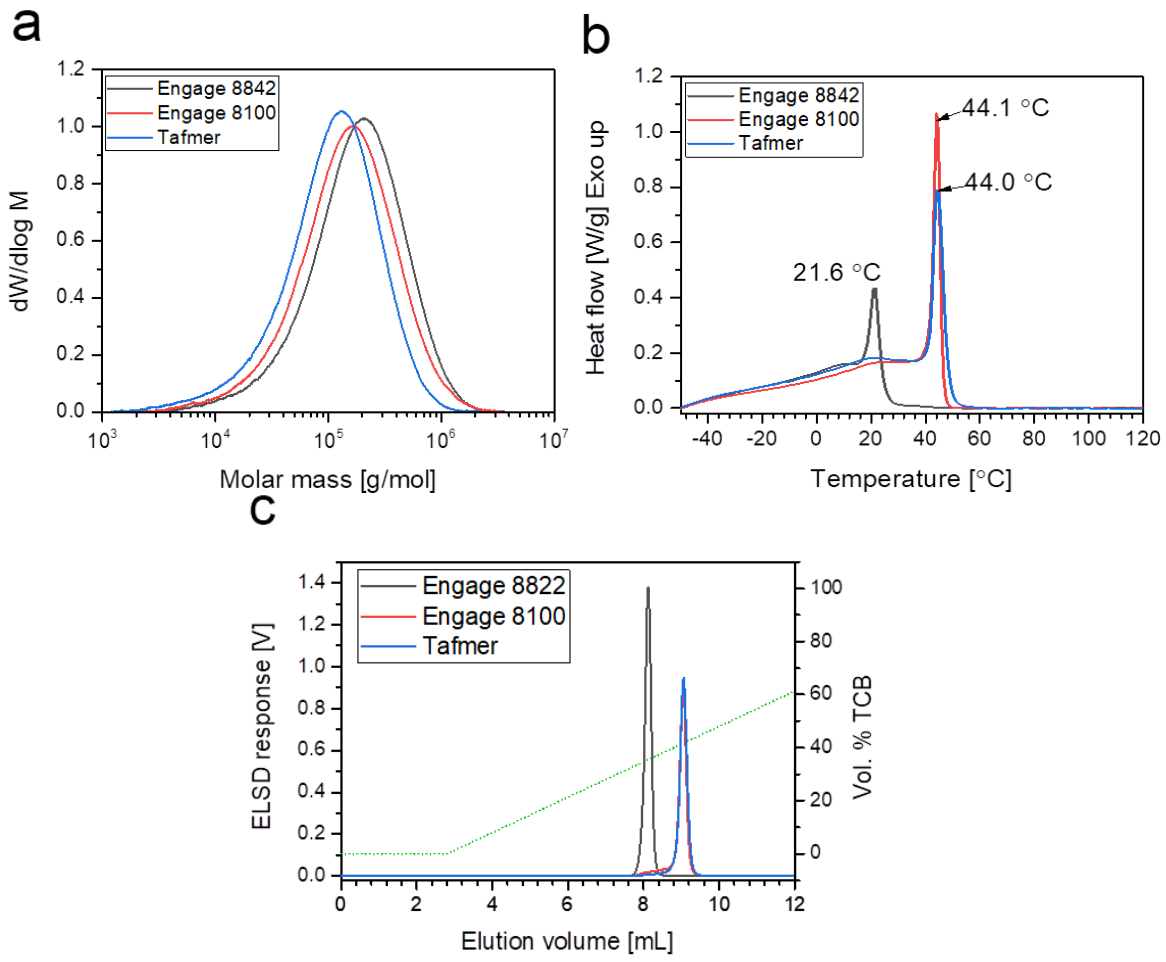

Figure 6.1. Molar mass distribution profiles of the three samples as determined HT-SEC (a) DSC first crystallization profiles (b) and HT-SGIC elugrams of the three LLDPE elastomers (c).

Figure 6.1a-c shows the molar mass distribution, DSC crystallization curves and the HT-SGIC peak elution behaviour of the three elastomers respectively. The DSC crystallization behaviour of these samples shows that Engage 8842 has a low crystallization temperature that is represented by the broad peak at 21.6 °C, attributed to higher comonomer content compared to the other samples.

The elution behaviour of these three samples in HT-SGIC also shows that the low comonomer content material is more retained and elutes last while Engage 8842 elutes first. This observed HT-SGIC elution behaviour and the comonomer content correlate with DSC crystallization behaviour of the samples. For an in-depth microstructural analysis, the samples were fractionated using p-MMF into several fractions for offline characterization.

Table 6.2 summarises the fraction recovered quantities, molar mass and chemical composition properties. Fig. 6.2 also summarizes the recovered fraction quantities as well as the peak molar mases, comonomer content and dispersities. Except for Engage 8100, 8 fractions were recovered from all the samples that were fractionated

6.3. Preparative fractionation

Table 6.2 A summary of p-MMF fractions of Engage 8842, Engage 8100 and Tafmer as determined by HT-SEC.

Fractions	**NS/SR[a] [mL]**	**[C][b] mol.%**	**Recovery Wt.%**	**M_p[c] [kg/mol]**	**M_n[c] [kg/mol]**	**M_w[c] [kg/mol]**	**Đ[c]**
			Engage 8842				
Fr 1	0.80	n.m	n.m	n.m	n.m	n.m	n.m
Fr 2	0.83	13.7	9.4	448.0	189.0	463.1	2.5
Fr 3	0.85	12.7	26.3	313.3	96.2	325.6	3.4
Fr 4	0.88	11.9	15.6	238.7	117.0	264.7	2.3
Fr 5	0.93	14.2	15.5	183.2	77.9	200.8	2.6
Fr 6	1.03	13.7	17.5	124.8	65.2	149.2	2.3
Fr 7	1.23	13.7	6.7	90.8	58.1	116.8	2.0
Fr 8	Soluble	13.6	8.8	75.9	38.2	93.6	2.5
Total recovery			**99.8**				
			Engage 8100				
Fr 1	0.80	9.2	37.5	291.1	183.6	310.4	1.7
Fr 2	0.83	9.9	17.8	192.3	133.9	205.8	1.5
Fr 3	0.85	10.8	13.1	149.1	105.4	160.3	1.5
Fr 4	0.88	11.2	8.7	122.3	86.7	131.1	1.5
Fr 5	0.93	11.7	5.1	100.8	73.6	107.3	1.5
Fr 6	1.03	10.8	9.9	88.3	60.1	95.0	1.6
Fr 7	1.23	9.7	3.8	55.3	43.9	65.0	1.5
Fr 8	Soluble	10.1	3.0	52.4	36.8	61.8	1.7
Total recovery			**98.9**				

			Tafmer				
Fr 1	0.8	9.6	15.2	129.0	55.8	168.7	3.0
Fr 2	0.83	8.4	23.6	107.2	40.6	111.5	2.8
Fr 3	0.85	10.2	14.8	91.3	37.9	98.1	2.6
Fr 4	0.88	9.8	7.7	110.8	65.8	113.3	1.7
Fr 5	0.93	10.2	14.0	80.6	46.6	91.0	2.0
Fr 6	1.03	9.9	7.9	72.9	50.4	84.6	1.7
Fr 7	1.23	10.0	7.2	78.5	53.8	86.5	1.6
Fr 8	Soluble	10.2	8.4	38.0	26.7	52.6	2.0
Total recovery			**98.8**				

[a] denotes non-solvent/solvent ratio, [b] comonomer content as determined by FTIR,
[c] molar mass properties as determined by HT-SEC, **n.m** denotes 'no material'

Figure 6.3 (a-c) present molar mass distribution curves of the fractions. Engage 8842 and Engage 8100 fractions are broadly distributed from fraction 1 to fraction 8 in an orderly manner. Furthermore, Engage 8100 p-MMF fractions exhibit narrower molar dispersity, indicative of more pronounced molar mass homogeneity than the Engage 8842 fractions. On the other hand, the Tafmer p-MMF fraction molar mass distribution curves do not show any observable trend between molar mass and fraction number. At present, an explanation for this failure of the same preparative-technique to produce fractions with dissimilar molar mass is undeveloped.

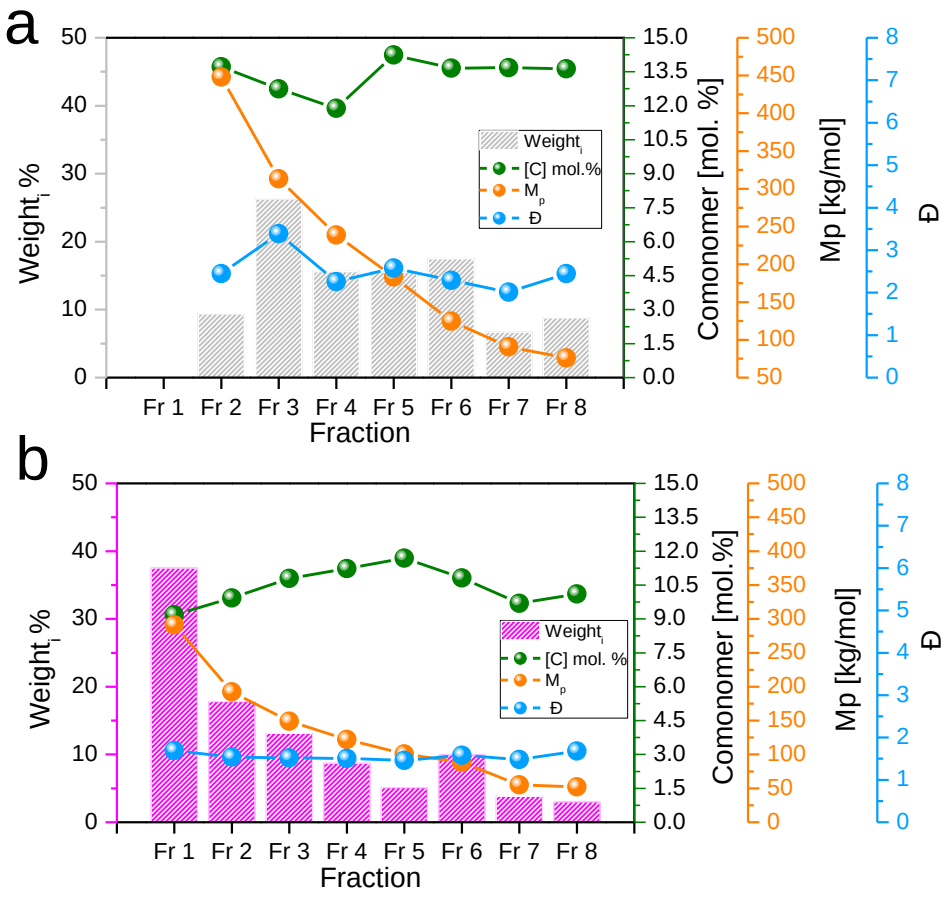

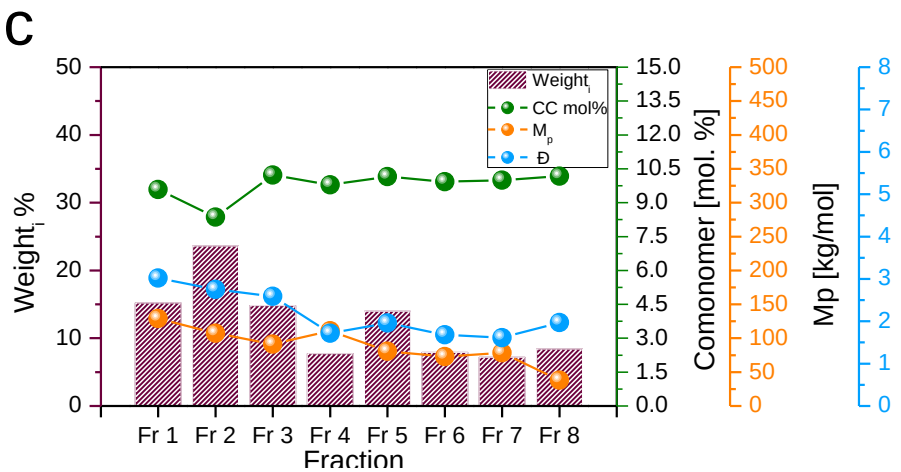

Figure 6.2. Graphs showing the recovered fraction quantities peak molar mass and dispersities of Engage 8842 (a), Engage8100 (b) and Tafmer (c).

Fig. 6.4a shows the fraction peak molar masses of the three samples. A greater variation in the peak molar mass is seen for the first fractions and decreases with increasing fraction number.

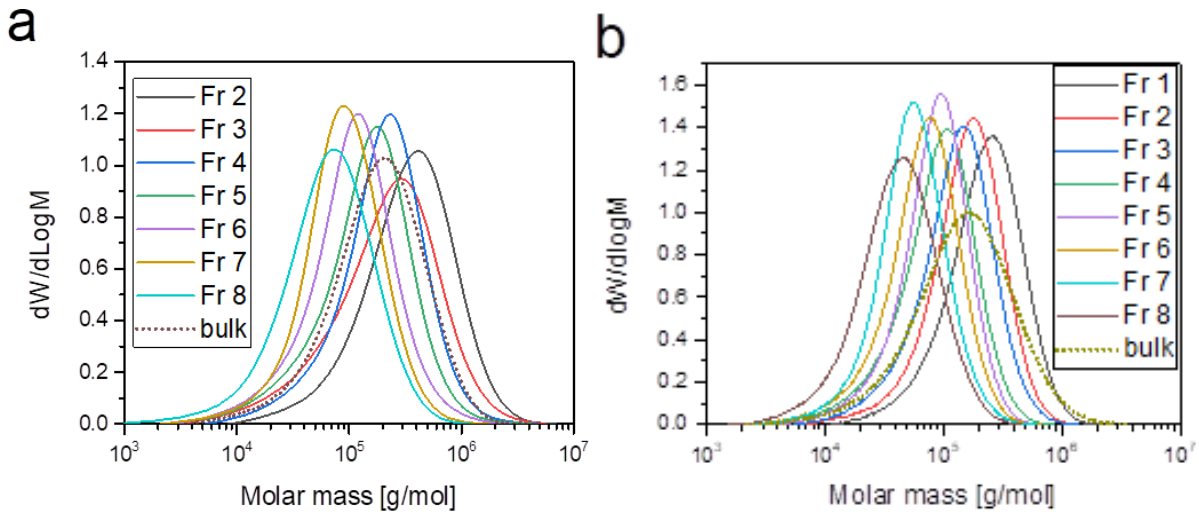

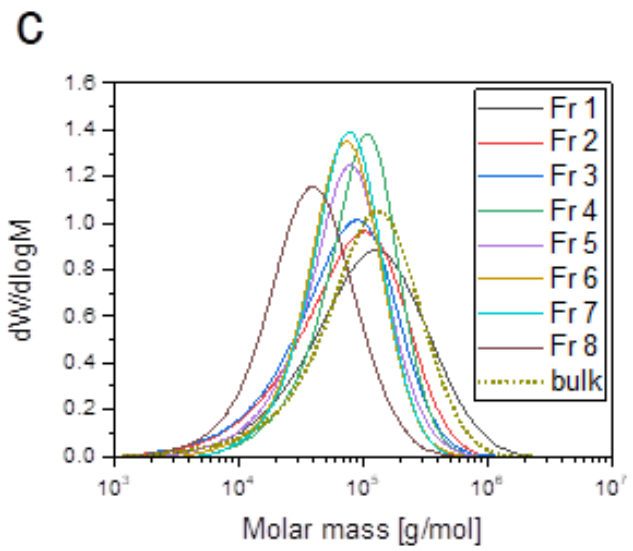

Figure 6.3. Molar mass distribution profiles of p-MMF fractions of the three samples obtained by HT-SEC. The fractions of Engage8842, Engage 8100 and Tafmer are shown in (a-c) respectively.

This trend can be directly related to the SEC findings reported in Fig. 6.1a as well as the plot showing the fraction weight against the molar mass (Fig. 6.4b). This means at any given solvent/non-solvent ratio, the fractions of Engage 8842 will consist of polymer chains with a slightly higher peak molar mass as compared to Engage 8100 and Tafmer. The same can be said when Engage 8100 is compared to Tafmer.

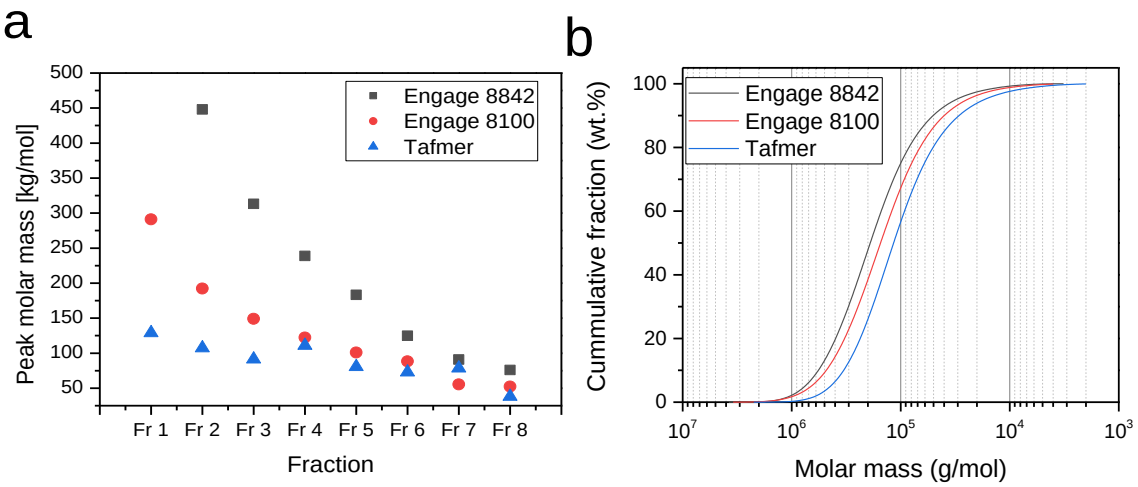

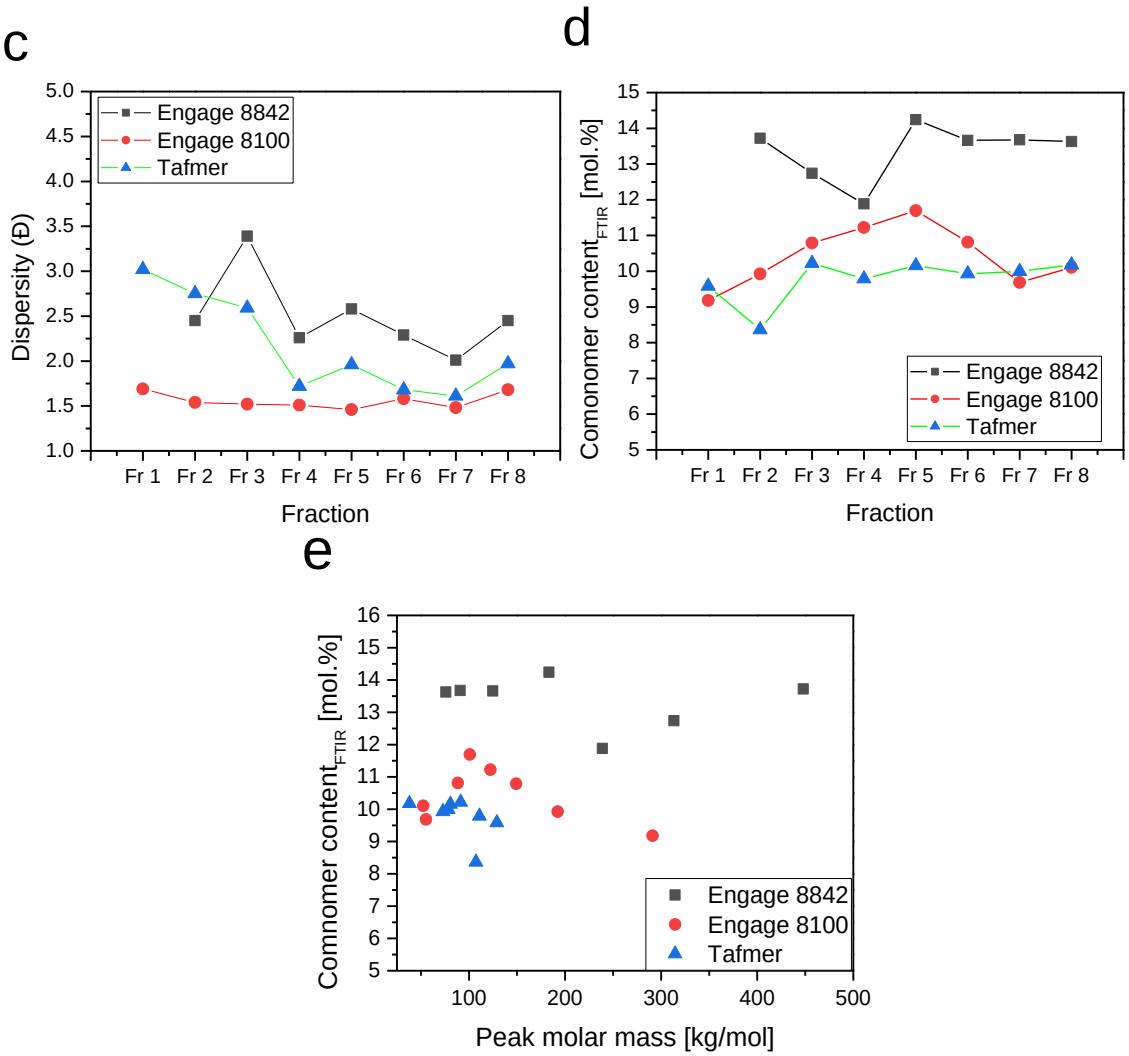

Figure 6.4. Plots showing the peak molar mass, cumulative fraction, dispersity, and comonomer content as a function of the fraction number for Engage 8842, Engage 8100 and Tafmer in (a-d) respectively; plot of fraction peak molar mass of Engage 8842, Engage 8100 and Tafmer fractions against the respective comonomer content (e).

The fraction dispersities are low as expected and are graphically illustrated in Fig. 6.4c. The fraction comonomer contents were calculated from FTIR analyses used the calibration curve mentioned in Chapter 4. The fraction comonomer contents are illustrated in Fig. 6.4d. As previously mentioned in the preceding chapters, FTIR determination comonomer content via a calibration curve is not as accurate as accurate as that obtained via ^{13}C-NMR. Fig. 6.4e relates the fraction peak molar mass to the comonomer content.

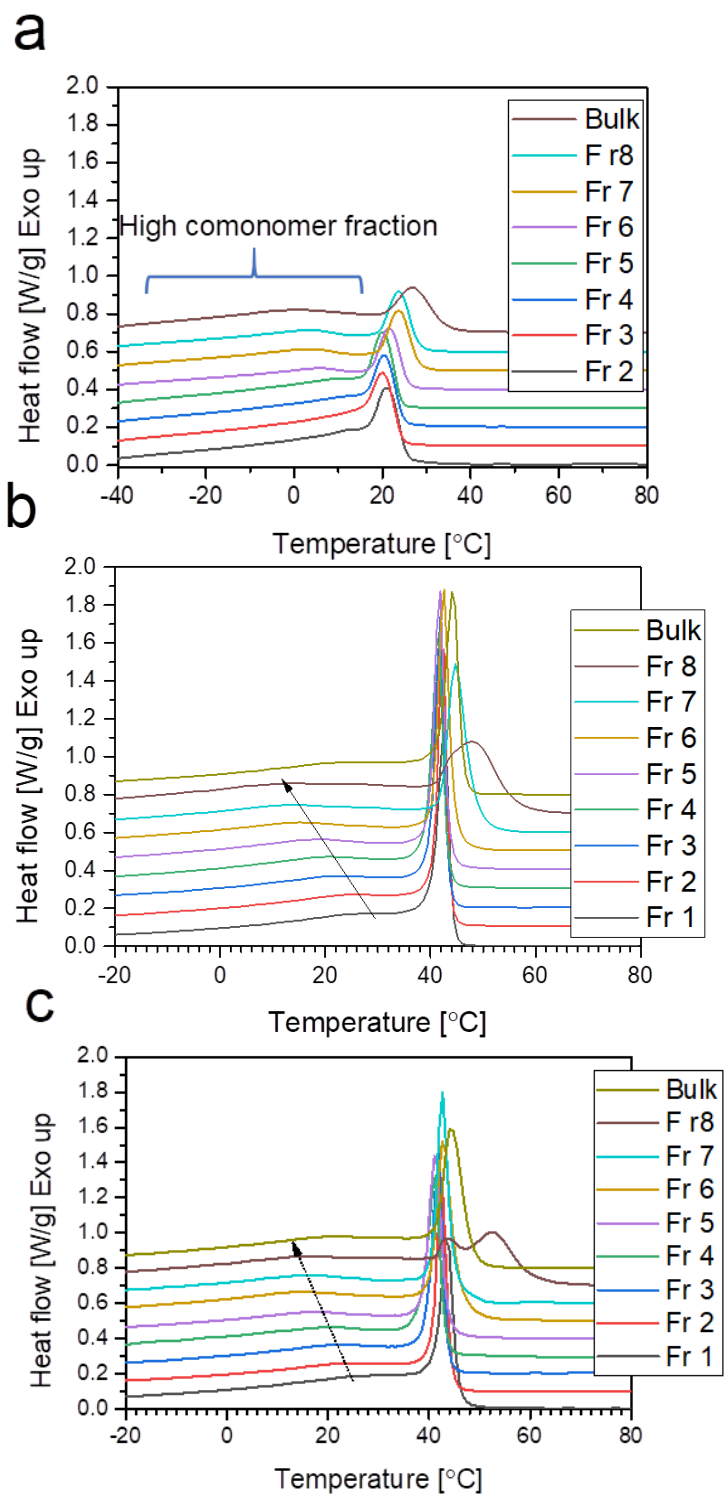

Figure 6.5. Relationship between the thermal behaviour of the p-MMF fractions and their bulk samples as recorded by their DSC cooling exotherms in the temperature range between -50 – 150 °C. The fractions of Engage 8842, Engage 8100 and Tafmer are shown in (a-c) respectively.

Here, it can be seen there is not a significant variation in the fraction comonomer content with molar mass. This is expected for p-MMF type fractionation since it is not affected by chemical composition. For more detailed information on the microstructure, particularly, the chemical composition distribution of these fractions and their respective bulk resins, it is necessary to employ other complementary analytical techniques such as DSC. This technique is widely used for thermal analysis of semicrystalline polyolefins.[1-3] DSC is based on the fact that molecular chains with varying amounts of SCB incorporation have varying lamellae thickness and crystallisable methylene sequence length.[4] Thus, both the chemical composition between polyolefin chains with varying molecular sizes and within the same polyolefin chain can be studied using DSC.

Figure 6.5 shows the cooling curves of the three elastomers and their fractions, respectively. It can be seen that all the thermograms show one main peak temperature and a shallower peak at low temperatures. This indicates presence of molecular chains with distinctly varying chemical composition. This is typical of less crystalline metallocene synthesized LLDPEs. Arndt[5] conducted DSC analysis of m-LLDPE elastomers with high 1-octene contents found similar thermal behaviour. The peak in the low temperature region was attributed to non-uniform comonomer incorporation between different polymer chains in the sample.[6]

Furthermore, the majority of the fractions for each sample crystallize within a similar temperature range. Razavi[7] studied the crystallization behaviour on DSC of m-LLDPE and m-VLDPE and showed that m-VLDPE exhibited several melting peaks some which with lower melting peaks and some higher than the crystallization temperature of the bulk which were attributed to molecular segregation. Zhang et al.[8] attributed the bimodal peak crystallization observed on the EO LLDPEs cooling thermograms to the metallocene-type catalyst. However, it can be seen that the crystallization temperature of the low molar mass fractions tends to increase and the peak also becomes broad; this is similar to the previous observations.

Note that the low molar mass (fraction 8) for TAFMER shows multimodal peak crystallization behaviour which extends to 52.4 °C. This indicates a complex composition. This can be attributed to molar mass influence as it is known that the crystallization of copolymers with low molar mass is more susceptible to the molar mass effect.[9,10] However, since molar mass has an influence on several properties of copolymers including its phase structure which dictate

their crystallinity, more powerful techniques that can probe further the composition of elastomers are essential.[11,12]

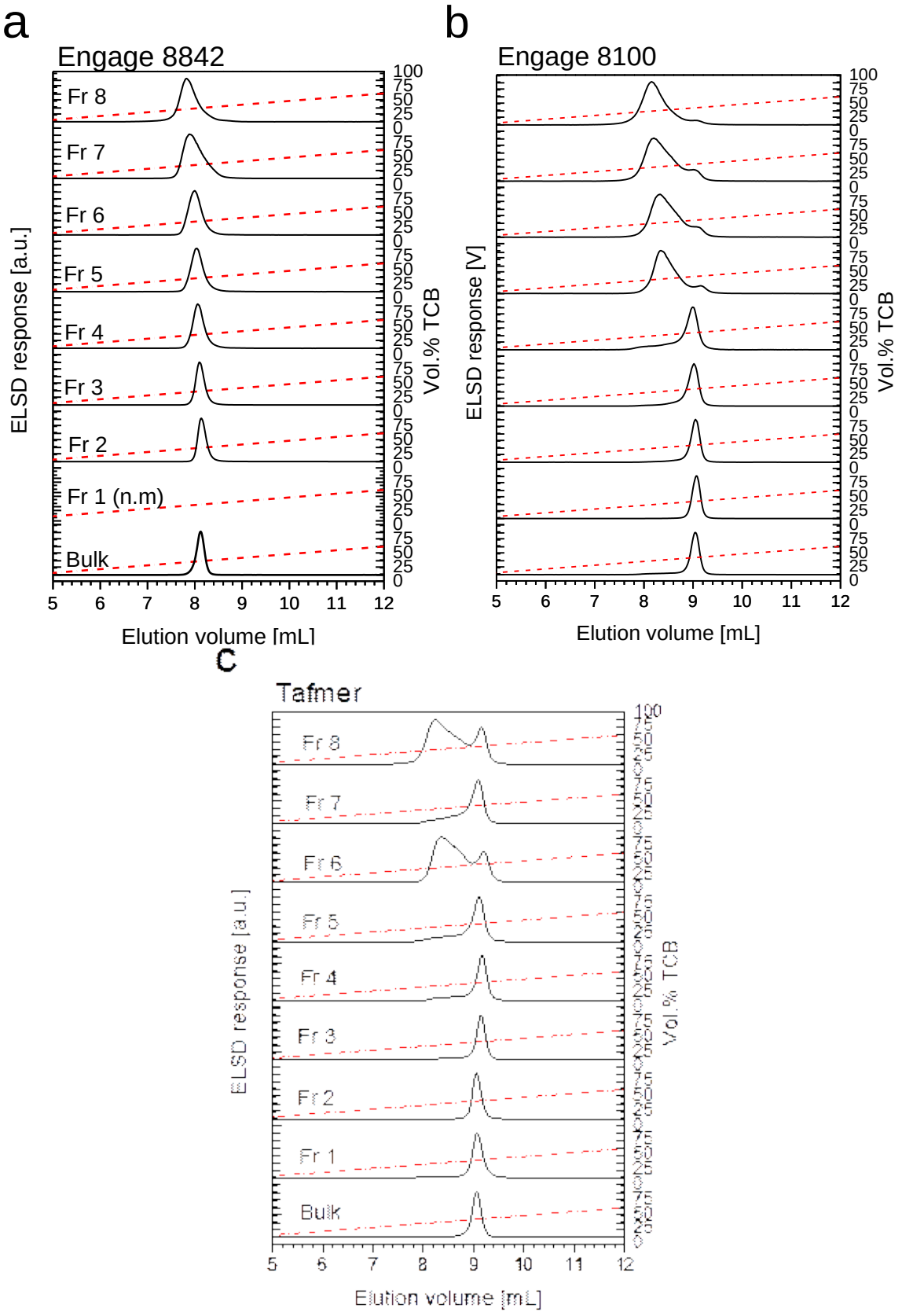

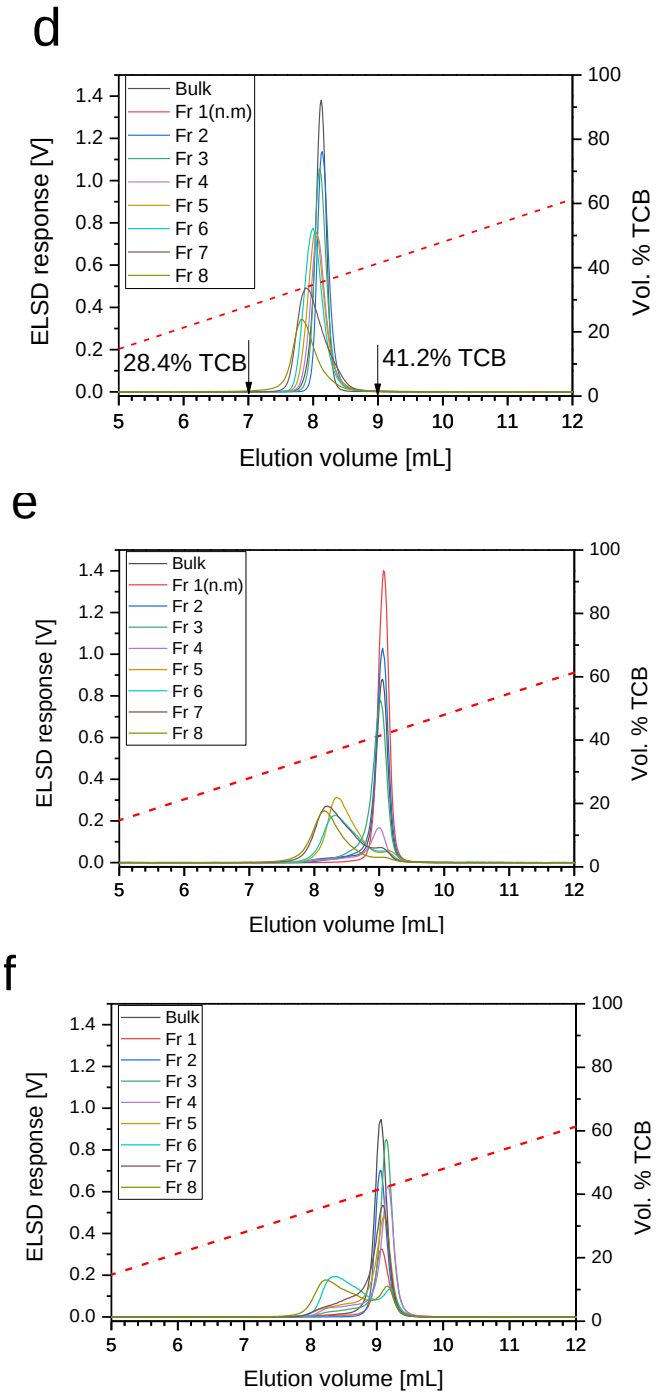

Figure 6.6. Elution behaviour of the Engage 8842, Engage 8100 and Tafmer bulk sample and their p-MMF fractions on HT-HPLC Hypercarb® stationary phase in a-c respectively. The elugrams of Engage 8842, Engage 8100 and Tafmer fractions and their bull samples are overlaid in d-f respectively.

HT-SGIC was used to analyse the p-MMF fractions and the results are summarised in Fig. 6.6. As seen in Fig. 6.6a, there is an observable trend between the elution volume and the fraction

number. The elution volume increases with increasing molar mass (from fraction 8 to 2). This observation is similar to the previously discussed p-MMF findings in Chapter 4 and 5. Moreover, Engage 8842 fractions show unimodal elugrams, which increase in broadness from fraction 2 to fraction 8. This indicates that the chemical homogeneity of the fractions decreases with decreasing molar mass.

The elution behaviour of Engage 8100 and its fractions is shown in Figure 6.6b. Fractions 1-4 show unimodal elugrams with similar peak maximum at about 9.0 mL. The similar elution volume of fraction 1-4 can be attributed to similar and narrow CCD of the fractions. On the other hand, fractions 5-8 elugrams show peak maxima at relatively low elution volumes (8.1 mL and 8.3 mL, respectively) and the second shoulder peak which extends to higher elution volumes.

The bimodal nature of the elugrams shows that these fractions constitute polymer chains that have relatively broader chemical composition distributions. Furthermore, the decreasing elution volume with decreasing molar mass for fraction 5-8 signifies the complex molecular structure of the fractions. However, these fractions exhibit very narrow dispersities (1.7 largest). This suggests that these fractions are homogeneous with respect to molar mass.

We further investigated the relationship between the M_p and elution behaviour in SGIC. As shown in Fig. 6.7, the elution volume of the fractions increases with increasing M_p.

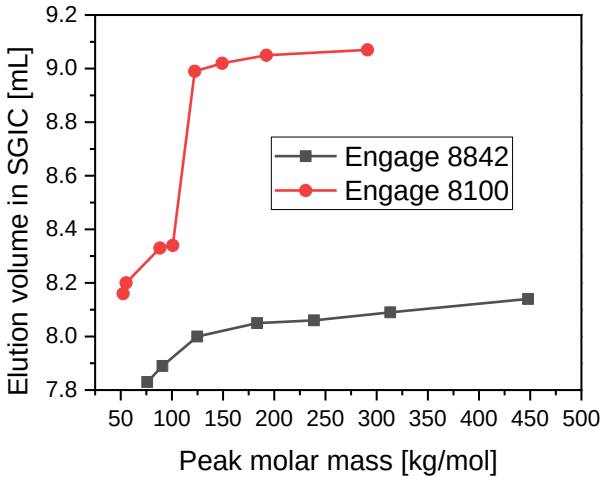

Figure 6.7. Correlation of peak molar mass to elution volume Engage 8842 and Engage 8100 fractions.

In addition, the comonomer contents of these fractions are not significantly different. This suggests that the molar mass has a pronounced effect on the adsorption-desorption mechanism of the molecules on the Hypercarb® stationary phase. According to Fig. 6.7, the low molar mass molecules are less retained while the opposite is true for high molar mass molecules irrespective of the chemical composition. Similar behaviour was observed for the LC 160 p-MMF fractions elution behaviour (Chapter 4). This indicates that Engage 8824 has a more homogenous chemical composition distribution while Engage 8100 and Tafmer fractions elute later in a broader elution volume.

This is also confirmed by their bimodal elution behaviour in SGIC previously shown in Fig. 6.6. Therefore, these results show that amongst these three samples, Engage 8842 has most homogeneous molecular structure. The bulk samples and fractions of Engage 8100 and Tafmer were analysed using HT-2D-LC using the similar conditions as those reported in Chapter 3. Figs. 6.8 and 6.9 show the 2D contour plots of the bulk samples and their respective fractions for samples Engage 8100 and Tafmer respectively.

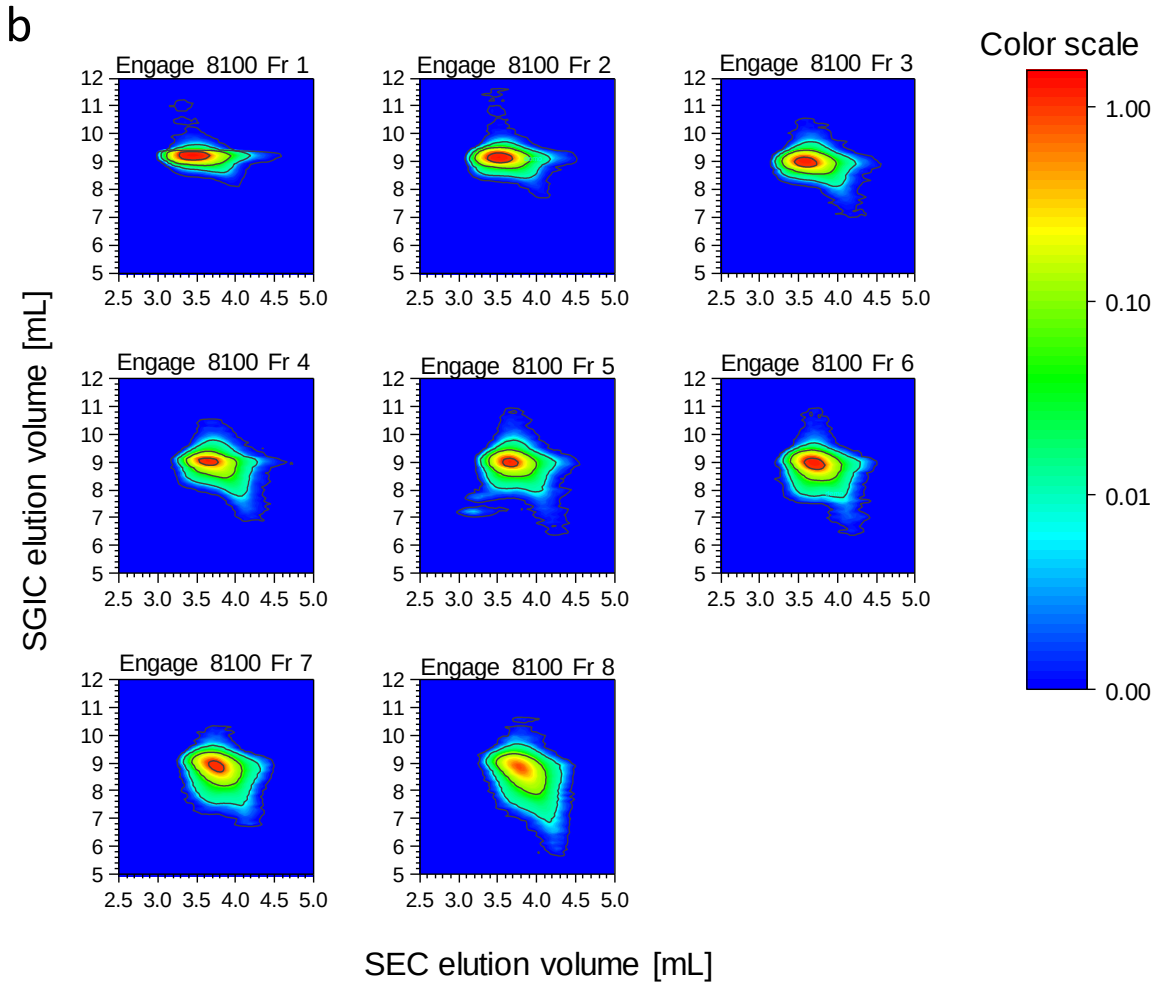

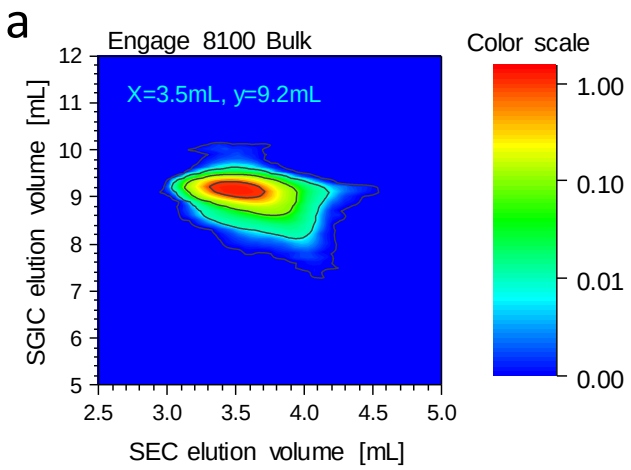

Figure 6. 8. 2D contour plots of fractions of Engage 8100 obtained from HT-2D-LC analyses.

The bulk analyses of the Engage 8100 and Tafmer show rather similar elution behaviour as was seen with the one-dimensional analyses. Therefore, from a bulk analysis point of view, there is not much that can be deduced from the molecular complexity of the samples. As already seen in the SEC analyses of the fractions (Fig. 6.3), the elution profiles are rather narrow which indicates molar mass homogeneity. However, as the fraction number increases, the SGIC elution becomes broader.

This was also seen in the one-dimensional SGIC analyses, Fig. 6.6. Tailing of the SGIC profiles occurs mainly towards low elution volumes which indicates an increase in the species which are retained to a lesser extent. From the HT-2D-LC contour plots, these can now be assigned as low molar mass species as seen in their high SEC elution volume. The same can be said for the Tafmer fractions, see Fig. 6.8. However, the fractions have narrower SGIC elution profiles as compared to the Engage 8100 fractions.

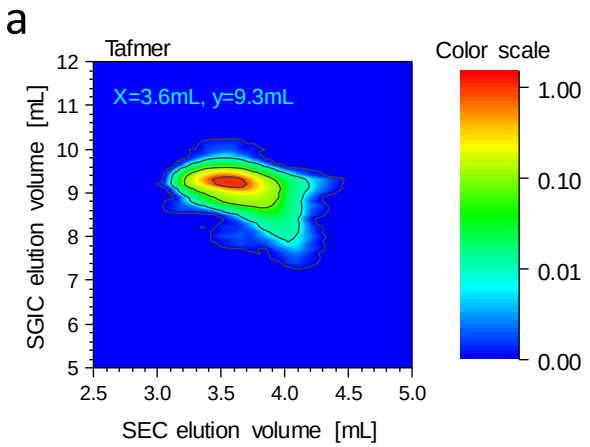

Figure 6. 9. 2D contour plots of fractions of Tafmer obtained from HT-2D-LC analyses.

6.4. Conclusion

Commercial samples that are seemingly homogenous and similar at bulk sample level exhibit microstructural inhomogeneity and differences. The only possible way to fully unravel these differences is via preparative fractionation. In the present chapter three commercial elastomers were fractionated via preparative molar mass fractionation and analysed using HT-SEC, DSC, HT-SGIC and HT-2D-LC. While the bulk samples show narrow molar mass and SGIC elution distributions, the fractions show multimodal chemical composition distributions. The common trend with the samples is the increase in the fraction chemical composition complexity with a decrease in the molar mass. While the role of molar mass cannot be discounted, it is undoubtable that prior preparative fractionation gives more information on the differences between samples.

6.5. References

1. Cheruthazhekatt, S.; Pijpers, T. F. J.; Mathot, V. B. F.; Pasch, H. *Anal. Bioanal.Chem.* **2013**, *405*, 8995–9007.
2. Zhang, M.; Lynch, D. T.; Wanke, S. E. *J. Appl. Polym. Sci.* **2000**, *75*, 960–967.
3. Schick, C. *Anal. Bioanal.Chem.* **2009**, *395*, 1589–1611.

4. Liu, W.; Zhang, X.; Bu, Z.; Wang, W.-J.; Fan, H.; Li, B.-G.; Zhu, S. *Polymer* **2015**, *72*, 118–124.

5. Arndt, J.-H.; Brüll, R.; Macko, T.; Garg, P.; Tacx, J. *Polymer* **2018**, *156*, 214-221.

6. Gabriel, C.; Lilge, D. *Polymer* **2001**, *42*, 297–303.

7. Razavi-Nouri, M. *Polym. Test.* **2006**, *25*, 1052–1058.

8. Zhang, K.; Liu, P.; Wang, W.-J.; Li, B.-G.; Liu, W.; Zhu, S. *Macromolecules* **2018**, *51*, 8790–8799.

9. Hosoda, S. *Polym. J.* **1988**, *20*, 383–397.

10. Tarasova, E.; Poltimäe, T.; Krumme, A.; Lehtinen, A.; Viikna, A. *Macromol. Symp.* **2009**, *282*, 175–184.

11. Podzimek, S. *J. Appl. Polym. Sci.* **2013**.

12. Mandelkern, L. *Crystallization of polymers*, 2nd ed.; Cambridge University Press: United Kingdoms, 2004.

Chapter 7

Conclusions and recommendations

Findings from previous results chapters are summarised in the conclusions section. Recommendations deduced from the findings are made in the subsequent section.

7.1. Conclusion

Four different preparative fractionation techniques were evaluated for characterization of ethylene-1-octene elastomers. It was shown that the suitability of a typical preparative fractionation method for LLDPE characterization is dictated by its sensitivity or lack thereof to the molecular structure dimensions (CCD and MMD). As such, of the four preparative fractionation methods investigated in the first results chapter, it was shown that p-MMF fractionation is selectively sensitive to molar mass rather than chemical composition, p-TREF used with an isocratic solvent is sensitive to chemical composition rather than molar mass.

The addition of a non-solvent to create a binary solvent mixture resulted in temperature-based fractionation techniques producing fractions with different molar masses. The fractions obtained revealed the complex nature of the sample LC 160. It can be concluded that the use of a binary solvent mixture in temperature dependent fractionations is one way to fractionate bulk resins according to molar mass. p-TREF in xylene showed good sensitivity to chemical composition although some fractions were recovered in very low quantities. However, p-MMF gave significant amounts of fractions with very narrow molar masses (mostly Đ less than 2).

The molecular structure of the eight fractions was successfully elucidated using p-MMF in combination with advanced analytical techniques such as DSC, CRYSTAF, FTIR, HT-SEC and HT-SGIC. When LLDPEs with increasing comonomer contents were fractionated with preparative molar mass fractionation and the fractions analysed with several techniques, it was revealed that the fractionation technique is not affected by chemical composition of the fractionated material. Small differences in chemical composition behaviour were observed for the first sample (4.4 mol.%) and this was attributed to the presence of a PE homopolymer and copolymer, which is typical of a ZN-catalyst LLDPE. The low molar mass fractions showed

decreased elution volumes in HT-SGIC for the mentioned sample. The fractions obtained from the rest of the samples (7.5, 10.0, and 11.1mol.% respectively) showed that elution behaviour was influenced by their respective bulk samples in HT-HPLC. Therefore, it can be concluded that p-MMF as a technique is not influenced by the chemical composition of the bulk sample, provided that the average comonomer content is high.

This makes the technique suitable for the comparison of elastomers with close comonomer contents. In the last chapter, three commercial elastomers were compared. At bulk sample level, the fractions appeared homogenous in both their molar mass and chemical composition distributions as investigated by HT-SEC and HT-SGIC respectively. However, when the bulk samples are fractionated and analysed with both HT-SEC and HT-SGIC, complex elution behaviour of the fractions is observed in HT-SGIC.

Furthermore, the elution behaviour of the fractions obtained from bulk samples with similar average comonomer contents is dissimilar. Coupling of HT-SGIC to HT-SEC also revealed broad chemical composition distributions for Engage 8100 fractions with low molar mass components tailing towards low SGIC elution volumes. Clear differences in the elution behaviour of the two sets of fractions in HT-2D-LC is clear testament preparative fraction is needed to reveal the microstructural differences.

7.2. Future work.

Preparative fractionation of LLDPE elastomers using p-TREF and p-SCF in which the mobile phase was a solvent mixture gave fractions with narrow molar mass distributions. It would be of interest to optimize the conditions for these methods to improve its selectivity since the technique is fast and requires less labour.

Thermal gradient interaction chromatography (TGIC) is another technique that can be used for the separation of chemically different macromolecules. It would be of interest to compare the bulk elution profiles to those of the fractions. Moreover, the technique can be tailored specifically for elastomer materials by using different solvent combinations.